Università degli Studi di Firenze

DOTTORATO DI RICERCA IN

"AGROBIOTECNOLOGIE PER LE PRODUZIONI TROPICALI"

CICLO XXV

COORDINATORE Prof. Stefano Mancuso

In vivo studies to characterize a protein involved in Golgi apparatus-mediated trafficking and a mitogen-activated protein kinase kinase kinase family (ANPs) involved in plant immunity

Settore Scientifico Disciplinare AGR/03

Dottoranda
Dott.ssa *Marti Lucia*

Tutor
Prof. *Mancuso Stefano*

Cotutor
Prof.ssa *De Lorenzo Giulia*

Anni 2010/2012

CONTENTS

PREFACE

Plants, as sessile organisms, must continually combine growth, development and defence events to adapt to fluctuating environmental conditions. This plasticity is made possible by the ability of the plants to perceive, transduce and integrate multiple signals from the environment, which allows them to properly adapt to environmental perturbations. As all living multicellular organisms, plants successful lifestyle depends on complex interactions among regulatory networks based on gene interactions, gene products, hormone pathways, metabolites and signaling pathways. All these processes could be now studied more in detail and *in vivo*, thanks to the advent and the progress of scanning confocal microscope, through subcellular dynamic analyses. The great help brought by this type of microscopy is closely linked to the discovery of the phenomenon of fluorescence; it is in fact possible to mark, with fluorescent molecules, particular biological elements of interest and follow their roles and space-time evolution through the confocal microscope.
During my thesis, I performed subcellular dynamics studies using *Arabidopsis thaliana* as a model plant.

In a first part of my work, I focused on mechanisms controlling the integrity of the Golgi apparatus. The plant Golgi is a highly polarized organelle and consists of different types of cisternae that are morphologically and functionally distinct (Neumann et al., 2003). Golgi is highly motile (up 4 μm sec-1) along the cytoskeleton (Boevink et al., 1998; Nebenfuhr et al., 1999). The Golgi apparatus, together with the endoplasmic reticulum (ER) is the heart of the

secretory pathway, which plays a fundamental role in both plant immunity and development. In general, all eukaryotic cells, unlike prokaryotes, developed an internal membrane system that controls the secretion of biomolecules and also mediates uptake of substances and delivery to specific intracellular locations. Many aspects of membrane trafficking are likely shared among eukaryotes, but the endomembrane system of higher plants displays distinct organizational features that may imply adaptive specializations in membrane trafficking.

The events comprising protein biosynthesis and subsequent export from the ER are, perhaps, the most conserved among kingdoms, but an important feature among plant endomembrane system is that, in addition to its role in protein sorting and protein modification, the Golgi apparatus plays also a pivotal role to transport building blocks to energy-rich compartment, including chloroplast, storage vacuole and cellulosic cell wall (Perrin et al., 2001; Vitale and Hinz, 2005; Radhamony and Theg, 2006).

In a widely accepted model, the membrane traffic machinery begins by translocation of newly synthesized proteins into the ER, then flows first to the Golgi, and subsequently to the plasma membrane (PM)/extracellular matrix (ECM). From the Golgi, vacuolar proteins are re-directed to the vacuole (by way of the late endosome) due to specific sorting signals. Conversely, endocytosed cargo from the PM/ECM travels by way of endosomes to the vacuole. This so-called retrograde pathway works as recycling mechanism. Some evidences had indicated that also peroxisomes and plastids take part of

endomembrane system (Titorenko and Mullen, 2006; Nanjo et al., 2006).

In addition to performing more "traditional" roles, secretory membrane trafficking has been shown to be involved in a variety of plant-specific processes. For example, it plays a prominent role in plant immunity. Plant cells, because of their sessile lifestyle, uniquely depend on the secretory pathway to respond to changes in their environments, either abiotic, such as the absence of nutrients, or biotic, such as the presence of predators or pathogens. These environmental stresses, cause significant intracellular restructuring in plants and certain molecules need to be transported to, or removed from, a given compartment. Cell surface proteins involved in pathogen recognition reach their cellular destination by exocytosis after folding and maturation in and trafficking through the ER and Golgi apparatus (Kwon et al., 2008a). Most compartments, including the cytoplasm, the ER, the nucleus, mitochondria, Golgi bodies, and peroxisomes aggregate beneath pathogen entry sites (Gross et al., 1993; Takemoto et al., 2003; Lipka et al., 2005; Koh et al., 2005).

The Golgi is subjected to a remodeling due to its continuous exchange of molecules with both other organelles or cytoplasm; in particular, there is a continuous anterograde and retrograde flow of membranes from and to the Golgi apparatus (Brandizzi et al, 2002b; daSilva et al., 2004). This raises a fundamental biological question: how does the Golgi maintain its integrity (architecture and composition), in spite of the intense turnover? In mammalian cells, some members of golgins family have been shown to contribute to the Golgi integrity (Barr and Short, 2003). Although golgin

homologous exist in plants, there is no evidences yet for their involvement in regulating Golgi function (Latijnhouwers et al., 2005; Stefano et al., 2006; Latijnhouwers et al., 2007) and in general little is known about mechanisms underlying Golgi integrity in plants. I therefore searched for elements that control Golgi integrity by performing a genetic screens of an EMS-mutagenized population of *Arabidopsis thaliana* plants stably expressing a Golgi marker.

In the second part of my thesis, I focused on subcellular dynamic events occurring during the immune response triggered by PAMPs (pathogen-associated molecular patterns) and DAMPs (damage-associated molecular patterns). Plants, unlike animals, lack specialized and mobile immune cells to combat pathogens. However, this is balanced by the capability of all plant cells to set a wide and complex repertoire of defense responses leading to immunity. This is activated by the recognition of non-self molecules. The perception of intruders is performed by two type of receptors: membrane-resident pattern recognition (PRRs), perceiving pathogen-associated molecular patterns (PAMPs) or damage-associated molecular patterns (DAMPs), and intracellular immune sensors, called resistance (R) proteins, which mediate recognition of pathogen effector proteins. The former response is named PAMP-triggered immunity (PTI), the latest is termed effector-triggered immunity (ETI). The recognition of the non-self molecular structures triggers a complex array of immune responses, including the generation of reactive oxygen species (ROS), nitric oxide, the plant stress hormone ethylene, activation of a mitogen-activated protein kinase (MAPK)

cascade as well as changes in gene expression (Felix et al., 1999; Zipfel et al., 2004; Zeidler et al., 2004). Three types of kinases form the core module of a MAPK cascade: MAP kinase kinase kinases (MAPKKKs), MAP kinase kinases (MAPKKs) and MAP kinases (MAPKs). Because very little is known about the subcellular dynamics of MAPKKKs during the immune response, I performed live cell imaging studies on a family of MAPKKKs (ANPs family) that has been recently shown to play an important role in immunity (unpublished data of G. De Lorenzo laboratory).

I. INTRODUCTION

I.1 PLANT IMMUNITY

During evolution, plants, due to its sessile lifestyle, have evolved a sophisticated immune system of the so called "innate" type to combat microbial attach. On the other hand, in order to be pathogenic, microbes must reach the plant interior either by penetrating the leaf or root surface directly or by entering through wounds or natural openings such as stomata. Once inside, they have cross another obstacle, the plant cell wall, a rigid, cellulose-based support surrounding every cell, before encountering the host plasma membrane. Here, they have to face a sentinel system that comprises the so called Pattern Recognition Receptors or PRRs (Jones and Dangl, 2006; Boller and Felix, 2009). The detection of specific Pathogen-Associated Molecular Pattern (PAMPs), also indicated as Microbe-associated molecular patterns (MAMPs), by PRRs represents the first of the two levels into which plant immunity is distinguished. This type of resistance is referred to as PTI, for PAMP-Triggered Immunity (Chisholm et al., 2006). PAMPs belong to the class of the so-called general elicitors, which also include damage-associated molecular patterns (DAMPs) (Darvill and Albersheim, 1984; Boller, 1995). DAMPs, originally indicated as endogenous elicitors, arise from the plant itself because of the damage caused by microbes or mechanical stress (Darvill and Albersheim, 1984). To counteract PTI, microbes have evolved effectors, against which plants have in turn evolved a second level of plant surveillance, known as Effector-Triggered-Immunity (ETI). This is a very robust response typically mediated by Resistance (R) proteins, which are

intracellular proteins of the nucleotide-binding site-LRR (NB-LRR) class that mediate, directly or indirectly, recognition of pathogen effectors, originally indicated as Avirulence (Avr) proteins (Jones and Dangl, 2006). Activation of R protein-mediated resistance also suppresses microbial growth, but only when the invader is already inside after a limited proliferation (Figure 1). ETI is often characterized by a local programmed cell death termed Hypersensitive Response (HR) at the infection site: here, a limited number of plant cells, those that take contact with the pathogen, die quickly, determining a necrotic lesion where the pathogen is confined and blocked (Godiard et al., 1994).

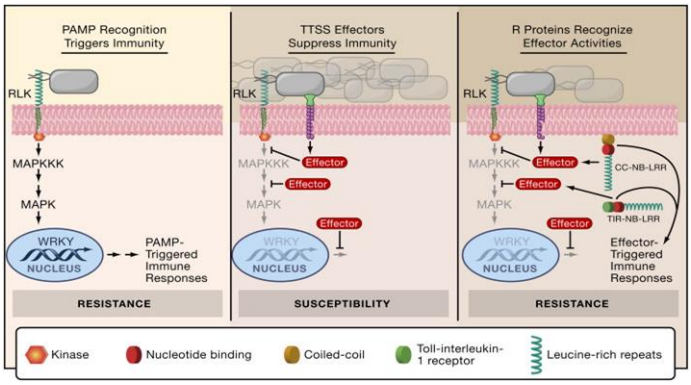

Figure 1. Model for the Evolution of Bacterial Resistance in Plants
Left to right, recognition of pathogen-associated molecular patterns (such as bacterial flagellin) by extracellular receptor-like kinases (RLKs) promptly triggers basal immunity, which requires signaling through MAP kinase cascades and transcriptional reprogramming mediated by plant WRKY transcription factors. Pathogenic bacteria use the type III secretion system to deliver effector proteins that target multiple host proteins to suppress basal immune responses, allowing significant accumulation of bacteria in the plant apoplast. Plant resistance proteins (represented by CC-NB-LRR and TIR-NB-LRR; see text) recognize effector activity and restore resistance through effector-triggered immune responses. Limited accumulation of bacteria occurs prior to effective initiation of effector-triggered immune responses. Adapted from Chisholm et al. (2006).

On the other hand Boller and Felix (2009) postulate only one form of plant innate immunity where both PTI and ETI coexist and DAMPs are included. These authors envision that effective innate immunity in plants, as in vertebrates, is mediated through a single overarching principle, the perception of signals of danger (Matzinger, 2002; Lotze et al., 2007; Rubartelli and Lotze, 2007). PAMPs, DAMPs, and effectors might appear to the plant as one and the same type of signal that indicates a situation of danger (Figure 2). Indeed, gene expression data indicate that considerable overlap exists between the defense response induced by MAMPs, DAMP and effectors (Tao et al., 2003; Navarro et al., 2004; Thilmony et al., 2006; Wise et al., 2007).

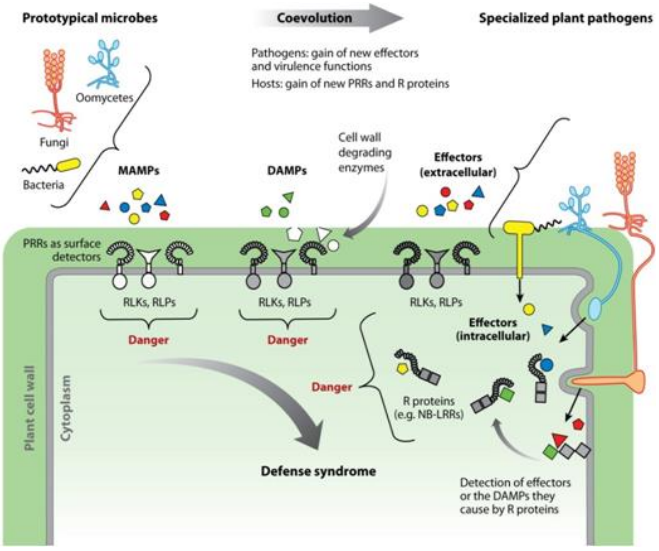

Figure 2. Microbe-associated molecular patterns (MAMPs), damage-associated molecular patterns (DAMPs), and effectors are perceived as signals of danger.
Extracellular MAMPs of prototypical microbes and DAMPs released by their enzymes are recognized through pattern recognition receptors (PRRs). In the course of coevolution, pathogens gain effectors as virulence factors, and plants evolve new PRRs and resistance (R) proteins to perceive the effectors. When MAMPs, DAMPs, and effectors are recognized by

PRRs and R proteins, a stereotypical defense syndrome is induced. RLK, receptor-like kinase; RLP, receptor-like protein; NB-LRR, nucleotide binding-site–leucine-rich repeat. Adapted from Boller et al. (2009).

The recognition of specific or non-specific elicitors is followed by a complex spectrum of reaction including molecular, morphological and physiological changes (Altenbach and Robatzek, 2007). Activation of PRRs or R proteins triggers early changes that occur within seconds to minutes and include ion-flux across the plasma membrane, an oxidative burst, mitogen-activated protein (MAP) kinase activation and protein phosphorylation (Schwessinger and Zipfel, 2008). Afterwards a substantial transcriptional reprogramming takes place within the first hour involving activities of WRKY transcription factors. Activation of transcription of genes related to the pathogenesis such as lytic enzymes (chitinase, glucanase, protease), proteins and metabolites with antimicrobial activities (defensins and phytoalexins, respectively) is also induced (Kombrink and Somssich, 1995).

Later changes include callose deposition, newly synthesized cell wall material, into the paramural space between the cell wall and the plasma membrane (Aist, 1976) which serves as a physical barrier at infection sites, and stomatal closure. Stomata provide a major entry point for many plant pathogens and *A. thaliana* stomata have been shown to close within 1 h in response to PAMPs as part of PTI (Melotto et al., 2006).

I.1.1 PAMPs, DAMPs and their receptors

PAMPs are molecular signatures typical of whole classes of microbes, and their recognition plays a key role in innate immunity. Endogenous elicitors (DAMPs) are similarly recognized. Recognition of PAMPs or DAMPs by PRRs is the prerequisite and the first step to trigger defence reactions effective against the invading microbes. Characterized PRRs belong to the superfamily of surface receptor-like kinases (RLKs) (Boller and Felix, 2009) that generally have an extracellular ligand-binding domain, a membrane spanning region, a juxtamembrane (JM) domain, and a serine/threonine kinase domain. The N-terminal extracellular domain of PRRs defines ligand specificity. The most studied of them include those with leucine-rich repeat (LRR) domains (LRR-RLKs), LysM domains (LYK) and the *Catharanthus roseus* RLK1-like (CrRLK1L) domain. These proteins recognize distinct ligands of microbial origin or ligands derived from intracellular protein/carbohydrate signals. From a simplistic viewpoint, kinases serve as switches that are turned on or off via conformational changes induced by ligand binding. The plant RLKs conserve an aspartate residue in the kinases catalytic loop required for catalytic activity. The activation loop becomes phosphorylated and structurally reoriented to enable substrate access and/or to enhance phosphotransfer efficiency (Adams, 2003). In Ser/Thr kinases the catalytic aspartate (D) is mostly preceded by an arginine (R). This kind of kinases are termed RD kinases, and RD motif facilitates phosphotransfer (Johnson et al., 1996b). However most RLKs are non-RD kinases, lacking an arginine preceding the catalytic

aspartate (Krupa et al., 2004). RLKs, in general, require additional proteins to modulate their function (Johnson et al., 1996a; Dardick and Ronald, 2006). An important example is BRI-associated kinase1 (BAK1), which interacts with many *Arabidopsis* RLKs and is required for their activity.

The best characterized plant PRRs are LRR-RLKs and include FLS2 (flagellin sensing 2), which recognize a conserved 22 amino-acid peptide (flg22) of the bacterial flagellin, and EFR, which binds a 18 amino-acid epitope (elf18) of the bacterial elongation factor EF-Tu (Boller and Felix, 2009; Lacombe et al., 2010). The rice LRR-RLK XA21 shares similar structure and is activated by a sulphated 17-amino acid peptide (AxYS22) conserved in strains of Xanthomonas (Lee et al., 2009). CERK1 belongs to a distinct subfamily of RLKs, chitin elicitor-binding protein (CEBiP), with LysM motifs. The proteins act for immune signaling triggered by fungal chitin, a long-chain polymer of an N-acetylglucosamine and the main component of cell walls of higher fungi. LysM motifs are required for glycan binding in the N-terminal ectodomain (Wan et al., 2008; Nakagawa et al., 2011). Besides PAMPs, plant-derived peptides and cell wall fragments acting as DAMPs are also perceived by RLKs to enhance resistance to bacterial and fungal pathogens. They have been proposed to function as secondary danger signals to prolong or amplify immune responses. For example, wounding, stress hormones and PAMPs significantly up-regulate the Arabidopsis PROPEP genes (Boller and Felix, 2009; Lee et al., 2011a) that encode the secreted peptides (PEP1–6). These bind PEPR1 and PEPR2 to trigger immune signaling (Krol et al., 2010; Yamaguchi et al., 2010).

Moreover plant cell wall-associated RLKs (WAK1 and WAK2) bind pectin and oligogalacturonides (OGs) and modulate both immunity and development (Kohorn et al., 2009; Brutus et al., 2010) (Figure 3).

FLS2/flg22. FLS2 perceives the conserved peptide of flagellin flg22 present in a broad class of bacterial plant pathogens including *Pseudomonas syringae* pv. *tomato* (Pto) DC3000 (Gomez-Gomez and Boller, 2000). FLS2 consists of an extracellular LRR domain with 28 repeats, a transmembrane domain and a cytoplasmic kinase domain (Boller and Felix, 2009). The catalytic loop of FLS2 contains the sequence CD instead of the RD. It is well-established that FLS2 forms heterodimers with BAK1 (Chinchilla et al., 2007; Schulze et al., 2010) in the presence of bound flg22. BAK1 is a common component in many RLK signaling complexes and was first identified for its requirement in brassinosteroid signaling via the receptor BRI1 ((Li and Nam, 2002). Immediately after FLS2-BAK1 activation, Arabidopsis BIK1 (a receptor-like cytoplasmic Kinase, RLCK) plays a pivotal role in MAMP signaling.

BIK1 interacts with FLS2 and BAK1, and flg22 triggers FLS2- and BAK1-dependent BIK1 phosphorylation (Zhang et al., 2010; Lu et al., 2010). Recently, ligand mediated receptor endocytosis has been identified as an additional FLS2 regulatory mechanism (Robatzek et al., 2006). After binding of flg22, FLS2 accumulates in mobile intracellular vesicles. This ligand-induced FLS2 endocytosis is followed by receptor degradation possibly via lysosomal and/or proteasomal pathways. Endocytosis and downstream signalling are

closely linked but it is not yet known if the actual internalization is required for signal transduction.
Responsiveness to flg22 is shared by members of all major groups of higher plants, indicating that the PRR for this epitope of bacterial flagellin is evolutionarily ancient. Indeed, orthologs of FLS2 with a high degree of conservation are present in genomes of all higher plants analyzed so far. Only the moss *Physcomitrella patens* contains many LRR-RKs in its genome but does not carry an FLS2 ortholog and also shows no response to flg22 (Boller and Felix, 2009).

EFR/EF-Tu. The elongation factor receptor EFR is another well studied receptor which can perceive the N-terminal acetylated peptide elf18 and elf26 of the bacterial elongation factor Tu (EF-Tu). The extracellular LRR domain of EFR (21 repeats) is highly glycosylated, and this seems to be important for ligand binding as mutation of a single predicted glycosylation site compromises elf18 binding (Haweker et al., 2010).
EFR and BAK1 have also been shown to interact in a ligand-dependent manner (Roux et al., 2011). Indeed, many of the signaling components downstream of EFR and FLS2 are shared and activation of EFR leads to activation of similar defence responses as those triggered by flg22 (Zipfel et al., 2006). In fact it has been shown that BIK1 is phosphorylated upon elf18 and flg22 treatment (Lu et al., 2010). Given the many parallels between FLS2 and EFR, it is possible that trans-phosphorylation of the EFR/BAK1 complex also occurs, although direct proof is still lacking.

In contrast to FLS2, but similarly to Xa21, N-glycosylation is critical for EFR function and EFR is subject to ER quality control that requires several chaperones involved in ER-QC for full activity (Haweker et al., 2010). Responsiveness to elf18/elf26 was found in various Brassicaceae species but not in members of other plant families tested, indicating that perception of EF-Tu as a PAMP is an innovation in the Brassicaceae (Kunze et al., 2004).

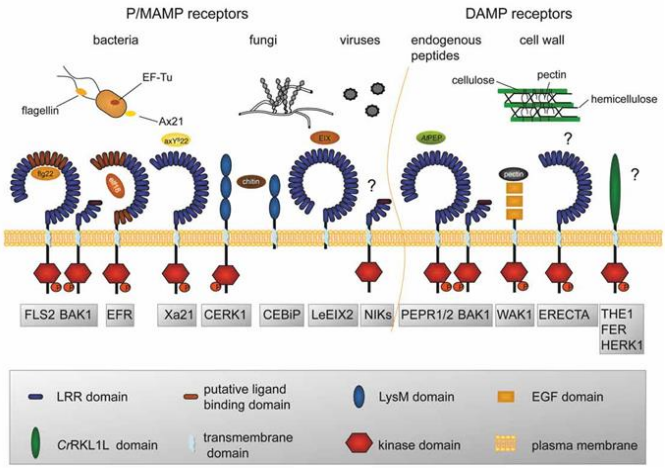

Figure 3. Membrane-associated pattern recognition receptors can perceive microbial patterns (P/MAMP) from different microbes such as bacteria, fungi, oomycetes or viruses. DAMPs can be released after wounding or pathogen attack. The LRR-RLKs FLS2, EFR and XA21 can perceive bacterial peptides such as flg22 from flagellin, elf18 from EF-Tu and AxYs22 from Ax21, respectively. Most likely LRR 1-6 and 19-21 of EFR are necessary for elf18 binding and receptor activation while LRR 9-15 of FLS2 are necessary for flg22 binding. CERK1/LysM-RLK1 is necessary for fungal chitin perception in Arabidopsis and acts cooperatively with CEBiP in rice, while tomato EIX2 can perceive the fungal ethylene inducing xylanase protein EIX. NIK1-3 were shown to be involved in virus resistance in tomato and Arabidopsis. They belong to the same LRR family II as BAK1, a small LRR-RLK with four and a half LRR-repeats that interacts with several ligand binding receptors such as FLS2, PEPR1/2 and BRI1 (not shown). DAMPs as e.g. the endogenous peptides AtPEPs are perceived by the redundant LRR-receptors PEPR1 and 2. Cell wall fragments can bind to WAK1 and activate oligogalacturonide-dependent defense responses. Other RLKs known to be involved in developmental processes as the LRR-RLK ERECTA and the CrRLK1L proteins FERONIA, HERCULES and THESEUS might be involved in damage associated defence responses. Adapted from Mazzotta and Kemmerling (2011)

Transient expression of the EFR gene in *Nicotiana benthamiana*, a plant lacking an endogenous EF-Tu perception system, conferred elf18/elf26 responsiveness to this plant species, directly demonstrating that EFR is the PRR for EF-Tu ((Zipfel et al., 2006) and, furthermore, that downstream elements of PRR activation are conserved between *Arabidopsis* and *Nicotiana*.

WAK1/OGs. The wall-associated kinases (WAK) family is another group of PRRs. These receptors contain epidermal growth factor (EGF)-like motifs in the extracellular domain, which can also bind cell wall components as pectin or oligogalacturonides (OGs) *in vitro* (Decreux et al., 2006). Oligogalacturonides (OGs) are linear molecules of two to about twenty α-1,4-d-galactopyranoslyuronic acid (GalA) residues that are released upon fragmentation of homogalacturonan (HG) from the plant primary cell wall (Cote et al. 1998) by wounding or by pathogen-secreted cell wall-degrading enzymes (for example polygalacturonases, PGs). Indeed, PGs are not elicitors per se, but are rather able to release elicitor-active molecules from the host cell wall. When the activity of a fungal PG is modulated by apoplastic PG-inhibiting proteins (PGIPs), long-chain oligogalacturonides are produced (De Lorenzo et al., 2001; De Lorenzo and Ferrari, 2002). OGs cannot be considered true PAMPs, since they are not derived from the pathogen. However, they are considered the classic examples of DAMPs, which are generated by the host cell during the infection process. OGs are also regulators of growth and development (Cervone et al., 1989). In fact OGs are potentially perceived not only during pathogen infection but also during normal

growth (Savatin et al., 2011), supporting the notion that a cross-talk exists between defense and developmental responses.

Through the use of a domain swap approach performed on the RLKs EFR and WAK1, it was demonstrated that a chimeric receptor comprising the WAK ectodomain fused with the EFR TM and intracellular kinase domain is able to perceive OGs and induce typical EFR-mediated responses, such as ethylene production and defense gene expression (Brutus et al., 2010). Similarly, a chimeric receptor comprising the TM and cytoplasmic kinase domains of WAK1 fused with the ectodomain of EFR is able to perceive elf18, triggering an oxidative burst in the *efr* Arabidopsis mutant that lacks EFR (Brutus et al., 2010).

PEPR1-2/AtPep1. Pep1 receptor1 (PEPR1) binds AtPep1, a DAMP derived from the precursor gene PROPEP1 (Yamaguchi et al., 2006). AtPep1 is a 23-amino-acid peptide representing a different class of endogenous elicitor that activates defence genes associated with the innate immune response (Huffaker et al., 2006). PROPEP1 is a member of a small gene family consisting of six annotated and one unannotated genes encoding precursors that, at their C-termini, contain homologue sequences to AtPep1 (Huffaker and Ryan, 2007). Some of these genes are expressed in response to PAMPs, and produce AtPep peptides that engage, in a feedback loop, to amplify defence signaling through both the Jasmonate/Ethylene and Salicylic Acid pathways (Huffaker et al., 2006; Huffaker and Ryan, 2007). PEPR1 and PEPR2 act redundantly to perceive AtPep1. BAK1 was

shown to interact with PEPR1 as well like FLS2 and EFR (Postel et al., 2010).

I.1.2 Basal defence

Induction of basal defence mechanisms occurs in response to PAMPs in both host and non-host plant species through a complex signal transduction pathway that includes a rapid depolarization of the plasma membrane potential, a rapid oxidative burst, and the activation of intracellular kinase cascades, generally followed by changes in gene expression.

Very Early Responses (1-5 Minutes)

Among the earliest and most easily recordable physiological responses to PAMPs and DAMPs in plant cell cultures, starting after a lag phase of ~0.5-2 min, is an alkalinization of the growth medium due to changes of ion fluxes across the plasma membrane (Boller, 1995; Nurnberger et al., 2004) which resulted in cytoplasmic acidification increasing influx of H^+ and $Ca2^+$ and a concomitant efflux of K^+; an efflux of anions, in particular of nitrate, has also been observed (Wendehenne et al., 2002). The ion fluxes lead to membrane depolarization. The rapid increase in cytoplasmic $Ca2^+$ concentrations serve as second messenger to promote the opening of other membrane channels (Blume et al., 2000; Lecourieux et al., 2002), or to activate calcium-dependent protein kinases (Boudsocq et al., 2010). In this regard, it is interesting that production of secondary

metabolites is enhanced in response to changes in cytoplasmic pH (Roos et al., 1998).

Another very early response to PAMPs and DAMPs, with a lag phase of ~2 min, is the oxidative burst (Chinchilla et al., 2007). Reactive oxygen species (ROS) may act as secondary stress signals to induce various defense responses (Apel and Hirt, 2004). The quantities of ROS produced can be cytotoxic and thus are expected to be antimicrobial and are thought to have direct (through cytotoxicity) and indirect (through signaling) roles in the plant cell death required for the HR. In addition, ROS drive the rapid peroxidase-mediated oxidative cross-linking of cell wall lignins, proteins, and carbohydrates, thereby reinforcing the wall against enzymatic maceration by the pathogen (Cote and Hahn, 1994).

O_2^- generating nicotinamide adenine dinucleotide phosphate (NADPH) oxidases are generally considered to be a major enzymatic source of ROS in the oxidative burst of plant cells challenged with pathogens or elicitors (Torres and Dangl, 2005; Torres et al., 2006).

AtrbohD is NADPH oxidase required for the production of ROS during infection with different bacterial and fungal pathogens, including *B. cinerea* (Torres and Dangl, 2005; Torres et al., 2006).

Other enzymes appear to be important in the elicitor-mediated oxidative burst, including apoplastic oxidases, such as oxalate oxidase (Dumas et al., 1993), amine oxidase (Allan and Fluhr, 1997), and pH-dependent apoplastic peroxidases (Frahry and Schopfer, 1998; Bolwell et al., 1995), which generate either O_2^- or H_2O_2.

Activation of Mitogen-Activated Protein Kinase (MAPK) cascades is another early response to PAMP and DAMP (Pedley et al. 2005). The

MAPK phosphorylation cascade is a highly conserved signal transduction mechanism that plays a key role in regulating many aspects of growth and development in eukaryotes. A MAPK cascade consists of a core module of three kinases that act in sequence: a MAPK kinase kinase (MAPKKK) that activates, via phosphorylation, a MAPK kinase (MAPKK), which activates a MAPK Once activated, MAPKs phosphorylate a number of different target proteins including transcription factors, other targets protein kinases, phospholipases, and cytoskeletal proteins, all of which effect changes in gene expression and/or physiological responses appropriate to the stimulus in question (Widmann et al., 1999).

Early Responses (5–30 Minutes)

Among the earliest responses there is an increased production of the stress hormone ethylene, receptor endocytosis as described for certain receptors in animals, and gene activation. The pattern of gene regulation in response to different PAMPs is almost identical, indicating that signaling through various PRR converges at an early step (Zipfel et al., 2006). Interestingly, among the induced genes, Receptor-like kinases (RLKs) are overrepresented. FLS2 and EFR are included in the induced genes, indicating that one role of early gene induction is a positive feedback to increase PRR perception capabilities (Zipfel et al., 2004).

A secretory machinery becomes also engaged in the execution of immune responses. Vesicle-associated and SNARE (soluble N-ethylmaleimide sensitive factor attachment protein receptor) protein-mediated exocytosis pathways are involved to drive secretion of

antimicrobial cocktails comprising proteins, small molecules, and cell wall building blocks into the apoplastic space. These pathways have important functions also in plant development and might have been recruited for immune responses. The driving forces of such focal accumulation is the rapid changes of the actin and tubulin network. Rearrangements of cytoskeleton produce a kind of physical barrier by locally increasing the density of cellular components (Frei dit and Robatzek, 2009). Bacteria and fungi have evolved molecules that intercept the secretion machinery by blocking vesicle formation from intracellular membranes (Kwon et al., 2008b).

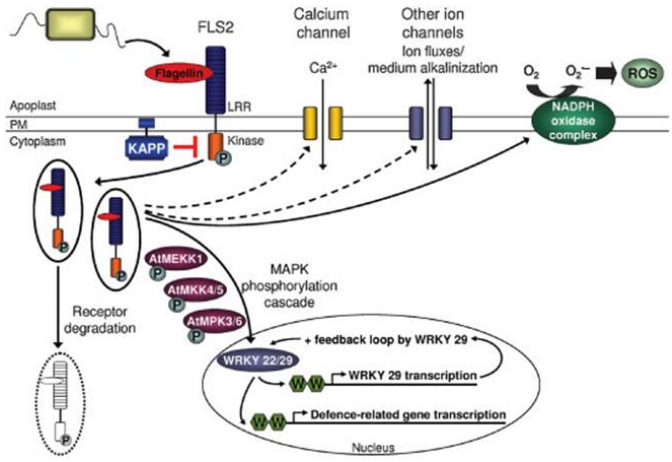

Figure 4. Plant very early/early responses to PAMPs. A current model for flagellin signalling in Arabidopsis

I.2 MAP KINASE CASCADES IN ARABIDOPSIS INNATE IMMUNITY

Protein kinases and phosphatases play a central role in signal transduction through the phosphorylation and de-phosphorylation of proteins. Both defense responses and developmental processes, like cell growth and differentiation, lead to their activation. One of the most common mechanisms is the mitogen-activated protein kinase (MAPK) cascade, comprising a class of protein kinases that plays a crucial role in the perception of external stimuli with subsequent changes in cellular organization or gene expression.

The progression of the signal through the MAP kinase cascade is mediated by the phosphorylation and comprise a series of sub-families, i.e., MAPKKK, MAPKK, MAPK, that are sequentially activated (Jonak et al., 2002; Tatebayashi et al., 2003). In general, MAP kinase signaling is initiated by the stimulus-triggered activation of a MAP kinase kinase kinase (MAPKKK or MAP3K). They are serine/threonine kinases which may be activated through physical interaction or phosphorylation by the receptor itself or intermediate bridging factors (Swarbreck et al., 2008) and in turn leads to the activation of downstream MAP kinase kinases (MAPKK or MAP2K) through phosphorylation on two serine/threonine residues in a conserved motif (Nakagami et al., 2005). Subsequently, the MAPKK phosphorylates the downstream MAPK on threonine and tyrosine residues sequentially leading to changes in its subcellular localization and/or phosphorylation of downstream

substrates including transcription factors which alter patterns of gene expression appropriate to the stimulus (Khokhlatchev et al., 1998; Widmann et al., 1999) (Figure 5).

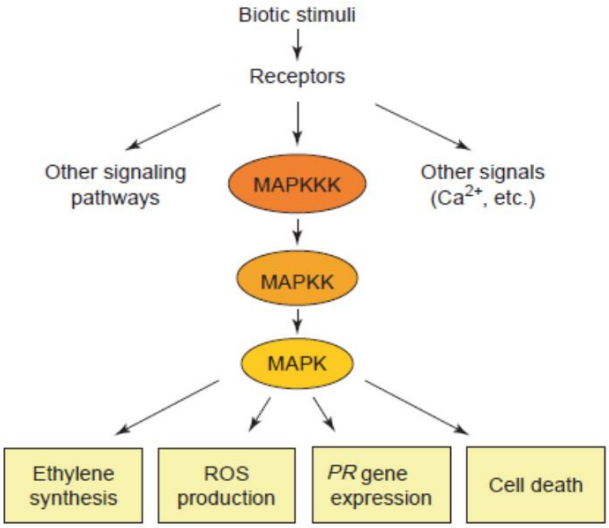

Figure 5. MAPK cascades and cellular responses.
They influence following the recognition of microbial pathogens. Adapted from Pedley et al. (2005)

An important point to note is that the MAPK cascade is highly specific for its substrate i.e., MAPKK can specifically and selectively interact with a specific MAPK. Among various MAPK modules the recognition of an appropriate specific substrate by MAPK depends upon the differential interaction of two sites i.e., catalytic site and docking site. A typical MAPK consist of an active site and a common docking furrow which are closely located and are implicated in recognition and binding of target proteins (Taj et al., 2010). MAPK

signaling location, specificity and duration are regulated by scaffolding proteins and MAPK phosphatases (Yoshioka, 2004). Scaffolding helps in holding the components of MAPK cascade via a single adapter together. Additionally, this arrangement also facilitate the interaction with the upstream factors that activates them, thus facilitating substrate recognition by the MAPK module (Whitmarsh et al., 1998; Morrison and Davis, 2003; Yoshioka, 2004).

The Arabidopsis genome encodes 60 MAPKKKs, 10 MAPKKs, and 20 MAPKs (2002). This indicates that MAPK cascades may not simply consist of single MAPKKKs, MAPKKs, and MAPKs connected together. Instead, it suggests that there is some level of redundancy, and that the spatial and temporal activities of different components may be strictly regulated to minimize the cross-talk.

A few PRRs have been documented to stimulate MAPK signaling upon perception of elicitors. These include the flagellin receptor FLS2 (Felix et al., 1999; Gomez-Gomez and Boller, 2000), the bacterial elongation factor EF-Tu receptor EFR (Zipfel et al., 2006) and the chitin receptor CERK1 (Miya et al., 2007).

The best-studied MPK3 regulates basal resistance to B. cinerea (Galletti et al., 2011), while MPK6 regulates defence gene expression and resistance to *B. cinerea* induced by OGs and flg22 (Galletti et al., 2011). MPK3 and MPK6 are activated by phosphorylation with a peak at 15 min after treatment with OGs, flg22 or elf18 (Denoux et al., 2008; Boller and Felix, 2009). In transfected protoplasts MPK3 and MPK6 phosphorylation has been shown to be induced by the expression of constitutively active forms of ANPs (a MAPKKK gene

family) obtained through deletion of the regulatory domain (ΔANPs) (Kovtun et al., 2000).

I.2.1 ANP gene family is involved in plant cytokinesis

The gene family Arabidopis NPK1-Related Protein Kinase (ANP), which includes *ANP1*, *ANP2*, and *ANP3*, constitutes a distinct branch of the MAPKKK phylogenetic tree (Jouannic et al., 1999).
ANP genes were isolated for their homology with the tobacco MAPKKK *NPK1 (Nucleus-and Phragmoplast-Localized Protein Kinase 1)* gene (Banno et al., 1993; Nishihama et al., 1997; Nakashima et al., 1998). NPK1 localizes to the phragmoplast and is involved in the formation of the cell plate and cytokinesis (Nakashima et al., 1998). Recently, NPK1 has been shown to be part of a MAPK signaling pathway involved also in cytoskeletal organization and comprising the NPK1-activating kinesin-like protein 1 (NACK1) and NACK2, NPK1, the NQK1 MAPK kinase (a MAPKK), and the NRK1 MAPK (NACK-PQR pathway) (Soyano et al., 2003). The activated pathway ultimately targets the tobacco MAP65-1a and 1b isoforms to promote microtubule (MT) dynamics (Ishikawa et al., 2002). Little is known about the Arabidopsis ANPs. Transient overexpression of constitutively active ANPs in protoplast cell cultures suggests that they may regulate oxidative stress– and auxin-related signaling pathways (Kovtun et al., 2000). Single-mutant plants homozygous for T-DNA insertions within ANPs are normal, likely due to functional redundancy. No homozygous triple mutants have been obtained, nor plant homozygous for two mutations and heterozygous for the third

mutation, suggesting that ANP1, ANP2 and ANP3 may be "collectively essential" (Krysan et al., 2002). Homozygous *anp2 anp3* double mutants show severe phenotypic changes, including an overall reduction in total plant size. The other mutants are indistinguishable from the wild type, with the exception of the *anp2* single mutant and the *anp1 anp2* double mutants, which showed a small increase in the hypocotyl length (8% for anp2 and 15% for *anp1 anp2*) (Krysan et al., 2002). Dark-grown *anp2 anp3* hypocotyls show numerous binucleate cells with cell wall stubs, swollen cells, shorter but wider hypocotyls. Reduced length and increased radial swelling have been reported for other Arabidopsis mutations that affect cell growth and division. The phenotype of ANP mutants is not "rescued" by hormone treatment (Krysan et al., 2002).

I.2.2 ANP1 is activated by H_2O_2

Induction of *MAPK* genes and increased MAPK kinase activity occurs when plants are subjected to many abiotic stresses such as touch, cold, salinity, genotoxic agents, UV irradiation, ozone, and oxidative stress (Mizoguchi et al., 1996). In many eukaryotes, the transduction of oxidative signals is controlled by protein phosphorylation involving MAPKs (Kyriakis and Avruch, 1996). Kovtun et al.(2000) have shown that, in Arabidopsis protoplast, H_2O_2 can activate ANP1, initiating a MAPK cascade leading to induction of MPK3 and MPK6. Constitutively active ANP1, obtained by expressing protein lacking the regulative domain (Δ-ANP1), mimics the H_2O_2 effect and initiates the MAPK cascade that induces

specific stress-responsive genes. Active ANP2 and ANP3, but not CTR1, also induced AtMPK3 and AtMPK6 activity, indicating that CTR1 and ANPs activate different MAPK cascades. The ability of ANPs to activate stress-related MPKs suggests that the ANP-mediated MAPK cascade is involved in stress signaling. Furthermore H_2O_2 can specifically induce the full-length ANP1 activity to the level of the constitutively active ANP1.

Interestingly, constitutively active NPK1 can partially block embryo development. In animals, induction of an oxidative stress-activated MAPKs also results in embryo arrest (Widmann et al., 1999). In addition, several H_2O_2-induced MAPK cascades regulate cell cycle progression and oxidative stress can block cell cycle progression in yeast, mammals, and plants (Kovtun et al., 2000). Furthermore, by transient expression analyses in maize and Arabidopsis protoplasts it was shown that constitutively active ANP1, ANP2, and ANP3 (Δ-ANPs) initiate a MAPK cascade that represses activity of two promoter responsive to auxin, GH3 and ER7. These results suggest that ANP1 antagonizes auxin-regulated growth pathways as a stress-protective mechanism (Kovtun et al., 2000).

I.2.3 ANP1 is not involved in flg22-triggered activation of MPKs in protoplasts

In a work published in 2002, four Arabidopsis MAPKKKs (CTR1, EDR1, MEKK1 and ANP1) from three different subgroups, were expressed in leaf protoplasts to determine whether any of them played a role in the flg22-triggered signaling pathway (Asai et al.,

2002). Constitutively active derivatives of these four MAPKKKs were constructed by deleting the putative regulatory domain. As mentioned before, MKK5 and MKK4 were identified as MAPKKs involved in MPK3 and MPK6 activation upon flg22 treatment. Then, which MAPKKK was responsible of the activation of MPKK5 was investigated by transiently expressing their constitutively active forms. It was found that MKK5 is specifically activated only by constitutively active MEKK1 (ΔMEKK1). Constitutively active ANP1 (ΔANP1) was found to not be involved in the flagellin transduction pathway (Kovtun et al., 1998).

I.3 THE PLANT SECRETORY SYSTEM

The secretory pathway of eukaryotic cells is a major site for the biosynthesis, folding, assembly, and modification of numerous soluble and membrane proteins as well as for the synthesis and transport of lipids, polysaccharides, and glycoproteins. It consists of the nuclear envelope (NE) and endoplasmic reticulum (ER), the Golgi apparatus, various post-Golgi intermediate compartments, the vacuoles and the small vesicular transport carriers that shuttle between these compartments (Bonifacino and Glick, 2004) (Figure 6). This pathway mediates the proper delivery and sorting of proteins to a variety of subcellular compartments. Proteins targeted to the various compartments start their journey after translocation to the ER, in a signal sequence-mediated process, and are subsequently transported to the Golgi apparatus. Additional sequences are required for targeting proteins to intermediate compartments on route to either vacuoles or the plasma membrane. The direction of transport is generally termed as anterograde transport and Golgi apparatus play a pivotal role. Moreover this process is not unidirectional as there exist a retrograde transport as well, where the plasma membrane is the starting membrane internalizing proteins and associated ligands to intracellular compartments through endocytosis or phagocytosis (Conner and Schmid, 2003; Gruenberg and van der Goot, 2006). Retrograde traffic will ultimately reach either the lytic organelles or the ER (Pelham et al., 1992), but by analogy to the early biosynthetic pathway, a recycling route also exists that returns essential components rapidly back to the plasma

membrane (Maxfield and McGraw, 2004). In most cases some pathogens, such as viruses, bacteria and protozoa take advantage of the route to the ER to enter the cytosol and often manipulate trafficking machinery of the host cell to satisfy their own purpose (Gruenberg and van der Goot, 2006).

An important feature of the plant secretory pathway is that, in addition to its role in protein sorting and protein modification, the Golgi apparatus plays a central role in the biosynthesis of cell wall polysaccharides (Perrin et al., 2001). The cell wall is a rigid but continuously remodelled structure as well and requires organized delivery of *de novo* synthesized components over the entire plasma membrane surface. Perhaps for this reason, the plant Golgi apparatus is distributed as individual stacks continuously migrating over the tubular cortical ER network (Boevink et al., 1998)and in close association with the so-called ER export sites (ERES) (daSilva et al., 2004).

Recent findings highlighted that the trans Golgi network (TGN) is a separate organelle in plants (Foresti and Denecke, 2008). The earliest characterized markers for the plant TGN are the SNAREs SYP61 and SYP41, and in protoplasts, these markers label punctate structures that are often physically separated from the Golgi bodies (Uemura et al., 2004). SYP61 labels organelles that exhibit a more variable size than Golgi bodies and can either be overlapping or be closely associated or found several microns separated from the nearest Golgi stack in the apical tobacco leaf epidermis cortex (Foresti and Denecke, 2008).

Plant cells also contain functionally distinct vacuoles that are supported by completely distinct trafficking routes and the storage vacuoles have unique functions in seeds and other tissues and are used for the accumulation of proteins, polysaccharides and lipids for a variety of applications (Robinson et al., 2005; Vitale and Hinz, 2005).

All of these organelles interact each other by small membrane transport vescicles which bud from a donor compartment using a complex of coat proteins system deforming the local membrane until a vesicle is freed by scission. Then these vesicles travel through the cytosol by association with cytoskeletal motors to reach their target compartment to deliver the cargo, helped by docking and tethering factors as well as members of the SNARE family protein. SNARE proteins operating as both target-specificity and membrane-fusion determinants in vesicle trafficking (Bassham et al., 2008).

As for mammals, plant cells contain the three major types of vesicles: COPI, COPII, and clathrin coated vesicles (CCV).

I.3.1 Vesicular trafficking

COPII-coat

Secretory organelles are finely interconnected through an extensive exchange of membranes and lumenal contents, which enables steady-state maintenance of the functional and morphological identity of each organelle within the pathway. Proteins are synthesized and modified in the ER; those that attain proper conformation leave the ER via COPII carriers to reach the Golgi for

further modification and sorting to the extracellular space, or storage and lytic organelles (Vitale and Denecke, 1999; Foresti and Denecke, 2008). In plants, proteins can also be sorted from the Golgi to the chloroplasts (Villarejo et al., 2005).

COPII assembly occurs at the ER. In vesicle formation at the donor compartments, GTPases Sar1 (secretion-associated, Ras- related protein 1) play roles in recruiting coat proteins to membranes (Stagg et al., 2007; Spang, 2008). The *Arabidopsis* genome encodes 3 Sar1 isoforms (Vernoud et al., 2003). Sec12, an ER membrane-associated guanine nucleotide exchange factor activates the cytosolic GTPase Sar1 (D'Enfert et al., 1991; Barlowe et al., 1994). This step is followed by the association of Sar1 to the ER membrane and by the recruitment of the COPII coat that is composed of the Sec23-24 and Sec13-31 heterodimer complexes (Barlowe et al., 1994; Miller and Barlowe, 2010; Barlowe, 2010)(Figure 7). Sar1 and Sec23-24 form a cargo recruitment complex that discriminates between transported and ER resident proteins (Miller et al., 2002; Mossessova et al., 2003; Miller et al., 2003; Tabata et al., 2009). Recently it has been suggested that the ER export of certain vacuolar sorting receptors might not occur via COPII transport machinery (Niemes et al., 2010).

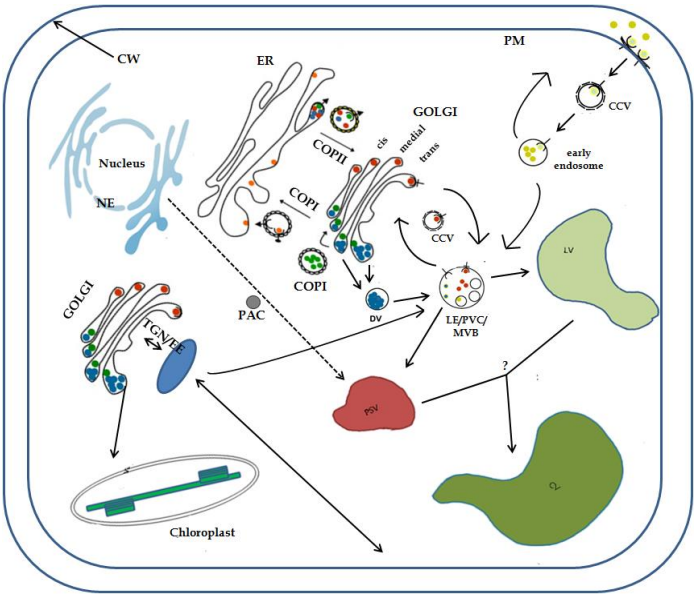

Figure 6. Simplified diagram of the plant secretory pathway illustrating the different route that proteins take to reach their destinations once they leave the ER.
Upon synthesis, most of the secretory proteins leave the ER and move to the Golgi. Proteins leaving the Golgi have different destinatios: ER (retrieval), vacuoles, plasma membrane (PM) and chloroplasts. Transport to the vacuole may take three different routes: directly from the ER via PAC vesicles; via a Golgi mediated dense vesicles route (DV) or a post-Golgi clathrin route (CCV) via TGN/early endosomal complex and prevacuolar compartment (PVC). IT represents one of the steps necessary for proteins to reach the vacuole as well. Protein transport to the PM may involve a recycling rndosome. The endocytotic route from the PM to the Golgi and mechanisms of protein transport to chloroplasts are yet to be defined. LV, lytic vacuole; PSV protein storage vacuole; CV, central vacuole; CW, cel wall; PM, plasma membrane; CCV, clathrin coated vesicles. Adapted from Paul et al. (2007) and Brandizzi not published.

In plants, the subcellular distribution of the ER export sites (ERES) has long been a matter of debate, but it seems to have finally been settled (Hwang and Robinson, 2009), at least for highly vacuolated cells. Several independent findings raise the possibility that different

plant cell types use diverse ERES–Golgi spatial organization to accomplish ER export.

The possibility that the ERES–Golgi organization differs among tissues has examples in non-plant systems. However, what is certain is that, at least in leaf epidermal cells, Golgi stacks and ER export sites (ERES) move as a unit (daSilva et al., 2004) and that Golgi stacks are tightly tethered to the ER. It has been shown that increased synthesis of membrane cargo destined to the plant Golgi indices a signal-mediated recruitment to ERES of a tobacco Sar1 isoform (daSilva et al., 2004) and sec24 (Hanton et al., 2007).

The GTPase Sar1 or COPII components can be used to visualize ERES (daSilva et al., 2004; Hanton et al., 2007).

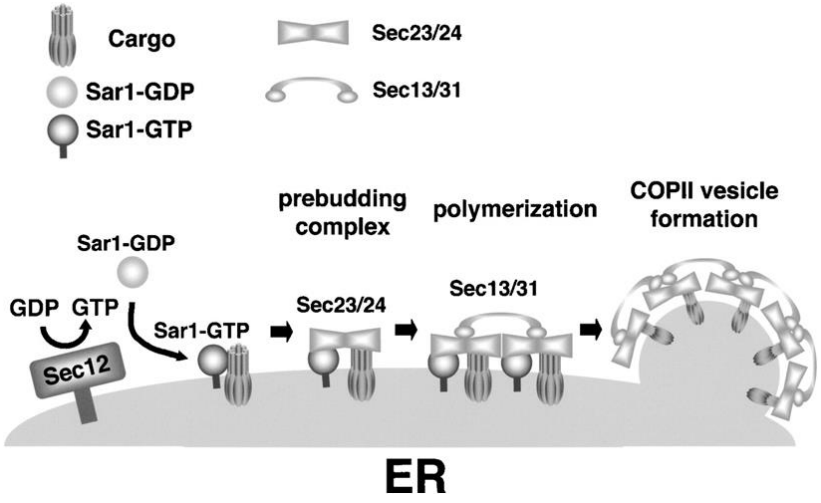

Figure 7. Vesicle formation at the transitional ER is accomplished by the COP-II coat system.

A coat-GTPase cooperates with a cargo-selective coat subunit to collect cargo molecules at the bud site, next a "cage" subunit is recruited from the cytosol to physically deform the lipid bilayer into a vesicle.

COP-I coat

Retrograde vescicles are also associated with Golgi trafficking and depends on COPI. This complex remains unclear although is responsible for retrograde traffic, either within the Golgi apparatus or between the Golgi and the ER. The COPI coat assembly is driven by a GTPase ADP ribosylation factor (ARF). The Arabidopsis genome encodes 12 ARF isoforms and of the 12 ARF isoforms, ARF1 is targeted to the Golgi and post-Golgi structures whereas ARFB localizes to PM. Their operating is regulated by two proteins: a guanine nucleotide exchange factor (GEF), and a GTPase-activating protein (GAP).

Plant cells contain multiple ARF GAPs (Vernoud et al., 2003) but relatively little is known about them.

Among the ARF-GEF, ARF1 is thought to control retrograde Golgi-derived COPI transport, which is indirectly required to maintain effective ER-derived anterograde COPII transport (Pimpl et al., 2003; Langhans et al., 2008). Like mammalian cells, plant species contain ARF-GEFs involved in Golgi-to-ER recycling that are sensitive to Brefeldin A drug (BFA), which can be detected by the rapid redistribution of Golgi membranes to the ER (Ritzenthaler et al., 2002).

COPI consists of two subunits that are F-COP and B-COP, which together constitute the coatomer (Figure 8). F-COP has four proteins (β-COP, γ-COP, δ-COP, and ζ-COP) and interacts with motifs on the cytoplasmic domain of receptor or other "cargo" proteins. B-COP, with three proteins (α-COP, β'-COP, and ε-COP) might be considered analogous to clathrin triskelions and constitutes the outer

cage of the vesicle. Plants have multiple genes encoding for COPI proteins and the multiplicity of COPI isoforms might suggest the existence of different classes of COPI coated vesicles. Indeed, an electron tomographic analysis of Golgi stacks in Arabidopsis, has revealed two differently sized COPI-vesicle populations: COPIa derived from cis-cisternae, and COPIb from medial and trans-cisternae (Donohoe et al., 2007).

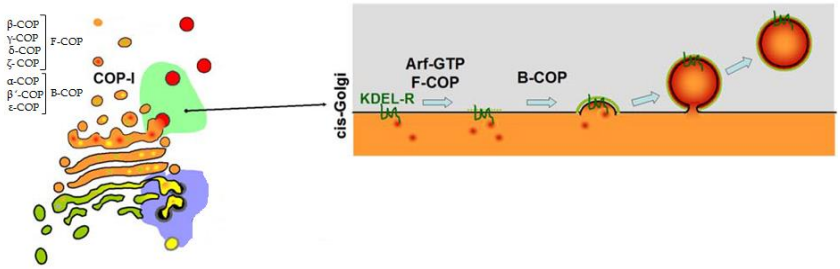

Figure 8. At the cis-Golgi, vesicle formation is accomplished by the COP-I coat system. Recovery of ER-resident proteins is accomplished by a cargo receptor called the KDEL-Receptor (KDEL-R, encoded by ERD2) which is a membrane protein that binds to ER-retrieval signals (KDEL-COOH) on the lumenal side, and recruits coat components on the cytosolic side. Adapted from Bassham et al. (2008).

Clathrin coated vesicles (CCVs)

The clathrin coats were the first proteinaceous vesicle coats to be observed and structurally characterised (Kirchhausen, 2000). They are found on two major compartments in most organisms, the TGN and the PM, and are involved in sorting cargo into various endosomes from both organelles. Clathrin-coated pits are also essential for signal transduction pathways, and for defining distinct membrane patches both at the PM and the TGN. The basic structural unit of the clathrin coat is the triskelion made of two protein chains

(heavy, CHC and light, CLC) (Fotin et al., 2004). Clathrin triskelions are the cage subunit for CCVs, and they require a peripheral and intrinsic membrane factors on the donor membrane, cargo-selective subunit , which is typically a member of the adaptor protein family (APs). Clathrin adaptors are recruited from the cytoplasm by an activated small GTP-binding protein from the ARF family (Stamnes and Rothman, 1993). The AP-complexes were the first clathrin-coordinating complex described, and come in four different types (reviewed in (Boehm and Bonifacino, 2001). Like in mammals, structural orthologues for each component of the four AP complexes (AP-1, to -4) have been identified in the Arabidopsis genome (Boehm and Bonifacino, 2001) (Figure 9).

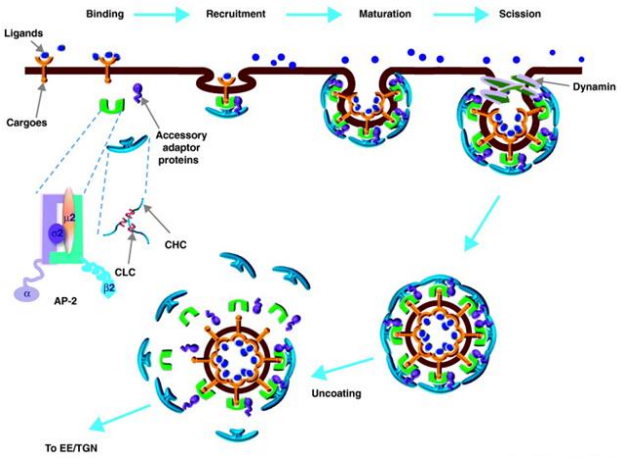

Figure 9. A representative model for CCV formation in plants.
Cargoes that need to be internalized from the PM are packaged by the co-operative assembly of the coat proteins that include clathrin, AP2-complex that consists of α, β2, μ2 and σ2 subunits, and associated accessory adaptor proteins recruited to the membrane. The membrane invaginates as more cargo and adaptor proteins are recruited and clathrin triskelia polymerize to form the cage. Dynamin assembles at the neck of the bud for scission of the CCV from the PM. Once a CCV pinches off, the coat falls off and the uncoated vesicle fuses with EEs/TGN for downstream processing of the cargo. Adapted from Chen et al. (2011).

Each AP-complex is made of 4 subunits: two large subunits (one of α, γ, δ, or ε and one of β1- β4; these subunits are distinct from the similarly named COP-I components), one medium subunit (μ1- μ4), and one small subunit (σ1- σ4). The AP-complexes recognize specific peptide motifs in the cytoplasmic tails of cargo proteins. These motifs fall into two classes, tyrosine motifs and di-leucine motifs (Boehm and Bonifacino, 2001; Dacks et al., 2008). These motifs are recognized mainly by either the μ or the β subunit of the complexes, though other subunits may also contribute to binding.

I.3.2 The secretory pathway in plant immunity

Vesicle trafficking plays a crucial role in PAMP perception and responses to pathogen attack (Frei dit and Robatzek, 2009). One of the first reactions observed in pathogen-attacked cells is the reorganization and polarization of the cytoskeleton to the site of attack (Schmelzer, 2002; Hückelhoven, 2007b), where aggregation of peroxisomes, endoplasmic reticulum and Golgi bodies supports rapid transport of antimicrobial compounds, proteins and cell wall material to the plant-pathogen interface (Takemoto et al., 2003; Lipka et al., 2005; Koh et al., 2005; Eichmann and Huckelhoven, 2008). Subcellular polarization processes are not limited to organelles and vesicles. Attacked plant cells seem to form detergent-resistant membranes (DRMs) or lipid rafts in the PM (Lipka et al., 2005; Bhat et al., 2005). Studies on DRMs revealed an enrichment of sphingolipids and sterols and an accumulation of proteins associated with signalling and response to biotic and abiotic stresses, cell wall

metabolism and cellular trafficking (Mongrand et al., 2004; Morel et al., 2006; Lefebvre et al., 2007).

Many of the processes that determine success or failure of pathogens take place at the cell surface and hence the apoplast constitutes a major battlefield of plant pathogen interactions. Correct localization of receptors at the cell surface is provided by the ER and the TGN, also involved in secretion into the apoplast. ER localization of PRRs is primarily for folding into their final configuration. ER chaperones are likely candidates for PRR folding. They include members of the heat shock protein Hsp90 family, the Hsp70 family member BiP and the ER-j proteins of the Hsp40 family. Indeed several genetic and biochemical studies have demonstrated that PRRs are clients of the ER quality control (ERQC) machinery (Beck et al., 2012). N-glycosylation is an important post-translational modification as well and is performed by the successive action of the oligosaccharyltransferase (OST) complex, the glucosidases I/II (GI/GII) and the UDP-glucose glycoprotein glucosyltransferase (UGGT) involving the ER chaperones calreticulin (CRT) and calnexin (CNX). ER-assisted glycosylation has been shown for Xa21, EFR, and FLS2 LRR-RLKs as well as for the LysM-RLK NFP (Nekrasov et al., 2009; Saijo et al., 2009; Lu et al., 2009; Li et al., 2009a; Haweker et al., 2010; Park et al., 2010; Lefebvre et al., 2012). However, an incomplete glycosylation profile does not always impede the function of receptors (Lefebvre et al., 2012).

PRRs have also been observed in other components of the secretory pathway. For example transient expression of OsCERK1- GFP in rice protoplasts revealed not only localization to the ER and the plasma

membrane but also to trafficking vesicles, probably resembling components of the Golgi-mediated secretory pathway (Chen et al., 2010). Alternatively, PRRs could be pass through the Golgi apparatus from the ER for subsequent modifications, as shown for EFR (Haweker et al., 2010) or FLS2. In particular a recent study has identified two reticulon-like group B proteins RTNLB1 and RTNLB2 that both associate with FLS2 (Lee et al., 2011b). Reticulons are ER resident proteins that have been associated with ER tubule formation and vesicle trafficking (Sparkes et al., 2010). In leaf protoplasts, a WAK1-GFP fusion protein is found in compartments labelled by Golgi markers and containing pectin. Its migration to the cell surface is far slower than that of BAK1-GFP and, interestingly, isoxaben, an inhibitor cellulose synthesis, delays the movement of WAK1-GFP, but not that of BAK1-GFP to the surface (Kohorn et al., 2006). Golgi-retention signals and mechanisms are therefore likely to play an important role also in the movement cell wall proteins.

The SNARE proteins drive the fusion of vesicles with the target membrane (Figure 10). Focal secretion of vesicle cargo to the site of fungal attack in *Arabidopsis* is likely mediated by the formation of a ternary SNARE complex of PEN1/AtSYP121, AtSNAP33 and the recently identified vesicle-associated membrane proteins (VAMP) AtVAMP721 and AtVAMP722 (Collins et al., 2003; Lipka et al., 2008; Kwon et al., 2008b). AtPEN1 (penetration mutant1 = AtSYP121) encodes the plasma membrane-resident syntaxin, a component of the vesicle-targeting machinery that plays a pivotal role in driving intracellular vesicle fusion (Jahn and Scheller, 2006). The role of vesicle transport and fusion proteins such as SNAREs in defence is

further highlighted by the rapid phosphorylation of PEN1/AtSYP121 and AtSYP122 after treatment with flg22 and of NtSYP121 after recognition of the effector Avr9; the rapid phosphorylation might induce secretion (Heese et al., 2005; Nuhse et al., 2007; Benschop et al., 2007).

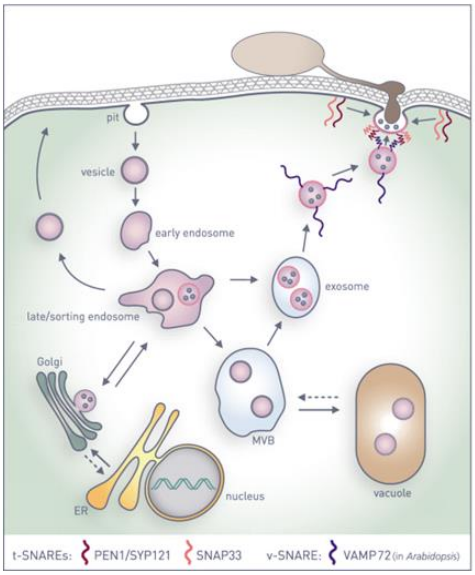

Figure 10. Model of SNARE-mediated vesicle trafficking in basal immunity.
In response to fungal attack, focal accumulation of the syntaxin PEN1/AtSYP121 and the SNAP-25-like protein AtSNAP33 is triggered. They form a binary t-SNARE complex marking the target membrane. Vesicles labelled with cognate v-SNAREs of the AtVAMP72 subfamily are trafficked to the target membranewhere they form a ternary complex and facilitate vesicle fusion . Thereby compounds exhibiting antimicrobial activities are delivered and secreted to combat fungal ingress. Exocytosis is in balance with endocytic processes in order to ensure cell integrity. Adapetd from Robatzek et al. (2007)

In Arabidopsis vegetative tissues, a multitude of SNARE genes is expressed, encoding four plasma membrane-resident syntaxins, two SNAPs, and five VAMPs (Uemura et al., 2004; Lipka et al., 2007). Conceptually, this provides ample opportunity for the formation of

distinct ternary SNARE complexes and thereby specific secretory pathways acting in diverse plant biological processes. The SNARE complex seems to participate also in important developmental processes because double mutants of *AtVAMP721* and *AtVAMP722* or of *AtSYP121* and *AtSYP122* show strong pleiotrophic effects such as necrotic leaf lesions and dwarfism (Assaad et al., 2004; Zhang et al., 2007; Kwon et al., 2008b).

The occurrence of MVBs and paramural bodies at cell wall appositions was observed in barley cells defending penetration by *B. graminis* ((An et al., 2006). Paramural bodies are multivesicular compartments situated between the cell wall and the PM. They may be the result of MVB fusion to the PM and subsequent secretion of internal vesicles and other compounds (An et al., 2006). Because MVBs are considered as endosome-derived prevacuolar compartments, this might point to an alternative secretory pathway in plant cells under attack from microbial pathogens (Huckelhoven, 2007).

Thus inward and outward host vesicle traffic is rapidly engaged and redirected in response to microbial attack. To date, endocytic localization of ligand-activated PAMP receptors has been demonstrated only for FLS2 and the tomato xylanase receptor LeEIX2 (Frei dit and Robatzek, 2009). (Robatzek et al., 2006) carried out a study on the dynamic changes at the subcellular level of FLS2 fused to the green fluorescent protein (GFP) and FLS2 was found to enter an endocytic pathway inhibited by MG132 (proteasome inhibitor) and chemicals interfering with endocytic trafficking.

Upon flg22 addition, membrane resident FLS2-GFP rapidly accumulated in intracellular vesicles that are likely trafficked for degradation. (Figure 11). This is reminiscent of ligand-induced receptor endocytosis in animals where dynamin was shown to interact with phospholipids and a number of proteins associated with the cytoskeleton (Konopka et al., 2006). Dynamin encodes a large GTPase involved in 'pinching off' coated pits to form clathrin-coated vesicles (CCVs).

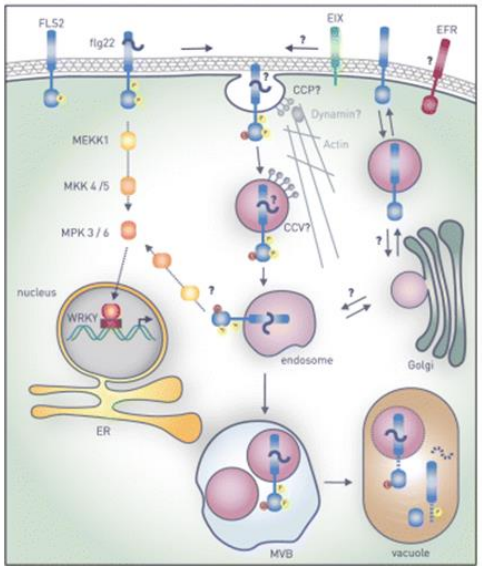

Figure 11. Model of flg22-mediated internalization of FLS2.
Upon flg22 binding to cell membrane resident FLS2, a MAP kinase cascade is activated that transmits the signal into the nucleus involving WRKY transcription factors Concomitantly, FLS2 is internalized into endosomal compartments, potentially comprising clathrin-coated pits (CCPs) and CCVs, involving the plant's cytoskeleton (actin and dynamin). FLS2 accumulates via endosomes to MVBs and is targeted to vacuoles for lysosomal degradation. Endocytosis of FLS2 likely requires FLS2 phosphorylation (P), and ubiquitination (ub). There is evidence for cell membrane FLS2 recycling in its flg22-unbound stage. Adapted from Robatzek et al. (2007).

The Arabidopsis dynamin-like protein 1 was implicated in plasma membrane vesiculation (Hong et al., 2003) but a role for dynamin-like proteins in receptor-mediated endocytosis has not yet been demonstrated in plants. Moreover FLS2 is phosphorylated after flg22 application and its phosphorylation appears to be a key to endocytosis. In fact FLS2 contains a PEST-like motif in its kinase domain which implicates ubiquitination, and more specifically, monoubiquitination as an endocytotic signal (Shih et al., 2000). Mutation of the PEST-like motif was found to compromise FLS2 endocytosis and downstream signalling but not flg22-triggered ROS (Robatzek et al., 2006). Taken together, it could be supposed that FLS2-mediated flg22 signalling might be initiated at the plasma membrane, but continue from intracellular compartments. The ubiquitination may also subject FLS2 to protein degradation via multivesicular bodies (MVBs) and the endosomal sorting complex required for transport (Robatzek et al., 2006).

The cytoplasmic tail of tomato xylanase receptor LeIX2 contains YxxØ motif as an endocytotic signal as well, and also the EFR receptor contains the YxxØ motif within its cytoplasmic juxtamembrane region, suggesting endocytic processes may be involved in EF-Tu signalling (Zipfel et al., 2006) and the involvement of CCVs (Baluska et al., 2005).

Upon ligand-dependent endocytosis, receptors may transit through the early endosome (EE) and subsequently in the late endosome (LE) and end up in the vacuole for degradation, or may recycle to the plasma membrane through the recycling endosomes. The sorting events (degradation or recycling) influence the cell response to the

stimulus. Recently, PGIP has been also shown to undergo tyrphostin A-23-sensitive internalization in endosomes followed by targeting to the vacuole, suggesting an involvement of CCVs. PGIP internalization may be related to pectin recycling (Sup et al., 2008).

Rab GTPases also play an important role in secretion and endocytosis (Yoshioka et al., 2009). However, uncertainties remain about the different trafficking pathways and there is still little or no insight into the functions of several major subclasses within the SNARE and Rab GTPase family.

Intracellular trafficking of vesicles is also a potent target for pathogen-produced effector proteins and compounds. For example brefeldin A, a compound from the fungus *Alternaria carthami*, promotes plant disease through interference in the formation of Golgi-derived vesicles (Driouich et al., 1997) and it is possible that one fuction of brefeldin A is to suppress plant immune response. Another compound is the conserved *P.syringae* effector HopM1 that interferes with the plant secretion system by association with the plant endomembrane system and degrading an ARF-GEF, probably by engagement of the plant ubiquitination-dependent proteasome machinery (Nomura et al., 2006). Thus, both fungal brefeldin A and bacterial HopM1 intercept the immune response secretion machinery by inhibiting vesicle formation rather than the later stage of vesicle fusion with the plasma membrane via ternary SNARE complex formation.

I.4 FLUORESCENT PROTEIN-BASED TECHNOLOGIES

All plant-microbe interactions are initiated at the level of the cell and these cellular interactions may be complex and crucial for both susceptibility and resistance to microbial growth. However, biochemical studies of tissue extracts do not provide high resolution of cellular responses in situations in which microbial-plant interactions are not synchronous or uniform within the plant; in such situations, therefore, the ability to visually detect interactions at a single cell level becomes particularly important.

Confocal laser scanning and video microscopy, computerized image processing, and an ever-increasing array of fluorescent probes that can be applied to living cells, collectively have opened up new and exciting opportunities for directly imaging cellular components and activities. Furthermore fluorescent protein technology applied to live cell imaging of plant has aided immensely in providing subcellular markers for the study of the complex spatial and temporal relationships among cellular organelles and to understand the intricate relationships among thousands of proteins. In addition the increase ease to generate transgenic plants and cells is an important aspect because it is possible to visualize fluorescent labeled cells components with a minimum of invasive manipulation.

The confocal laser scanning microscope (CLSM) eliminates out-of-focus blur while providing temporal resolution. This capability presents obvious advantages when organelles and proteins have to be visualized in living cells rather than in fixed sections.

Furthermore, the advent of confocal microscopes with spectral imaging capabilities has provided the possibility of viewing separate overlapping spectra of multiple fluorochromes. Another advantage of CLSM is the ability to minimize interference of innate plant autofluorescence from such sources as cell walls, vacuolar contents, and chlorophylls.

Spinning-disc confocal microscope technology has improved imaging time resolution in comparison to CLSM, making possible the imaging of live cells in realtime with minimal photo-toxicity. Conventional confocal microscopy relies on laser scanning over a specimen driven by the mechanical movement of mirrors, whereas spinning-disc confocal microscopy is based on the utilization of a spinning disc with multiple pinholes. When coupled to an electron-multiplying CCD digital camera, scanning rates as fast as 1,000 frames/s can be achieved (Nakano, 2002). Not only does this technology facilitate the imaging of protein localization, it also enables the direct estimation of protein velocity, trajectory, distribution, and activity. Recent applications of this technology provided dynamic imaging of a cellulose synthase subunit (AtCesA6) in the plasma membrane and intracellular organelles as a citrine-YFP fusion (Paredez et al., 2006; Persson et al., 2007).

Cell biology has undergone a renaissance since the cloning of GFP from the jellyfish *Aequorea victoria* (Prasher et al., 1992). Fluorescent proteins are widely accepted tools for studying protein localization, interactions, and dynamics. Although the first to be adopted and adapted as protein reporters in plant endomembranes were the blue-shifted GFP variants, mGFP4 and mGFP5 (Haseloff et al., 1997;

Siemering et al., 1996), numerous fluorescent proteins have since been developed and cover nearly the entire visible spectrum. The development of these fluorescent proteins has enabled to visualize multiple proteins simultaneously to gain information regarding localization, dynamics, and interactions (Hanton and Brandizzi, 2006). Descendants of wild-type GFP include enhanced GFP, enhanced CFP (ECFP), and enhanced YFP (EYFP). ECFP and EYFP have also been further improved by modifications that have increased the brightness of these fluorochromes and reduced their ability to form dimers. Cerulean CFP, for instance, possesses improved brightness (e.g. quantum yield and extinction coefficient) and fluorescent lifetime (Rizzo et al., 2004). Citrine (Griesbeck et al., 2001) and Venus YFP (Nagai et al., 2002) display improved stability at lower pH ranges and increased folding at 37 °C. For the red side of the spectrum, DsRed was cloned from the coral Discosoma and added to the fluorescent protein repertoire (Matz et al., 1999). However mutational studies using DsRed have produced the monomeric red fluorescent protein (mRFP1; (Campbell et al., 2002). Currently, there are about 10 mRFP1 variants differing in spectral properties, which include mCherry (Shaner et al., 2004) and mPlum (Wang et al., 2004; Wang and Tsien, 2006).

Another advance in fluorescent protein technology has been the development of ‘‘photoactivatable’’ fusion proteins. One of the first to be developed was a photoactivatable GFP (PA-GFP; (Patterson and Lippincott-Schwartz, 2002).

Recent developments in bioimaging for protein interactions include fluorescence resonance energy transfer (FRET) and bimolecular

fluorescence complementation (BiFC) or split-YFP. FRET is an elegant and powerful technique for testing protein-protein interaction events in living cells. The basic principle of FRET is that energy from an excited donor molecule is transferred to an acceptor fluorochrome when the donor fluorescence overlaps with the absorption spectrum of the acceptor. Such energy transfer can occur when donor and acceptor molecules are in close proximity and therefore are most likely interacting (Jares-Erijman and Jovin, 2003). Generation of a FRET signal depends not only on the overlap of the emission spectrum of the donor fluorophore and the excitation spectrum of the acceptor fluorophore but also on the orientation of the fluorophores toward each other in a distance range of 2 to 10 nm (Gadella, Jr. et al., 1999). Energy transfer from the donor to the acceptor leads to a reduction in the donor's fluorescence intensity and a decreased lifetime in the excited state. The process will lead to an increase in the fluorescence intensity emitted from the acceptor. The fluorescent protein pair most commonly used is CFP and YFP. However as the mutations that generate differences in the spectral properties of ECFP and EYFP fluorescent proteins are usually limited in number, there is the possibility that the CFP and YFP may form heterodimers. Therefore, in experimental setups that adopt fusions of CFP and YFP to proteins to be tested for interactions, a FRET signal may be generated by the multimerization of the fluorescent proteins rather than to specific interactions of the proteins that these are fused to. To overcome this possibility, monomeric fluorescent protein variants are more efficient for FRET applications. Lack of dimerization properties increases the confidence that a FRET signal

is the result of a genuine interaction between proteins rather than of dimerization of fluorescent proteins.

Protein-protein interactions can be analyze by BiFC as well where the N-terminus half of YFP is fused to a protein and the C terminus of YFP to a putative interacting partner. In theory, detection of the YFP signal in cells coexpressing the two fusions means that the two protein fused to the half YFP, as the YFP signal is detectable when the N- and C-terminal halves come in close proximity to form an intact YFP molecule.

GFP and its spectral variants have also been used in fluorescence recovery after photobleaching (FRAP) analyses to study protein traffic in plant endomembranes. FRAP is a powerful technique that enables the estimation of protein mobility within live cells. Exposing a subcellular population of fluorescently tagged fusion proteins to high-intensity laser light for a period of time causes irreversible fluorophore photobleaching within a defined area. Over time, if surrounding nonphotobleached fusion proteins migrate into the photo-bleached region, a fluorescence recovery in the bleached area will occur. Measurement of the fluorescence recovery over time allows direct estimation of protein mobility.

AIM OF THE THESIS

The capacity of plants to survive adverse conditions and reach reproductive maturity critically depends on their ability to continuously adapt to changes in the environment. Therefore, plants have evolved an array of intricate regulatory mechanisms that involve the generation of signaling molecules mediating the activation of adaptive responses. In particular, the activation of pathogen-specific defense mechanisms upon microbial infection and the acquisition of architectural and physiological adjustments to environmental changes permit survival, development, and reproduction of plants.

Secretion of proteins and other molecules is the primary means by which a cell interacts with its surroundings. In response to pathogen attack, the expression of the protein secretory pathway genes is upregulated to favor synthesis of protein necessary for resistance (Jelitto-Van Dooren et al., 1999; Wang et al., 2005). In fact plant cells, because of their sessile lifestyle, are uniquely reliant on the secretory pathway to respond to changes in their environments, either abiotic or biotic. Secretion is required not only for the delivery of antimicrobial molecules, but also for the biogenesis of cell surface sensors to detect microbes. Thus the secretory pathway plays an important role in defense. Compared to yeast and mammals, the secretory pathway of plants has unique features, which include the presence of protein storage vacuoles, mobile polarized Golgi stacks as well as a distinctive organization of the endosomal compartments (Hanton et al., 2007; Rojo and Denecke, 2008). The organelles involved in the pathway accomplish their functional tasks and communicate with other secretory organelles while maintaining a

morphological and functional identity. How this is achieved is a fascinating question that is largely unanswered, especially in the plant system. Interestingly, secretory organelles can remodel their structure over time and yet maintain their functional and morphological independence from other organelles in the same pathway and the Golgi apparatus plays a pivotal role in this complex machinery.

Also a MAP kinase cascades play an important role in innate immunity. A MAP kinase cascade is composed of three components: a MAP kinase (MAPK), a MAP kinase kinase (MAPKK), and a MAP kinase kinase kinase (MAPKKK). When plasma membrane receptors are stimulated by an extracellular ligand MAPKKKs are activated. Activation of the MAPKKK causes a phosphorylation cascade that culminates in the activation of the MAP kinase, which then phosphorylates various downstream targets, for example transcription factors (Asai et al., 2002). The gene family Arabidopsis NPK1-related Protein Kinase (ANPs), which includes ANP1, ANP2, and ANP3, constitutes a distinct branch of the MAPKKK phylogenetic tree. Little is known about the Arabidopsis ANPs. Kovtun et al. (2000) proposed their involvement in H_2O_2 signal transduction, one of the early defense responses induced by the perception of elicitors. Therefore it has been recently shown that the ANPs family plays an important role in immunity (unpublished data of G. De Lorenzo laboratory).

The aims of my thesis work were:

1. To characterize a protein involved in Golgi-mediated trafficking;
2. To study the sub-cellular localization and elicitor-regulated dynamics of the Arabidopsis NPK1-related proteins (ANPs).

II. MATERIALS AND METHODS

II.1 CHARACTERIZATION OF A PROTEIN INVOLVED IN GOLGI-MEDIATED TRAFFICKING

II.1.1 Fluorescent proteins and molecular cloning

The fluorescent proteins used in this study were based on fusions with mGFP5 (Haseloff et al., 1997), EYFP (Clontech, California, http:// www.clontech.com), and monomeric RFP (Campbell et al., 2002). Wild-type and mutant *GOLD36* cDNA were amplified from cDNA of wild-type Col-0 and *gold36* plants, respectively. The cDNA was subcloned in the binary vector pFGC5941 and expressed under the control of the CaMV 35S promoter. mRFP fusions of wild-type and mutant *gold36* were generated by overlapping PCR of cDNA sequences (i.e. *GOLD36* cDNAs and mRFP) followed by subcloning in pFGC5941. Constructs were confirmed by sequencing.

II.1.2 RNA extraction and PCR analysis

RNA extraction was performed using the RNeasy Plant Mini Kit (Qiagen, http://www.qiagen.com). Reverse transcription experiments
were performed using the Superscript III First Strand Synthesis Kit (Invitrogen, http://www.invitrogen.com). PCR experiments were performed in standard conditions and were carried out using 0.2 mM dNTPs, 0.2 lM primers, and 1 unit of Taq polymerase (Promega, http://www.promega.com).

II.1.3 Plant materials and growth conditions

I used wild-type plants of *Arabidopsis thaliana* (ecotypes Columbia and Landsberg erecta), a transgenic Arabidopsis line (ecotype Col-0) expressing ST-GFP. I also used the Arabidopsis mutant *gold36–1* from the ABRC consortium. Plants used in this work were all stable transformants obtained with a floral dip method (Clough and Bent, 1998), and subsequent selection on MS medium supplemented with Gamborg's B5 vitamins, 1% (w/v) sucrose, the appropriate antibiotics, and 0.8% (w/v) agar. Seeds were surface-sterilized and were grown at 21°C under 16 h light/8 h dark conditions. Cotyledons used in this work were harvested from 7-day-old seedlings. For antibiotic selection, seeds were stratified on selective medium (see above) for 5 days, then the selected seedlings were transferred to MS medium without antibiotics for 2 days prior to analysis. Selective antibiotics were glufosinate ammonium salt (BASTA; final concentration 20 μg/ml), kanamycin (100 μg/ml), or hygromycin (15 μg/ml).

II.1.4 Isolation of the *gold36* mutant and genetic analyses

M1 and M2 ST-GFP seeds were prepared as described earlier (Faso et al., 2009). Thirty seeds from each M2 line were grown for 7 days and analyzed using confocal microscopy for displacement of the ST-GFP marker. The *gold36* homozygous mutant was crossed with Landsberg erecta to generate a mapping population. The polymorphism between the two ecotypes was analyzed using a combination of

cleaved, amplified polymorphic sequence markers and simple sequence length polymorphism markers (Konieczny and Ausubel, 1993; Bell and Ecker, 1994). The rough map was performed on 57 individuals showing the aberrant phenotype. Identification of SNPs in the rough-mapped region was achieved as follows. Genomic DNA was submitted to the Michigan State University Research Technology Support Facility for sequencing using the Illumina Genome Analyzer II (GA II) (Bentley et al., 2008). DNA was prepared and sequenced using standard kits and protocols from Illumina Inc. The final library was sequenced in seven of the eight flow cell lanes; sequencing was performed for 50 cycles. Image analysis was performed on instrument using Real Time Analysis (RTA) v 1.4. Base calling, read passing, and error analysis were performed off instrument using the Illumina GA-Pipeline v1.4. A total of 154.8 million reads (7.74 Gbp as sequence) were generated. The default CHASTITY filter of the GA-Pipeline was used for determining passed filter (PF) reads; 114.6 million reads (74%, 5.73 Gbp) passed filtering. PF reads were aligned to the Arabidopsis thaliana genome sequence (TAIR8) using the short read alignment program Bowtie (Langmead et al., 2009)(v 0.10.0). Alignment parameters were adjusted to allow up to three mismatches in the seed (the first 28 bases). The Bowtie output was converted to MAQ map format using Bowtie-Maqconvert from the Bowtie distribution. MAQ (Li et al., 2008) (v 0.7.1) was used to assemble aligned reads into a consensus to identify putative SNPs. Raw SNPs were filtered with MAQ's SNP filter, increasing the minimum depth to call a SNP to five reads. As SNPs of interest should be homozygous, the variants were further

filtered to only those in which ≥80% of the overlapping reads supported the SNP call.

II.1.5 Confocal laser scanning microscopy

An inverted laser scanning confocal microscope (LSM510 META, Carl Zeiss, http://www.zeiss.com) was used for confocal analyses. For GFP5 and YFP imaging, settings were as described earlier (Brandizzi et al., 2002a; Hanton et al., 2007). Imaging of DiOC6-stained cells and of *gold36* cells labeled with propidium iodide or expressing mRFP constructs was carried out as described in (2009). FRAP analyses were conducted as described earlier (Brandizzi et al., 2002b). All confocal images were acquired with 1-lm pinhole settings. Post-acquisition analyses were performed with the Zeiss AIM software. PaintShop Pro was used for further image handling. Images reported in microscopy figures are representative of at least five independent experiments.

II.1.6 Fluorescent dyes and drug treatments

Cellular nucleic acids were stained by immersing cotyledons in a solution with propidium iodide (PI; Invitrogen; working solution: 1 μg/ml) in water for 15 min. Endomembranes were stained with the general endomembrane dye DiOC6 (working solution: 1.8 μM; Molecular Probes, http://www.invitrogen.com) in water for 30 min, as described earlier (Zheng et al., 2004). Wortmannin (working solution: 33 μM; Sigma, http://www.sigmaaldrich.com) was used on

intact tissue for 12 h. All stock solutions were kept at -20°C, and working solutions were prepared fresh just before use. For analysis and observation at the microscope, samples were mounted on a slide with the solution in which they were last treated.

II.2 SUB-CELLULAR LOCALIZATION AND ELICITOR- REGULATED DYNAMICS OF THE ARABIDOPSIS NPK1-RELATED PROTEINS (ANPs)

II.2.1 Fluorescent protein and molecular cloning

The fluorescent ANPs used in this study were obtained by fusions with eGFP by Multisite Gateway® Recombination Cloning Technology (Life Technologies). In particular ANP1 and ANP3 full-length cDNA clones were obtained from Riken BioResource Center, Experimental Plant Division (http://www.brc.riken.jp/lab/epd/). ANP2 full-length cDNA was generated by RT-PCR using RNeasy plant mini kit (Qiagen) for total RNA extraction from wild-type Col-0 and Superscript III (Life Technologies) for cDNA synthesis. Each cDNA was used as templates for cloning. Entry clones pEntry-ANP1, pEntry-ANP2 and pEntry-ANP3 were obtained by using pDONR221/Zeo vector (Life Technologies) in a BP clonase reaction. Subsequently multisite recombination was performed by using each entry vectors containing the sequences codifying ANPs, pEN-R2-F-L3, containing the sequence codifying eGFP and p2GW7,0, containing 35S promoter sequence. In this single multisite LR clonase reaction 35S::ANPx-eGFP constructs were generated and transferred in the destination binary vector pB7m34GW. Both entry and destination Gateway compatible vectors described before were obtained from Plant System Biology, a Ghent University research department (http://gateway.psb.ugent.be/) and described in (Karimi et al., 2002). Binary vectors containing 35S::ANPs-eGFP

constructs were amplified in *Escherichia coli* (One Shot® Mach1™ strain; Life Technologies) and used for *Agrobacterium tumefaciens* (strain GV3101) transformation

The sGFP was carried out as described previously for ANPs. The LR clonase reaction was performed by using pH7m24GW binary vector as a destination plasmid to form 35S::eGFP (sGFP). The same vector was used for cloning ANP2-eGFP and ANP3-eGFP cassettes to obtain 35S::ANPx-eGFP for rescuing *anp2 anp3* phenotype, as it confer resistance to hygromycin.

II.2.2 RNA Extraction and PCR analysis

RNA extraction was performed using the RNeasy plant mini kit (Qiagen, http://www.qiagen.com).

Reverse transcription experiments were performed using the Superscript III first-strand synthesis kit (Invitrogen). PCR experiments were performed in standard conditions and were carried out using 0.1 mM deoxynucleotide triphosphate (dNTPs), 0.1 µM primers, and 1 unit of Taq polymerase (Promega, http://www.promega.com).

II.2.3 Plant materials and growth conditions

Arabidopsis Col-0 plants were used for plant transformation using the floral dip method (Clough and Bent, 1998) and transformants were obtained on MS/2 medium 1% sucrose supplemented with

glufosinate ammonium salt (BASTA; final concentration 20 µg/mL) or Hygromicin (Hyg; 25 µg/mL) and 0.7% (w/v) agar.
Seedlings transient expression of organelle markers was performed as described in (2009b).
For confocal microscopy analyses, seeds were surfaced, sterilized, germinated and grown for 5 days in Petri dishes containing Murashige and Skoog agar plates supplemented with 1% Sucrose.
The *anp2anp3* double mutants (in the Ws background) were kindly provided by Patrick J. Krysan (Department of Horticulture, University of Wisconsin).

II.2.4 Spinning Disck an Confocal Laser Scanning Microscopy analysis

An inverted Spinning-disk confocal microscope (Model: CarvX ; manufacturer:CrEST-Italy) was used for localization analyses. Imaging was performed using CFI Planfluo 40x (1,4 NA) oil immersion objectives (NIKON) through 70 µm pinhole disk set at 6000rpm. The GFP and DCF-DA were excited using 473 nm wavelength laser light while Propidium Iodide (PI) were excited using 532 nm laser light, and were detected using a cooled charge-coupled device CCD camera (CoolSNAP HQ2, Photometrics, USA) through omega band-pass filters, respectively XF100-2 and XF101-2. The CCD camera, Z-motor and Confocal head were controlled with Metamorph software (Molecular Devices, USA).
Colocalization analyses were performed using an inverted laser scanning confocal microscope (LSM780 NLO; Carl Zeiss). Imaging of

ANPs-GFP, MT-rk, PT-rk and PI were performed using 488-nm excitation of an Argon ion laser, 25 mW for GFP and 543-nm He/Ne laser, 5mW for mCherry and PI; a 488/543/633 beam splitter was used for acquisition. Imaging was performed using 40x Zeiss plan-neofluar oil, 1.3 NA, DIC.
Images reported in microscopy figures are representative of at least five independent experiments.

II.2.5 Fluorescent Deys and elicitor treatments

Cellular nucleic acid were stained by immersing cotyledonds in solution with PI (Invitrogen; working solution 2µg/mL) in water for 15 min.
ROS detection was performed by using DCF-DA at a final concentration of 100 nM in water for 2 min.
OGs (100 µg/mL) and elf18 (100 µM) elicitation was carried out immerging cotyledons in a water solution performing a time course from 15 to 30 min.
All stock solutions were kept at -20˚C and working solutions were prepared fresh just before use. For analyses and observation at the microscope, samples were mounted on a slide with the solution in which they were last treated.

OGs with an average DP of 9 to 16 were prepared as described in Bellincampi et al.(2000). Matrix-assisted laser desorption/ionization time-of-flight MS was used to verify the DP of OG preparations. The

elf18 peptide was synthesized by Prof. Maria Eugenia Schininà ("Sapienza" Università di Roma).

III. RESULTS

III.1 CHARACTERIZATION OF A PROTEIN INVOLVED IN GOLGI-MEDIATED TRAFFICKING

To learn more about the elements involved in the early secretory pathway, I have used a confocal microscopy based approach to find ethyl methanesulfonate (EMS) mutants with obvious alteration of the distribution of a fluorescent marker destined to the Golgi apparatus (Boulaflous et al., 2008). Because the Golgi is a central organelle for protein traffic in the secretory pathway, defects in Golgi protein distribution in the mutants allow the identification of mutants with defects in Golgi morphology and/or defects in protein transport to and from the Golgi (Boulaflous et al., 2008). In this studie I describe the identification and characterization of a recessive EMS mutant showing partial distribution of the Golgi marker ST-GFP (Boevink et al., 1998) to the ER. The mutant, named *gold36* (for Golgi defects 36), had defects in both general ER protein export and ER organization. The mutation responsible for the phenotype was pinpointed through a combination of classical mapping procedures and deep sequencing of the mutant genome.

III.1.1 Identification of a mutant with altered distribution of the Golgi marker, ST-GFP

In a microscope-based screen of cotyledons of 1-week-old Arabidopsis seedlings for altered subcellular distribution of ST-GFP (Figure 1 A), a well-established trans-Golgi membrane marker

(Boevink et al., 1998), we isolated *gold36*, a mutant with an ST-GFP signal distributed to the Golgi and an underlying network (Figure 1B). The network defined unusual structures in epidermal cells (Figure 1B). Generally, in the mid to lower sections of each cell I found one large globular structure (≤10 µm) that contained Golgi stacks (Figure 1B, see star) and that was distinguishable from the nucleus (Figure 2), and also smaller circular structures at the cell's periphery (Figure 1B, empty arrow). Both types of structures were highly motile.

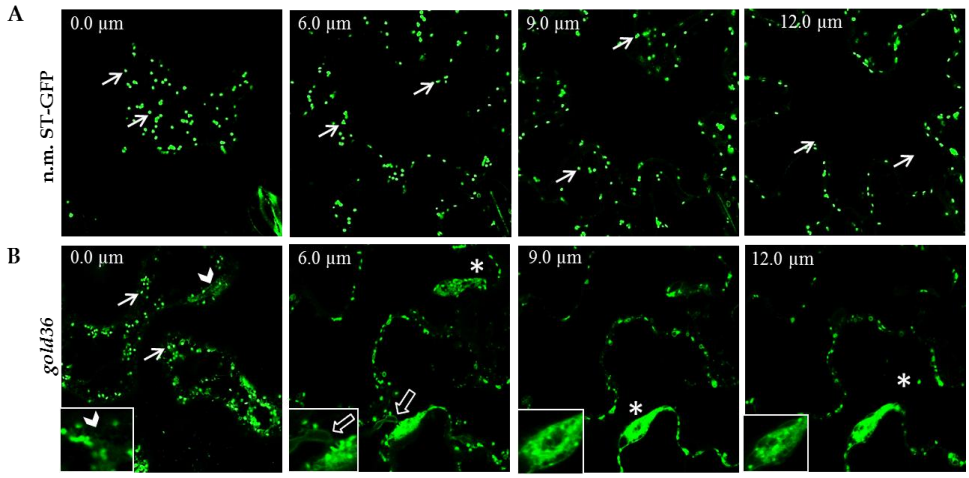

Figure 1. Figure 1. *gold36* shows clear defects in the distribution of the Golgi membrane marker, ST-GFP.

(A) Confocal optical sections (numbers at the left corner indicate depth of sections in microns) of cotyledons of non-mutagenized ST-GFP (n.m. ST-GFP, control) from the cell cortex (0.0 µm) to mid-section (12.0 µm) showing that the fluorescence of the marker is distributed at Golgi stacks (arrows). (B) In contrast to the control, the ST-GFP marker in the *gold36* mutant is partially distributed to Golgi
stacks (0.0 µlm section, arrow) and a network (0.0 µm section,empty arrowheads). ST-GFP is distributed also to circular structures (6.0 µm frame, empty arrows) and large globular structures (9.0 and 12.0 µm frames, stars). Insets: magnification of areas of interest.

As evidenced by treatment with the general plant endomembrane dye DiOC6 (Zheng et al., 2004; Faso et al., 2009), the phenotype was present also in segregating plants of the F2 mapping population from crosses of the *gold36* mutant with *Arabidopsis thaliana* Landsberg erecta (Ler) ecotype that did not express ST-GFP, thereby excluding the possibility that the phenotype was due to over-expression of the transgene (Figure 3).

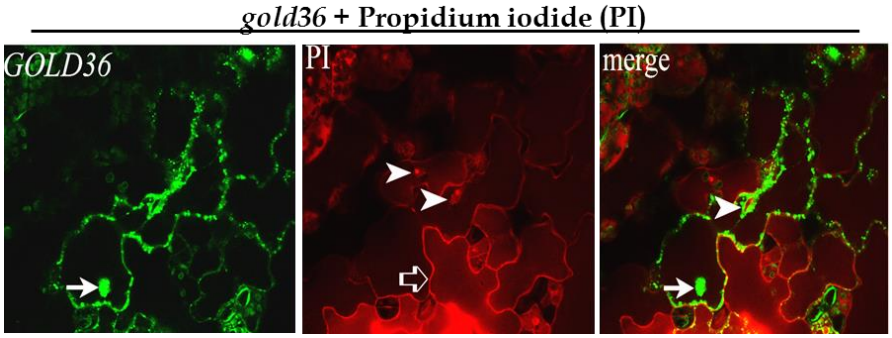

Figure 2. The large *gold36* aggregates are not nuclei.
Confocal images of *gold36* cotyledon epidermal cells treated with propidium iodide (PI) showing nuclei (arrowheads) and cell wall (empty arrow) labeled by the dye. A large aggregate (arrow) is distinguishable from the nucleus (arrowhead) (merged image).

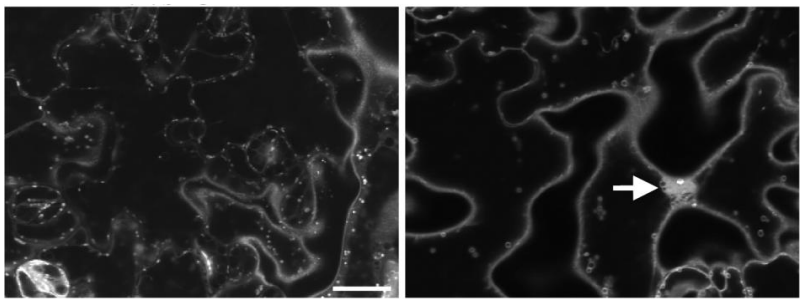

Figure 3. The *gold36* structures are not the result of ST-GFP expression.
Confocal images of cotyledon epidermal cells of non-mutagenized ST-GFP (n.m. ST-GFP) or a segregating L*er* × *gold36* F2 individual that did not express ST-GFP. Treatment with the general endomembrane dye DiOC6 shows the presence of *gold36* structures (arrow) only in the mutant.

Analyses of T1 *gold36* cotyledon epidermal cells stably expressing G-yk, a cis-Golgi marker (Nelson et al., 2007), showed that the fluorescence pattern of ST-GFP overlapped that of G-yk (Figure 4), indicating an abnormal distribution of another Golgi marker of earlier cisternae than the trans- Golgi in *gold36* and excluding the possibility that the partial redistribution of a Golgi marker was specific to ST-GFP and trans-Golgi proteins.

Because the membranous network highlighted by the Golgi markers in the *gold36* mutant background resembled that of the ER (Figures 1 and 4), I analyzed T1 *gold36* cotyledons expressing the ER lumenal marker, ER-yk (Nelson et al., 2007). Confocal microscope analyses confirmed that the network was indeed ER (Figure 5) and, thus, that in the *gold36* mutant the Golgi markers are partially redistributed to this organelle.

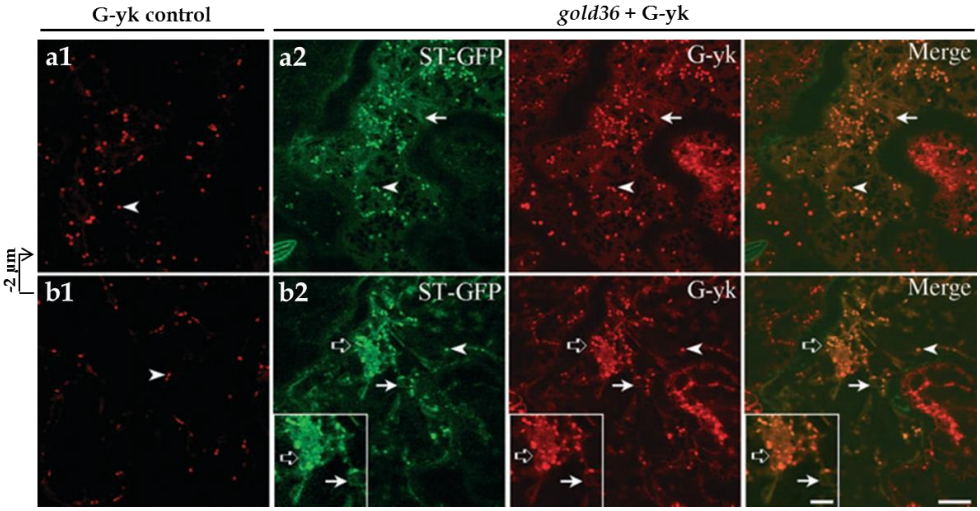

Figure 4. The *gold36* structures are not specific to ST-GFP.
Two confocal optical slices [(a), cortical region and (b), 2 µm deeper than (a)] of cotyledon epidermal cells stably expressing the cis-Golgi marker G-yk either in the Col-0 (a1, b1

control) or *gold36* background (a2, b2). Similarly to the control, in *gold36*, G-yk is clearly distributed to Golgi stacks (a, b arrowheads). In *gold36*, G-yk is also partially redistributed to a cortical network (a2, arrow) and to the same structures labeled by ST-GFP, such as a large globular structure (b2, empty arrows) and smaller circular structures (b2, arrows). Insets in b2: magnification of areas of interest. Bars = 10 µm (main image); 5 lm (inset).

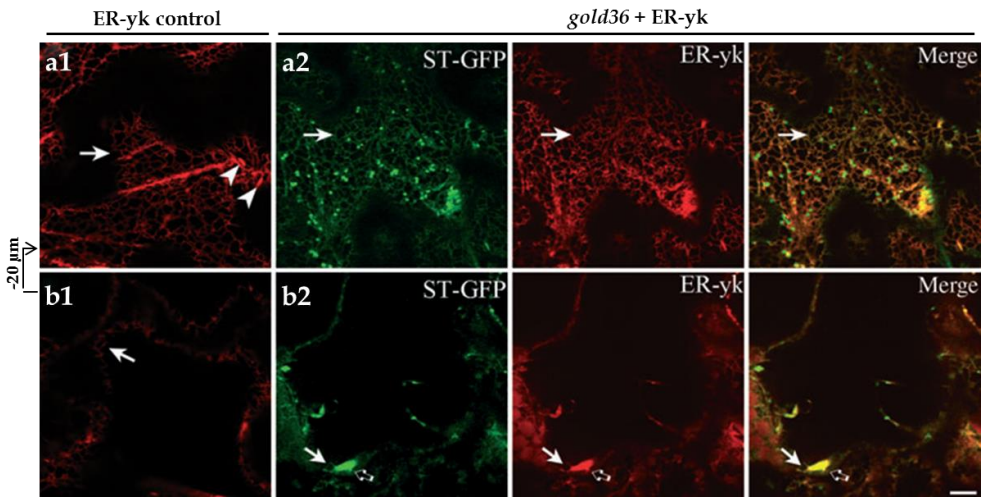

Figure 5. The network highlighted by the Golgi markers in *gold36* corresponds to ER.
Two confocal optical slices [a, cortical region and b, 20 µm deeper than (a)] of cotyledon epidermal cells stably expressing ER-yk, which labels the ER, either in the Col-0 [control, (a1, b1), arrows] or *gold36* (a2, arrows) background show that the network highlighted by ST-GFP corresponds to ER. The ER is part of the *gold36* aberrant structures (b2, arrows and empty arrows). In (a1), arrowheads point to ER fusiform bodies which are also labeled by ER-yk, as also reported for other ER soluble and secreted markers (Hawes et al., 2001; Hayashi et al., 2001; Estevez et al., 2006; Faso et al., 2009). Bar = 10 lm.

The imaging of the smaller circular *gold36* structures indicated that they were part of the ER network (Figures 1, 4 and 5); I aimed to test whether the larger globular structures were in continuity with the ER or formed an isolated compartment. To this end, I photobleached the ER-yk fluorescence in the large globular structure and followed its recovery over time. As shown in Figure 6, ER-yk photobleaching was followed by fluorescence recovery albeit to a much slower recovery rate than previously described for lumenal ER GFP (Tolley et al.,

2008), indicating not only that the large globular structures did not form a separate compartment from the general ER, but also suggesting that the defects in ER organization may limit diffusion of proteins in this organelle.

The obvious defects in ER morphology raised the question whether the ER export activities of this organelle would also be compromised.

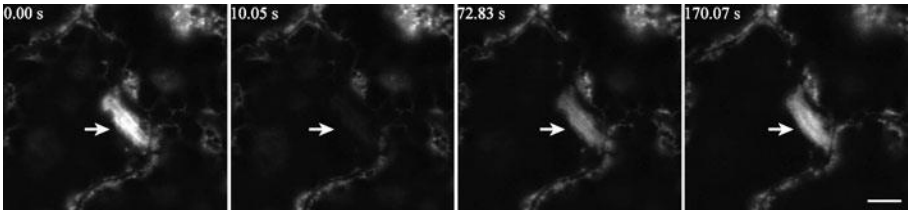

Figure 6. The large globular structures are not isolated bodies.
Images from a FRAP experiment on the ER-yk fluorescence in a large globular structure (arrows) in a *gold36* cotyledon epidermal cell stably expressing the ER marker show fluorescence recovery upon selective bleaching. Cells were treated with latrunculin B (25 lM) (Brandizzi et al., 2002b) to reduce the structure's movement. Only the signal from the YFP channel is shown for clarity. Time of acquisition of single frames is indicated in seconds (s) at the top left corner. Bar = 5 lm.

III.1.2 The *gold36* mutant has defects in ER protein export

The evidence that two Golgi markers were partially distributed to the *gold36* ER (Figures 1 and 4) suggested defects in ER protein export. To test this possibility, I aimed to establish the distribution of a bulk-flow reporter such as a soluble marker destined to the apoplast [sporamin signal sequence-mRFP fusion, secRFP (Faso et al., 2009)]. In Col-0, the marker reached its destination (Figure 7a1,b1), as expected (Faso et al., 2009). However, analyses of cotyledon epidermal cells of T1 *gold36* seedlings expressing secRFP showed partial retention of the marker in the ER network (Figure

7a2,b2), in clear contrast with the control. Interestingly, I also found that in *gold36*, secRFP was retained within the large globular structure and showed evident signal within the smaller circular structures at the cell's periphery (Figure 7a2,b2). Combined with the evidence of a redistribution of Golgi markers in the ER (Figures 1 and 4), partial retention of secRFP in the ER supports our hypothesis that the *gold36* mutant has defects in ER protein export.

III.1.3 The *gold36* phenotype is linked to a mutation in the At1g54030 locus

Therefore, I next sought to identify the mutation responsible for the *gold36* phenotype. To generate a mapping population, I crossed the *gold36* mutant with Ler. The genomic DNA of 57 F2 plants exhibiting the recessive phenotype was analyzed and a candidate region with the mutation was rough mapped between F11F12 and F14J16 BAC clones on chromosome 1 at a 2.2-Mbp intervals. To identify the point mutation, the genomic DNA of the *gold36* mutant was sequenced by Illumina Genome Analyzer II (Solexa).

Within the candidate region, 147 homozygous single nucleotide polymorphisms (SNPs) were identified, of which 18 were found within transcription units. Seven of these SNPs were found within coding regions, but only four were predicted to be non-silent mutations. Among these, only one SNP resulted in a typical G/C-to-A/T EMS transition (Maple and Moller, 2007), which caused a CCT → CTT codon change in the At1g54030 locus (herein named *gold36*)

and resulted in the missense mutation of a proline residue in position 80 into a leucine residue (P80L) at transcriptional level (Figure 8a).

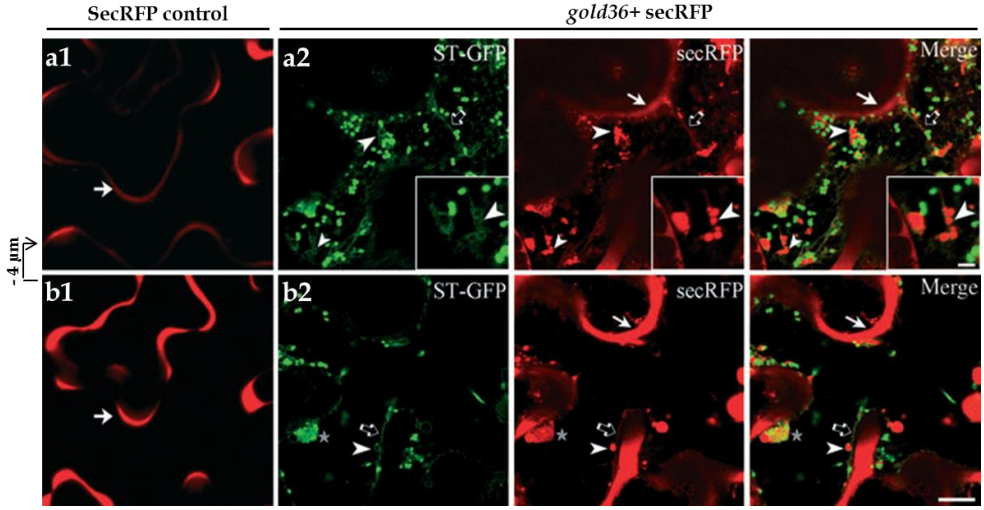

Figure 7. In addition to a partial distribution of Golgi markers in the ER, *gold36* also shows defects in ER export of a soluble secretory marker destined to the apoplast.
Two sequential confocal optical slices of either control [Col-0 transformed with secRFP (a1, b1), or *gold36* cotyledon epidermal cells transformed with the soluble apoplastic marker, secRFP (a2, b2)]. The marker is clearly visible in the apoplast in control and *gold36* cells (arrows); however, in *gold36* cells, the marker was also partially retained in the ER network labeled by ST-GFP (empty arrows) where it was distributed in bright circular structures (arrowheads), as well as in the globular structures (stars). Insets in (a2): magnification of areas of interest. Bars = 5 µm (b), 2 µm (inset).

To test whether such mutation was indeed responsible for the observed phenotype, I analyzed T1 *gold36* seedlings stably expressing the cDNA of either GOLD36 or GOLD36^{P80L} under the control of a CaMV 35S promoter using a confocal microscope. I found that the *gold36* phenotype was complemented by the wild-type cDNA but not by the cDNA bearing the mutation (Figure 8b,c),

indicating that the P80L missense mutation was indeed responsible for the phenotype.

III.1.4 A *gold36* knock-out mutant phenocopies the *gold36* phenotype

Because I was working with a missense mutant, I aimed to compare the phenotype with that of a knock-down/ out mutant. This experiment was important to distinguish whether the ER integrity defects of the *gold36* mutant were linked to the presence of the GOLD36^{P80L} mutant protein or to GOLD36 reduced/absent transcript levels. To do so, I isolated a T-DNA Col-0 insertion line (SALK_030621) in the first exon from the ABRC stock center (*gold36–1*; Figure 8a). RT-PCR of homozygous lines for the T-DNA insertion did not show presence of transcript compared to controls (Col-0, non-mutagenized ST-GFP, and *gold36* backgrounds) (Figure 9a), indicating that *gold36–1* is most likely a knock-out. To test whether the *gold36* phenotype was linked to an aberrant protein product (i.e. *gold36*^{P80L}) or abnormal GOLD36 transcript levels, I aimed to compare the *gold36–1* subcellular phenotype with that of *gold36*. To this end, I transformed *gold36–1* with ST-GFP.

I found that the distribution of ST-GFP in transformed *gold36–1* T1 cotyledons clearly phenocopied that of *gold36*, in that ST-GFP was partially redistributed to the ER, as well as to globular and circular structures (compare Figures 1 and 9b). In addition, complemented lines (*gold36–1* transformed with 35S::GOLD36) did not have such structures (Figure 9c). Together, these data confirm the forward

genetics analyses showing that the *gold36* phenotype was linked to the GOLD36 locus.

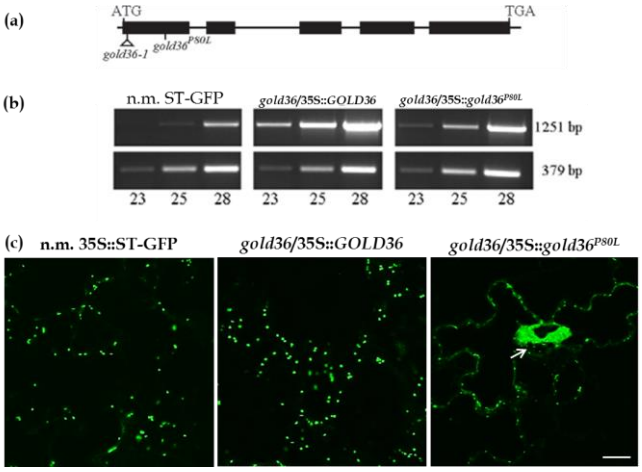

Figure 8. The mutation responsible for the *gold36* phenotype resides in the At1g54030 locus.
Diagram of the At1g54030 locus showing exons (filled boxes), the position of CCT → CTT EMS responsible for the P80L mutation (GOLD36^{P80L}) and the insertion site of the T-DNA in the *gold36–1* line. (b) RT-PCR to amplify wild type and mutated *GOLD36* cDNA (1251 bp; top images) and UBQ10 (PCR control, 379 bp; bottom images) in non-mutagenized ST-GFP (control) and *gold36* backgrounds showing higher levels of transcripts in the *gold36* lines compared to the control, as expected for transformed lines. PCR cycles are indicated below the RT-PCR panels. (c) Confocal images of cotyledon epidermal cells of either control plants or *gold36* transformed with wild-type and mutant GOLD36^{P80L}, showing that the *gold36* phenotype is complemented by GOLD36 but not by its mutant sequence. Arrow points to an aberrant *gold36* structure. Bar = 20 μm.

Importantly also, the evidence that a knock-out mutant phenocopied *gold36* suggested not only that GOLD36^{P80L} is a non-functional protein, but also indicated that the ER integrity defects of the *gold36* mutant are not linked to the presence of the aberrant protein GOLD36^{P80L} product in the ER but rather to the absence of intact GOLD36 transcript.

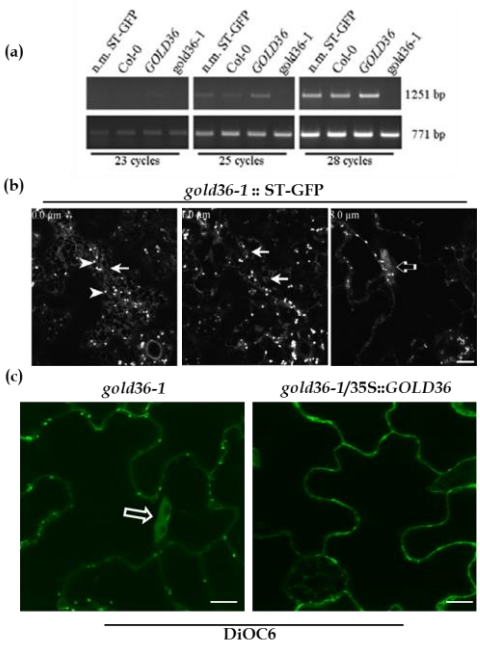

Figure 9. A *gold36* knock-out mutant phenocopies the *gold36* phenotype.
(a) RT-PCR analysis for the *GOLD36* transcript in non-mutagenized ST-GFP, Col-0, *gold36*, and *gold36–1* backgrounds showing non-appreciable levels of *GOLD36* in the *gold36–1* background compared to the others, and suggesting that the line is most likely a knock-out. Top panel: *gold36*; bottom panel: UBQ10. PCR cycles are indicated below the RT-PCR panels. (b) Three sequential confocal optical slices of *gold36–1* cotyledon epidermal cells stably expressing ST-GFP. Note the partial distribution of ST-GFP in the ER (panel 0.0 µm, arrow) besides Golgi stacks (panel 0.0 µm, arrowheads) and the presence of aberrant circular (panel 1 µm, arrows) and large globular (panel 8 µm, empty arrow) structures in the ER. Bar = 20 µm. (c) Confocal images of cotyledon epidermal cells of either *gold36-1* or complemented *gold36-1* treated with DiOC6 showing the presence of the aberrant structures only in the *gold36-1* line (arrow). Bar = 10 µm.

III.1.5 GOLD36 is targeted to the vacuole, but GOLD36^{P80L} is retained in the ER

Analyses of the primary sequence of GOLD36 indicate that the protein contains 417 amino acid residues with a predicted molecular mass of approximately 46 kD. GOLD36 is annotated as MVP1 (Agee et al., 2010) and as a member of the superfamily of plant GDSL-like

lipases; however, unlike all the other members, it does not contain the flexible active site serine in the canonical GDSL motif located near the N-terminus that is essential for lipase activity in this family (Brick et al., 1995). In accordance with this finding, absence of lipase activity of GOLD36/MVP1 has been confirmed recently (Agee et al., 2010). SignalP 3.0 prediction server (Emanuelsson et al., 2007) indicates the presence of an N-terminal signal sequence for insertion in the ER. The protein sequence does not have obvious retention signals, suggesting that it may be exported from the ER to distal compartments such as the vacuole and the apoplast. To investigate this possibility, I aimed to examine GOLD36 localization using a stable transformation system. I first transformed *gold36* plants with a GOLD36 fusion to a monomeric red fluorescent protein (mRFP; 35S::GOLD36-mRFP). mRFP is more resistant to low pH than GFP (Shaner et al., 2005); therefore, it is better suited as a marker for acidic compartments such as the apoplast or the vacuole than GFP. Confocal analyses showed that the GOLD36-mRFP was clearly localized in the vacuole (Figure 10a). GOLD36-mRFP complemented the *gold36* phenotype (Figure 10a), indicating that the protein is a functional fusion; therefore, its distribution must at least partially overlap with that of the endogenous GOLD36. Because the mRFP signal was confined to the cell body rather than in the apoplastic space in plasmolyzed *gold36* cotyledonal epidermal cells expressing GOLD36-mRFP, I concluded that GOLD36-mRFP is not secreted to the apoplast (Figure 10b). Further evidence that GOLD36 is directed to the vacuole is provided in Figure 10c.

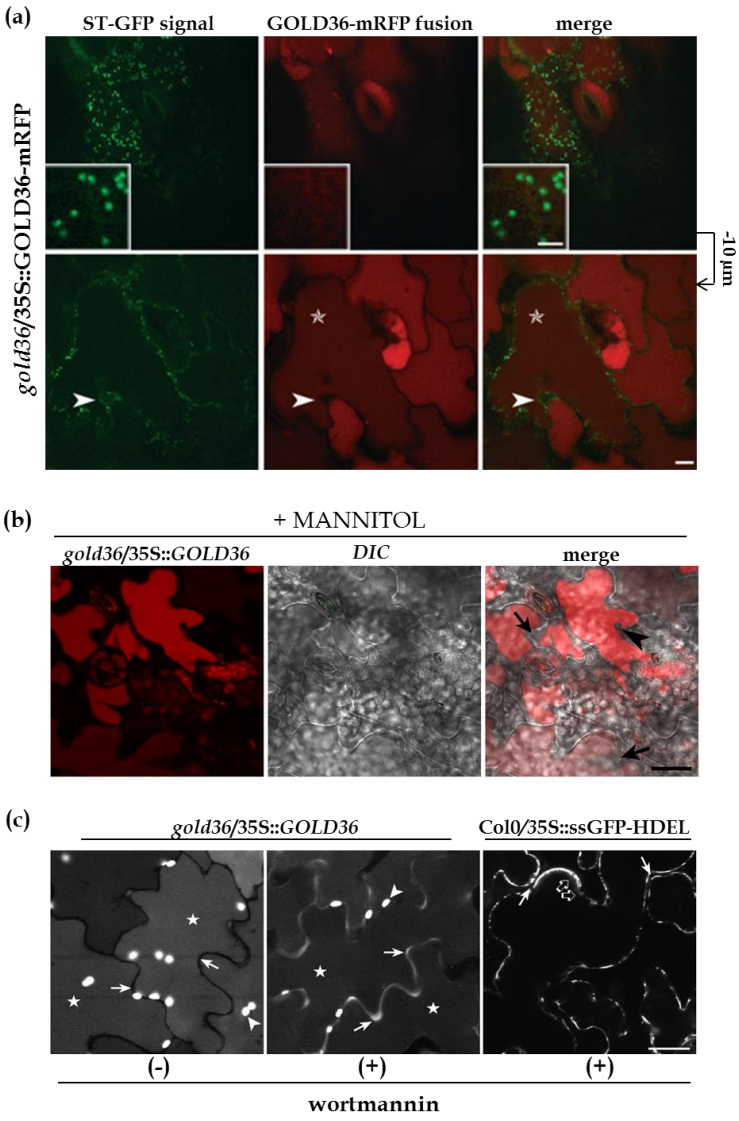

Figure 10. GOLD36 is a vacuolar protein but its P80L mutant is retained in the ER.
(a) Sequential confocal optical sections of *gold36* cotyledon epidermal cells expressing GOLD36-mRFP fusion. Optical slice position is indicated on the right side of the images. GOLD36-mRFP is localized in the lumen of the central vacuole (star) and complements the *gold36* phenotype; note that ST-GFP fluorescence is mainly localized in the Golgi stacks (main image and insets). Arrowhead points to a nuclear envelope, often seen in cotyledon epidermal cells expressing ST-GFP (Faso et al., 2009). Bars = 20 lm (a), 5 lm (insets).
(b) Images of cells *gold36*/35S::GOLD36-mRFP plasmolyzed in mannitol (0.5 M for 20 min) show that the fluorescent signal is present within the cells rather than in the apoplast. For

clarity, only the GOLD36-mRFP signal is shown. Arrows point to cell areas with evident plasmolysis. An arrowhead points to a nucleus visible in negative contrast with the vacuolar fluorescence signal. Bar = 50 µm. (c) GOLD36-mRFP is partially redistributed to the apoplast in the presence of wortmannin. Bar = 20 µm

In fact to further ensure that GOLD36-mRFP was directed to the vacuole, I used wortmannin, a specific inhibitor of phosphatidyl-inositol 3-kinase, which has been used to perturb traffic to the lytic vacuole in cells of yeast (Schu et al., 1993); (Wurmser et al., 1999), mammals (Davidson, 1995; Arighi et al., 2004) and plants (Matsuoka et al., 1995; daSilva et al., 2005; Wang et al., 2009). Because in the presence of the drug, proteins destined to the vacuole are secreted (Kim et al., 2001; Pimpl et al., 2003; daSilva et al., 2005), I hypothesized that GOLD36-mRFP would be at rerouted to the apoplastic space if the vacuole was its final destination. Upon wortmannin treatment of *gold36*::GOLD36-mRFP cotyledons, I found that GOLD36-mRFP was partially secreted to the apoplastic space, confirming the hypothesis that GOLD36-mRFP is destined to post-ER compartments, specifically the vacuole.

As shown in figure 10c, confocal images of *gold36*::GOLD36-mRFP cotyledons plasmolyzed in mannitol (0.5 M) either untreated (control) or treated with wortmannin, and images of treated and plasmolyzed cotyledons stably expressing the ER lumenal marker [ssGFP-HDEL; (Brandizzi et al., 2003)]. The mRFP signal is exclusively visible in the vacuoles (stars) in the control, while it is also visible in the apoplast (arrows) in the wortmannin-treated sample. Consistent with the known effect of the drug on rerouting

vacuole-destined proteins to the apoplast, these data support post-ER traffic of GOLD36-mRFP.

As expected, wortmannin did not have an effect on the distribution of the ER lumenal marker ssGFP-HDEL, which was retained in the ER (empty arrows). In the *gold36*/35S::GOLD36-mRFP only the mRFP channel is shown for clarity. Note the presence of chloroplasts (arrowheads) that are visible in the *gold36*/35S::GOLD36-mRFP images but not in the ssGFP-HDEL image because the microscopy imaging settings for mRFP enable also the capture of the chlorophyll autofluorescence signal. Finally, I aimed to compare the fluorescence of GOLD36-mRFP with that of the GOLD36^{P80L} mutant (Figure 11). Analyses of T1 *gold36* transformants expressing GOLD36^{P80L}-mRFP showed that, in clear contrast to the wild-type protein, the mutant protein fusion was retained in the ER network where it accumulated in bright, large structures (Figure 11). As expected from experiments using the untagged GOLD36 (Figure 8c), GOLD36^{P80L}-mRFP did not complement the *gold36* phenotype.

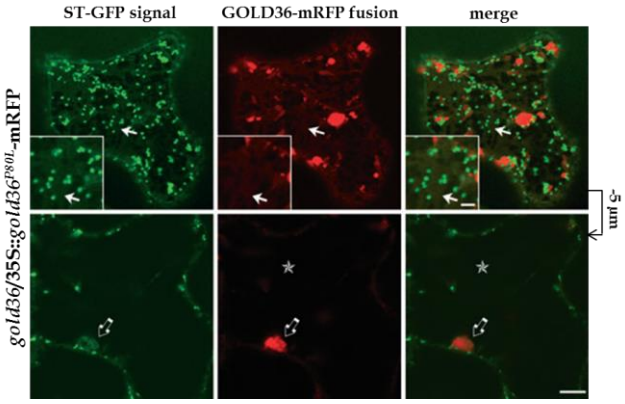

Figure 11. GOLD36^{P80L}-mRFP did not complement the *gold36* phenotype
GOLD36 cells expressing GOLD36^{P80L}-mRFP show ER (arrows) and globular structures (empty arrow) due to lack of complementation. In clear contrast to GOLD36-mRFP, the GOLD36^{P80L}-mRFP signal is in the ER but not in the vacuole (star). Insets magnification of areas of interest. 10 µm, 5 µm (insets).

III.1 SUB-CELLULAR LOCALIZATION AND ELICITOR- REGULATED DYNAMICS OF THE ARABIDOPSIS NPK1-RELATED PROTEINS (ANPs)

III.2.1 Sub-cellular localization and dynamics of ANPs

To elucidate the function of ANPs in immunity, I investigated the subcellular localization of the ANP proteins under normal conditions and upon elicitation.

To this aim GFP tag was fused to the C-terminal of each member of the ANP family placed under the control of CaMV 35S promoter and the chimeric proteins were stably expressed in *Arabidopsis thaliana*, ecotype Columbia-o (Col-0). Fluorescence was observed by using a spinning-disk confocal microscope in cotyledon epidermal cells of 6-day-old seedlings homozygous for the construct expressing the chimeric proteins. Plants expressing a soluble GFP (sGFP) were also analysed, as controls.

Control seedlings expressing sGFP showed fluorescence distributed throughout the cytoplasm and the nucleoplasm (Figure 12a). In contrast seedlings expressing each of the three ANP-GFP, showed a punctuate fluorescence mainly restricted to small (4-6 μm) motile bodies that were distributed in the cortical cytoplasm of the cells (Figure 12b), as well as to a confined zone of cytoplasm leaning to the plasma membrane probably due to the presence of the large central vacuole (data not shown).

The motion of the small bodies was analysed by collecting time-lapse images at 0.5 second intervals in a single focal plane and

velocity of individual small bodies was measured. The speed of the movement reached up to 10 µm sec^{-1}.

Upon elicitation with either OGs (100 µg/mL) or elf18 (1µM) for 15-20 min, fluorescence was still visible on the small bodies, but also appeared in I) the cell periphery, likely at the plasma membrane; II) a large structure likely corresponding to the nucleus and III) large discoid bodies (10-12 µm) that were mobile (4 µm sec^{-1}) and often organized in pairs (Figure 12 c,d). Some of the discoid organelles were stably associated to the putative nuclei, generally situated in the mid to lower sections of each cell (Figure 1 c and d, see stars).

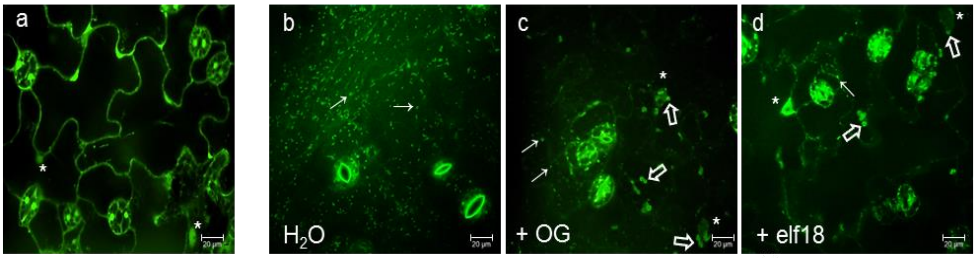

Figure 1. Expression of ANP3-GFP proteins.
Spinning disk confocal microscope analyses of cotyledon epidermal cells stably expressing sGFP (control) show fluorescence distributed throughout the cytoplasm and in the nucleoplasm(star) (a). In contrast to the control plants, transgenic ANP-GFP plants show that the fusion protein is distributed in numerous, small and motile fluorescent bodies (4-6 µm) (arrows). Upon elicitation with OG (c) and elf18 (d), fluorescence is still present in the small bodies (arrows), and appears also in larger discoidal motile organelles (empty arrows) and in a large structure, likely corresponding to the nucleus (stars).
Similar results were obtained with the ANP1-GFP and ANP2-GFP fusions.

III.2.2 GFP constructs are targeted to the mitochondria, plastids and nucleus

The nature of the different organelles was determined by confocal microscope analyses and by transiently expressing (Li et al., 2009b), in the transgenic seedlings, different red-fluorescent organelle markers, for the cis-Golgi (G-rk), peroxisomes (px-rk), mitochondria (mt-rk) and plastids (pt-rk) (Nelson et al., 2007), or by specific staining. The small motile bodies were thus identified as mitochondria by colocalization with mt-rk (Figure 13a).

The large structures were confirmed to be nuclei by propidium iodide (PI) staining (Figure 13b), while the large discoid organelles that appeared upon elicitation with OGs and elf18 were labeled by pt-rk and were therefore identified as plastids (Figure 13c).

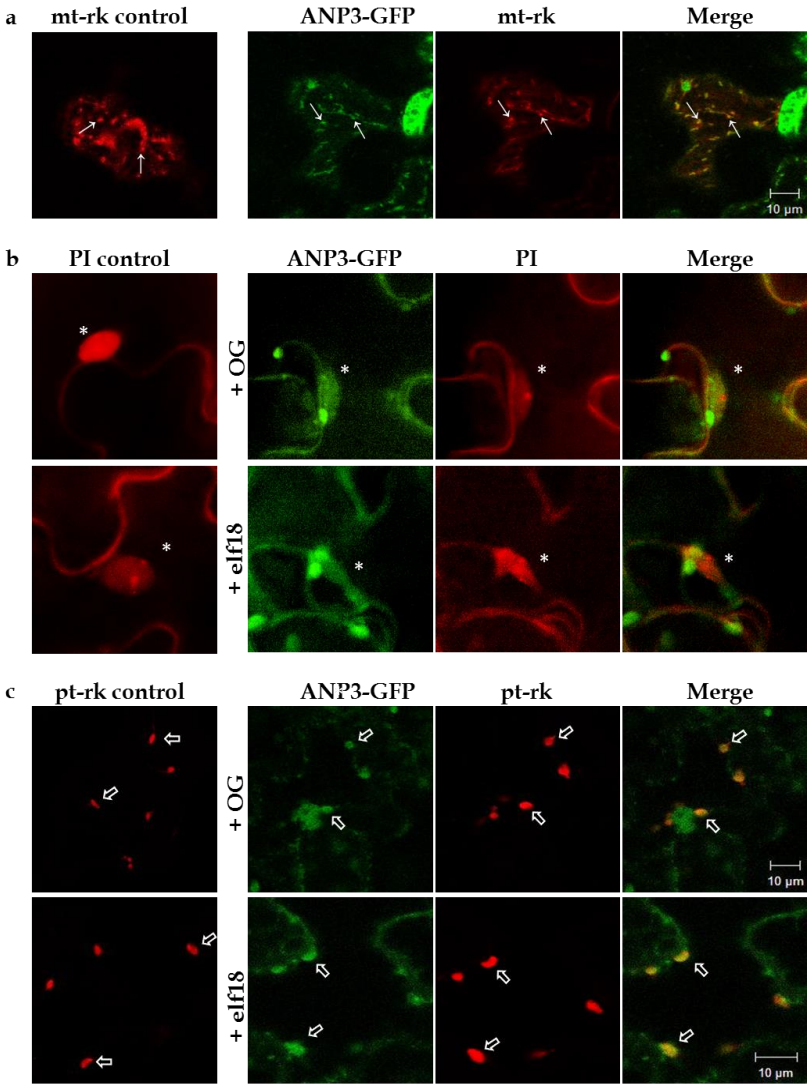

Figure 13. ANP3-GFP protein locates to mitochondria, nucleus and plastids.
High magnification of spinning disk and confocal microscope analysis of cotyledon epidermal cells of either control (Col-0) or transgenic ANP3-GFP plants transiently expressing (a) mitochondrial marker (mt-rk) show that ANP3-GFP protein is clearly associated to mitochondria (cortical region, arrows). (c) a plastid marker (pt-rk) show that the large discoid organelles that appear upon elicitation with OGs and elf18 are plastids (empty arrows), or (b) treated with propidium iodide, which labels the cell wall and nucleic acid in the nucleoplasm, show that the presence of the large structure, after elicitation, perfectly merged with the nucleus (star). Similar results were obtained with the ANP1-GFP and ANP2-GFP fusions.

No changes in the localization of fluorescent ANPs occurred upon control treatment with oligomannuronides (OM, 100 µg/mL) and tri-galacturonic acid (OG_3, 100 µg/mL), wall-derived molecules known to have no biological activity in Arabidopsis (Fig 14).

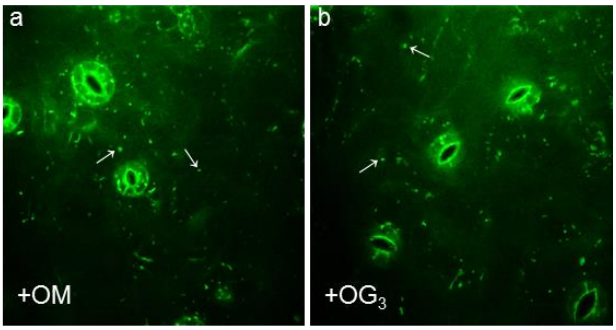

Figure 14. OM and OG_3 treatment do not change the localization of fluorescent ANPs. Incubation with inactive cell wall-derived molecules, such as oligomannuronides (OM, a) and OG trimers (OG_3, b) do not change ANP3 subcellular localization. Similar results were obtained with the ANP1-GFP and ANP2-GFP fusions.

III.2.3 Phenotype of *anp2 anp3* double mutant is rescued by 35S::ANP3-GFP

To assess whether the chimeric ANP-GFP proteins are functional, I determined whether the *anp2 anp3* phenotypic alterations (cytokinesis-related defects leading to multinucleate cells and formation of cell wall stubs, reduced root length and reduced plant growth) are rescued by the expression of the fluorescent ANP3. As a control, sGFP was expressed in the same mutant. Confocal microscopy analysis showed the presence of many polynucleate cells with cell wall stubs in the *anp2 anp3* mutant expressing sGFP (Figure 15a). On the contrary, no defective cells were observed in the *anp2 anp3* mutant expressing ANP3-GFP, indicating that the fusion protein was

able to rescue the cytokinesis-related defects (Figure 15b). The length of the root of *anp2 anp3* is also rescued by the expression of fluorescent ANP3, but not by sGFP (Figure 15c). These results demonstrate that ANP3 tagged with GFP is functional.

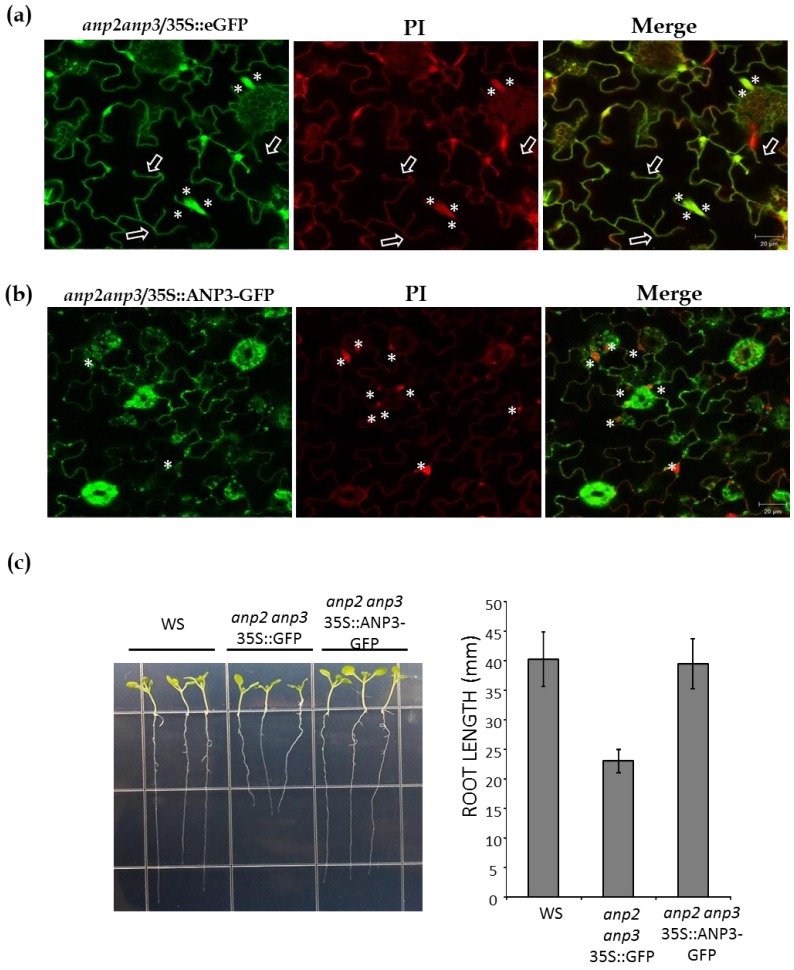

Figure 15. Phenotypes of the double *anp2 anp3* mutant are rescued by 35S::ANP3-GFP.
(a and b) Confocal microscope analyses in cotyledon epidermal cells of double *anp2 anp3* mutant stably expressing either a soluble GFP (eGFP) or the ANP3-GFP fusion under the control of the CaMV 35S promoter show that *anp2 anp3* phenotype (polynucleate cells and cell wall stubs in (a), indicated by stars and arrows respectively), is complemented by the fluorescent ANP3 in (b) but not by GFP. (c) Likewise, length of the root is rescued by the ANP3-GFP fusion but not by GFP. Similar results were obtained with ANP2-GFP.

III.2.4 Localization of ANPs upon elicitation coincides with sites of ROS production

The oxidative burst is a very early response to elicitors and the role of ANPs in H_2O_2 signaling has been proposed on the basis of a protoplast-based assay (Kovtun et al., 2000). Because the association with mitochondria and plastids, well known sites of ROS generation, suggests an involvement of ANPs in either ROS generation and/or transduction, the kinetics of internal ROS signal was examined by using 2-7-dichlorofluorescein diacetate (DCF-DA) staining to detect peroxides generated in response to OGs and elf18 by confocal microscope analysis. DCF-DA is a good tool for real-time detection of increased intracellular concentrations of ROS (Ashtamker et al., 2007), although it is dependent on peroxides activity in a particular cellular compartment (Gerber and Dubery, 2003).

DCF-DA-stained cotyledon epidermal cells showed a basal-level signal that accumulated, on the cell cortex, in the small motile bodies, likely corresponding to the same basal localization of ANPs proteins, i.e. the mitochondria (Figure 16A). Upon elicitations with OGs and elf18 a considerable increase of the DCF-DA signal was observed. Notably, fifteen minutes after elicitation, the pattern of DCF-DA fluorescence was very similar to that of ANP-GFP plants (Figure 16 B and C). To verify this, a DCF-DA staining was performed on seedlings stably expressing mt-rk or pt-rk confirming that peroxides accumulate in response to both OGs or elf18 in mitochondria, plastids and nucleus (Figure 17).

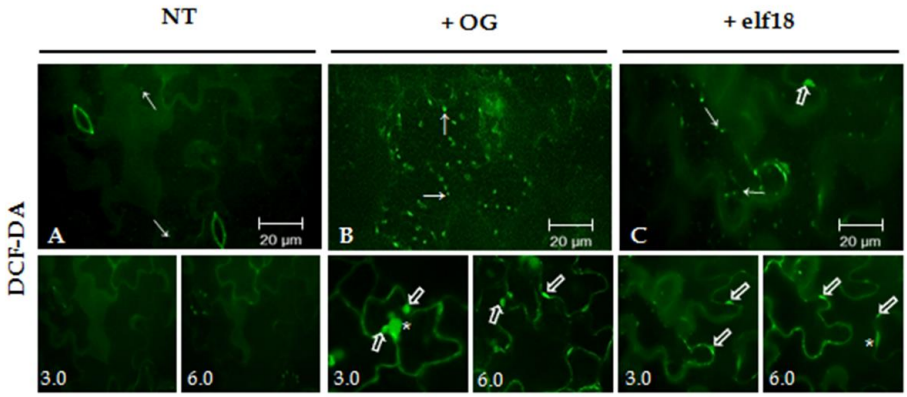

Figure 16. 2-7-dichlorofluorescein diacetate (DCF-DA) staining shows a fluorescence pattern very similar to that observed in ANP-GFP plants
2-7-dichlorofluorescein diacetate (DCF-DA) staining was used to detect peroxides generated in response to OGs and elf18 by confocal microscopy analysis. Notably, cotyledon cells exhibited a fluorescence pattern very similar to that observed in ANP-GFP plants after a 15 min treatment with either elicitor.

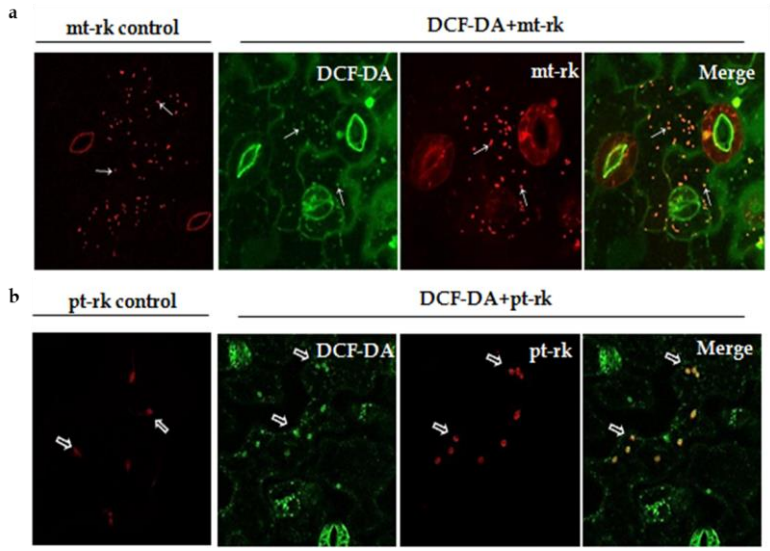

Figure 17. Subcellular localization of ANPs matches with intracellular ROS production sites.
DCF-DA staining of transgenic seedlings expressing mt-rk or pt-rk showed that peroxides accumulate in response to both OG or elf18 in mitochondria, plastids and nucleus (a and b).

III.2.5 *anp* triple mutant is defective in elicitor-triggered intracellular ROS production

Analysis of single, double and triple *anp* mutants has demonstrated that ANPs play an important role in immunity (unpublished data of G. De Lorenzo laboratory). In particular, because the triple *anp* KO mutant is not available, likely due to lethality, a triple *anp* mutant was generated by expressing, in a β-estradiol-inducible manner, an artificial microRNA that targets *ANP1* messengers in the *anp2 anp3* double KO mutant background, and two two lines (# 2.5 and # 8.7) were selected for further analyses. I have analyzed both extracellular and intracellular ROS production after elicitor treatments, by DCF-DA staining, in the two triple *anp* mutant lines, grown in the presence of DMSO alone (mock control) or β-estradiol (Figure 18). In confocal cortical slices, that allow a better vision of the apoplast, WT cotyledon epidermal cells treated either with OGs or elf18 showes an an increase of extracellular ROS (Figure 18 b and c) that was not visible in cotyledons treated with H_2O (Figure 18 a). This elicitor-triggered response was much lower in the *anp* triple mutant (Figure 18 k and l). I then investigated intracellular ROS production with deepr confocal sections and observed that, in WT cotyledon epidermal cells, DCF-DA stained mitochondria both in H_2O- and elicitor-treated samples (Figure 18 m-r), and plastids and nucleus only in the presence of elicitors (Figure 18 n and o, q and r). On the contrary, in the triple *anp* mutant, DCF-DA staining displayed only the presence of mitochondria, and elicitor applications did not vary the basal intracellular ROS production (Figure 18 w and x). Taken

together, these data demonstrate that ANPs are required for elicitor-regulated production of extra- and intracellular ROS.

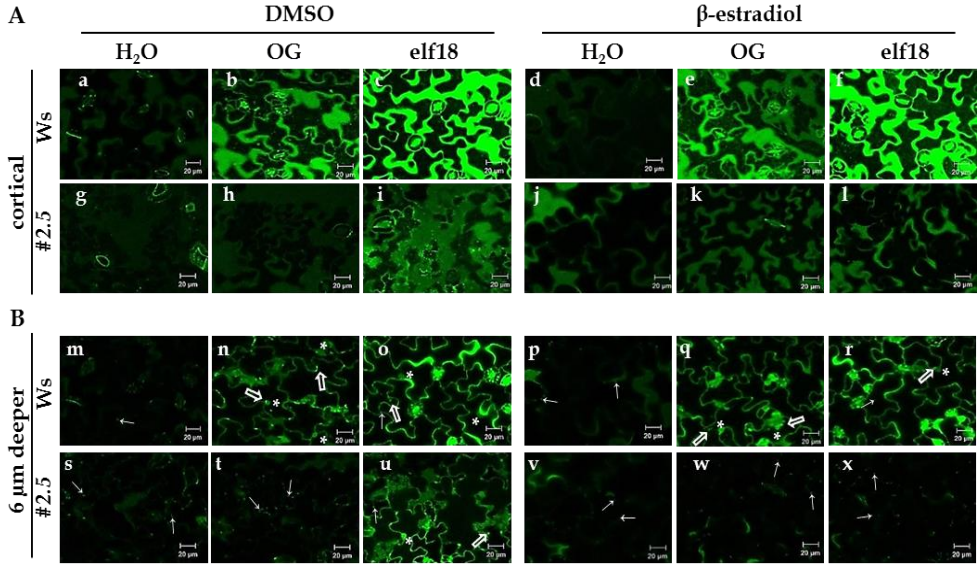

Figure 18. ***anp*** **triple mutant is defective in elicitor-triggered ROS production.**
DCF-DA staining was used to detect peroxides generated in response to OGs and elf18 by confocal microscopy analysis in wild type (Ws) and the *anp* triple mutant line #2.5. Two confocal optical slices [cortical region showing extracellular ROS (A) and 6 µm deeper section showing intracellular ROS (B)] of cotyledon epidermal cells were analyzed. After 15 min treatment with either elicitor, Ws cotyledons show presence of ROS into mitochondria (arrows), plastids (empty arrows) and nucleus (stars) (n,o-q,r), whereas *anp* triple mutant cotyledons display no ROS accumulation over that observed in untreated seedlings (w,x). Similar results were obtained in 3 different experiments (n=5). and for the # 8.7 line.

IV. DISCUSSION

IV.1 CHARACTERIZATION OF A PROTEIN INVOLVED IN GOLGI-MEDIATED TRAFFICKING

It is generally believed that the morphological and functional integrity of the ER depends on the activity of ER proteins that either reside in the organelle or that are associated with its surface. The data shown in this work demonstrated that reduced export of a small vacuolar protein affects the integrity of the ER in Arabidopsis. In particular, I demonstrate that an EMS mutant has obvious displacement of membrane and soluble markers destined to post-ER compartments as well as large defects in ER
network organization. Using a combination of classical positional cloning and next-generation whole genome sequencing, the mutation responsible for the phenotype was mapped to a missense mutation in the GOLD36 (At1g54030) locus. I established that while wild-type GOLD36 is targeted to the vacuole, the mutant *gold36* bearing a missense P80L residue switch is retained in the ER. However, I also found that a knock-out mutant phenocopied the *gold36* subcellular phenotype. Together these data propose the concept that a reduced or absent function of a distally targeted secretory protein can influence ER morphological and functional integrity.

IV.1.1 GOLD36^{P80L} is the product of an EMS allele with a unique subcellular phenotype

GOLD36 coincides with the described MVP1, which was identified through a screen for EMS mutants with defects in the targeting of a

delta-TIP to the vacuole (Agee et al., 2010). The mvp1 allele carried a mutation that causes the missense G57E residue shift in *gold36*/MVP1; the resulting mutant showed one large membranous aggregate per cell, which, similarly to the mutant described here, contained membrane markers destined to the ER and Golgi (Agee et al., 2010). Such structures also retained membrane markers destined to post-Golgi compartments (Agee et al., 2010), indicating that similarly to *gold36*, MVP1 had defects in protein traffic at these structures. Here, I show that, differently from MVP1, *gold36* additionally has a strong phenotype in the cortical ER with obvious retention of proteins destined to post-ER compartments in the cortical ER. Although such difference with MVP1 may be explained on the basis that the mutation in the *GOLD36* allele encoding GOLD36^{P80L} may be stronger compared to that of MVP1, our data combined with those of (Agee et al., 2010) indicate that *gpld36*/MVP1 is an important protein for ER functional and morphological integrity in plants.

IV.1.2 GOLD36/MVP1 is a vacuolar protein

I show that a GOLD36-mRFP fusion is localized at the vacuole and that the fusion is functional, complementing the mutant phenotype. Transient expression experiments in Arabidopsis have indicated that a GFP fusion of wild-type GOLD36 (MVP1-GFP) was localized in the ER, ER fusiform bodies, and transvacuolar strands (Agee et al., 2010), which are thin tubular structures containing cytoplasm, ER and Golgi membranes (Knebel et al., 1990; Nebenfuhr et al., 1999;

Hoffmann and Nebenfuhr, 2004). However, it was not shown whether the ER-localized MVP1-GFP could complement the phenotype (Agee et al., 2010). It is possible that the ER localization of MVP1-GFP reflects the distribution of the protein pool in transit to other compartments. Lower tolerance of GFP than mRFP to acidic pH may also partially explain a lack of visualization of the marker in the vacuole (Tamura et al., 2003; Shaner et al., 2005). Furthermore, ER fusiform bodies are generally labeled by any ER luminal protein including soluble inert ER GFP-markers (Hawes et al., 2001); (Hayashi et al., 2001; Estevez et al., 2006; Faso et al., 2009) raising the possibility that the MVP1-GFP localization in these structures may be transient. Nonetheless, the vacuolar localization of GOLD36-mRFP proposed in our work is consistent with proteomics studies that retrieved the At1g54030 product in the Arabidopsis vacuole (Carter et al., 2004), further adding to our microscopy and genetic complementation evidence that the vacuolar localization of GOLD36-mRFP reflects the distribution of the endogenous protein. It is also worth noting that, in clear contrast to the vacuolar distribution of GOLD36, the GOLD36^{P80L} mutant was localized in the ER. In addition, the phenotype of GOLD36/ GOLD36^{P80L} plants was not complemented and was similar to the knock-out mutant *gold36–1*. Together, these data suggest that GOLD36^{P80L} is a non-functional protein. Secretory malfolded proteins, which may prove a hazard for the cell if delivered to distal compartments, are retained in the ER via quality control mechanisms (Brandizzi et al., 2003; Anelli and Sitia, 2008). Therefore, the ER distribution of GOLD36^{P80L} may be the consequence of the missense amino acid mutation in a critical

residue necessary for proper folding. Alternatively, I cannot exclude that the ER retention may be linked to non-productive interactions of GOLD36^{P80L} with ER partners that would normally facilitate ER export of GOLD36.

IV.1.3 Although GOLD36 reaches the vacuole as a final destination, it influences ER integrity

In most eukaryotes, the membranes of the ER assume a network-like morphology characterized by the presence of interconnected cisternae as well as tubules that undergo continuous fusion and fission (Sparkes et al., 2009). Little is known about how the complex morphology of the ER is formed and maintained, or what role the overall structure plays in the functions of the ER. It is becoming increasingly clear that ER proteins or ER-associated proteins influence the ER morphological integrity. ER tubules are pulled and extended from a membrane reservoir as cytoskeletal elements, such as microtubules in mammalian cells (Vedrenne and Hauri, 2006) or as actin filaments in plant and yeast cell polymers (Prinz et al., 2000; Brandizzi et al., 2003; Sparkes et al., 2009). Tubules are then stabilized by cytoskeleton independent mechanisms; recently, ER-associated proteins including reticulons and DP1/Yop1p proteins have been implicated in such mechanisms ((Voeltz et al., 2006). Similarly, ER associated dynamin-like proteins such as the mammalian atlastin and its yeast functional hortologue, Sey1p, have also been implicated in the remodeling of the ER (Hu et al., 2009; Orso et al., 2009). The ER morphology is also known to change to accommodate an overload of

membrane proteins as a consequence of over-expression or defects in ER export (daSilva et al., 2004; Stefano et al., 2006; Runions et al., 2006). The data show that GOLD36 is a vacuolar protein and that a *gold36* knock-out mutant phenocopies the *gold36* subcellular phenotype. These data show that, although GOLD36 does not accumulate in the ER

at a steady state, the mutant phenotype is linked to reduced or absent GOLD36 presence in the ER. In light of this, I speculate that GOLD36 is a factor that, while in transit to its final destination, influences the integrity of the ER. This model proposes that GOLD36 participates in the maintenance of ER integrity by either working as a chaperone of other proteins that are necessary for ER integrity or by binding to and reducing the activity of proteins destined to non-ER compartments that may have deleterious effects in the ER. The model in which GOLD36 functions as a molecular chaperone is intriguing, as it may add to the repertoire of known chaperones involved in ER protein folding and maturation (Anelli and Sitia, 2008). In addition, the model would be consistent with growing evidence that ER quality control relies not only on the ERAD pathway, but also on ER chaperone-mediated protein transport of terminally malfolded proteins to the vacuole for disposal (Spear and Ng, 2003; Pimpl et al., 2006). Here I have not pursued a secondary aspect of our work on detailing the nature of the small circular structures visualized in the ER by confocal microscopy and that of the crystalline structures contained within the *gold36* aggregates visualized by electron microscopy. Those may be supernumerary aggregates of the GOLD36^{P80L} or of other proteins that arise as a consequence of the

GOLD36^{P80L} mutation. I also cannot reject the possibility that such structures may be modified ER fusiform bodies. The genetic and microscopy analyses show that GOLD36^{P80L} is not a dominant mutation and that the GOLD36 is phenocopied in the *gold36* knock-out background.

It is interesting to note that the *gold36* mutant has defects in ER protein export, as evidenced by the partial retention of a bulk flow marker in the ER. This observation leads us to ask whether GOLD36 is also required for ER protein export or whether the alteration of the ER morphology

causes defects in ER export. In this model, the effect of reduced activity of GOLD36 on protein export would be indirect but it would underscore the importance of the overall integrity of the ER structure in the export functions of this organelle.

Here, I described an EMS mutant that was identified through the powerful techniques of confocal microscopy and forward genetics coupled with a next-generation sequencing approach. These results demonstrate that microscopy-based screens that rely on morphological and functional analyses of secretory organelles are useful and exciting resources for the identification of players in the integrity of organelles of the early secretory pathway. Our data add to the repertoire of factors that are known to influence the activity and the morphology of the ER and propose the concept that the activity of distally localized protein may influence the organelle's integrity. The identification of GOLD36 is an exciting starting point toward the identification of interacting partners to establish which

other factors function with this protein to influence the activities of the ER.

Microarray analysis showed the induction of the expression of GOLD36 following to the pathogen attack such as *Agrobacterium tumefaniens*, *Pseudomonas siringae*, and after methyl jasmonate treatment (Agee et al., 2010).

Recently (Nakano et al., 2012) demonstrated that this vacuolar protein interacts with a protein complex called PYK10, involved in defense responses. PYK10 is localized at the level of ER bodies, which are involved in the synthesis of molecules with antimicrobial funtion. These data suggest that GOLD36 may have a role in immunity.

IV.1 SUB-CELLULAR LOCALIZATION AND ELICITOR- REGULATED DYNAMICS OF THE ARABIDOPSIS NPK1-RELATED PROTEINS (ANPs)

A very early event in the transduction of elicitor signal is the activation of kinase cascades. Unpublished data of prof. G. De Lorenzo laboratory have shown that the Arabidopsis NPK1-Related Protein Kinases (ANPs) are involved in defence-related response to both DAMPs and PAMPs (OGs and elf18, respectively). Indeed, both double and triple *anp* mutants show a defective activation of the immune responses in terms of induction of defense genes, MAPKs activation, induction of resistance against pathogens. So far only a role in the regulation of cytokinesis and development (Krysan et al., 2002), and in the inhibition of auxin-induced gene activation, likely through a role in the response to ROS (Kovtun et al., 2000), had been described for these proteins.

I performed a subcellular study of the dynamics of ANP-GFP fusion proteins in normal condition and upon elicitation to better understand the function of these proteins in immunity. By confocal microscopy analyses I established that, in seedling epidermal cells, ANPs are mainly localized in cytoplasm and are associated to mitochondria in non-elicited conditions. After elicitor perception they associate also to plastids and the nucleus. These results are in agreement with bioinformatics intracellular localization predictions, by using MultiLoc and TargetP softwer (Emanuelsson et al., 2000; Hoglund et al., 2006), which mainly analyzes the N-terminal amino acid sequence of the proteins of interest to predict organelle targeting

specificity (Table 1). In particular MultiLoc predicted a dual targeting nature, to either plastids or mitochondria, for all three ANPs, and provided a high score for the nuclear localization.

Table 1. Summary of predicted and experimental intracellular localization of ANP proteins compared with other proteins used as negative or positive control.

		MultiLoc				TargetP		Localization	
Protein	**Locus**	**N**	**M**	**P**	**M/**	**M**	**P**	**Pre**	**Ex**
ANP	At1g09000	0.99	-	-	0.96	0.23	0.08	N,M/P	N,M,P,C,PM
ANP	At1g54960	0.99	-	-	0.97	0.23	0.20	N,M/P	N,M,P,C,PM
ANP	At3g06030	0.97	-	-	0.96	0.25	0.17	N,M/P	N,M,P,C,PM
ACO1	At4g35830	-	0.57	0.99	-	0.16	0.06	M,	M
ACO3	At2g05710	-	0.99	0.51	-	0.13	0.91	M,	M
GTP-BD	At4g02790	-	0.96	0.98	0.74	0.79	0.10		M
ProR	At5g52520	-	0.90	0.97	-	0.63	0.72	M,	M,P
AspRs	At4g33760	-	0.73	0.97	0.97	0.31	0.36	M,	M,P
MPP	At3g16480	-	0.94	0.84	0.89	0.64	0.57	M,	M,P
DCL	At1g01040	0.93	-	0.66	-	0.09	0.07	N,	N
HTR12	At1g01370	0.52	-	-	0.88	0.63	0.27	N,M/P	N
MC	At1g02170	-	-	-	-	0.17	0.73	Other	C
GSTF7	At1g02920	-	-	-	-	0.33	0.03	Other	C

[a] N = nucleus; M = mitochondria; P = plastids; C = cytoplasm; PM = plasma membrane
[b] Data obtained from the Arabidopsis Subcellular Database (SUBA 3 - http://suba.plantenergy.uwa.edu.au)
[c] (Baudisch and Klosgen, 2012)

The presence of amphiphilic α-helical regions can be also considered as a potential indicator of a mitochondrial targeting domain (Berglund et al., 2009) and can be detected using softwares for secondary-structure predictions, such as PsiPred (Bryson et al., 2005). Furthermore, a low content of arginines, together with a high abundance of proline and serine in the N-terminal portion has been

associated with plastid targeting, whereas a high arginine content to a mitochondrial targeting (Berglund et al., 2009). I performed these analyses of the first 68 amino acids of ANPs, thus excluding the kinase domain. Predictions suggested the presence of short α-helical regions in each of the N-terminal portion of ANPs; in addition, a high content of arginins and several serines and prolines suggests dual targeting (Figure 1).

Figure 1. Amino acid sequence of the N-terminal of ANPs.
Analyses were performed by using the PsiPred predictor on the first 68 amino acids of ANPs, thus excluding the kinase domain. Underlined sequences represent predicted α-helix. Amino acid arginine is colored in red, serine in green and proline in blue.

IV.2.1 Role of ANPs in ROS production

Because ANPs are localized in subcellular sites of ROS production and because I observed no peroxide production in the *anp* triple mutant upon OG and elf18 treatment, a possible functional model in immunity of these triple kinases can be proposed (Figure 2).

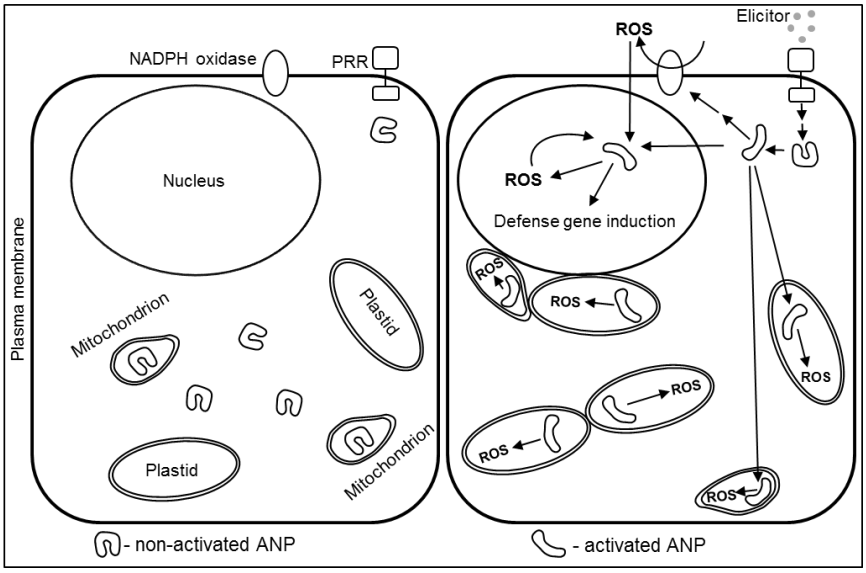

Figure 2. A model for ANP proteins function.
See description in the text.

In non-elicited condition ANPs are located in mitochondria and cytoplasm in a "closed"non-activated form. "Relocation" into the nucleus, plastids and plasma membrane occurs upon elicitation. What is the possible significance of ANP localization? Mitochondrial localization may not be required only for a defense response, since ANPs are also involved in cytokinesis. Indeed Segui-Simarro and collegues hypothesized that mitochondria provide an efficient means to deliver ATP for cell cycle and cytokinesis activities (Segui-Simarro et al., 2008). The perception of elicitors by the specific receptors initiates a cascade of responses and among them there is the conversion of ANPs in an "opened" activated form. Probably this step occurs in the cytoplasm. In a second phase, responsible for the actual signaling response, the activated forms are transported to the

plasma membrane, where they are involved in transduction leading to extracellular ROS production that are formed through the NADPH oxidases, and to the nucleus and plastids, where they are involved in intracellular ROS production and signal transduction leading to defense gene induction. This mechanism is in agreement with the absence of the DCF-DA fluorescence, and thus the intracellular ROS production, in the *anp* triple mutant. Recently, it was demonstrated that disturbance of ROS homeostasis induces atypical tubulin polymer formation and affects mitosis (Livanos et al., 2012). Therefore, ROS imbalance may affect directly the mechanism of the formation of the new cell wall. This may explain the presence of polyucleate cells in *anp2 anp3* and in the *anp* triple mutant. Thus ANPs emerge as central regulatory elements that orchestrate a plethora of events ranging from the division and development to those following to pathogen attack.

Literature Cited

Mitogen-activated protein kinase cascades in plants: a new nomenclature (2002) Trends Plant Sci **7**: 301-308

Adams JA (2003) Activation loop phosphorylation and catalysis in protein kinases: is there functional evidence for the autoinhibitor model? Biochemistry **42**: 601-607

Agee AE, Surpin M, Sohn EJ, Girke T, Rosado A, Kram BW, Carter C, Wentzell AM, Kliebenstein DJ, Jin HC, Park OK, Jin H, Hicks GR, Raikhel NV (2010) MODIFIED VACUOLE PHENOTYPE1 is an Arabidopsis myrosinase-associated protein involved in endomembrane protein trafficking. Plant Physiol **152**: 120-132

Aist JR (1976) Papillae and related wound plugs of plant cells. Annu Rev Phytopathol **14**: 145-163

Allan AC, Fluhr R (1997) Two distinct sources of elicited reactive oxygen species in tobacco epidermal cells. Plant Cell **9**: 1559-1572

Altenbach D, Robatzek S (2007) Pattern recognition receptors: From the cell surface to intracellular dynamics. Mol Plant-Microbe Interact **20**: 1031-1039

An Q, Huckelhoven R, Kogel KH, van Bel AJ (2006) Multivesicular bodies participate in a cell wall-associated defence response in barley leaves attacked by the pathogenic powdery mildew fungus. Cell Microbiol **8**: 1009-1019

Anelli T, Sitia R (2008) Protein quality control in the early secretory pathway. EMBO J **27**: 315-327

Apel K, Hirt H (2004) REACTIVE OXYGEN SPECIES: Metabolism, Oxidative Stress, and Signal Transduction. Annu Rev Plant Biol **55**: 373-399

Arighi CN, Hartnell LM, Aguilar RC, Haft CR, Bonifacino JS (2004) Role of the mammalian retromer in sorting of the cation-independent mannose 6-phosphate receptor. J Cell Biol **165**: 123-133

Asai T, Tena G, Plotnikova J, Willmann MR, Chiu WL, Gomez-Gomez L, Boller T, Ausubel FM, Sheen J (2002) MAP kinase signalling cascade in Arabidopsis innate immunity. Nature **415**: 977-983

Ashtamker C, Kiss V, Sagi M, Davydov O, Fluhr R (2007) Diverse subcellular locations of cryptogein-induced reactive oxygen species production in tobacco bright yellow-2 cells. Plant Physiol **143**: 1817-1826

Assaad FF, Qiu JL, Youngs H, Ehrhardt D, Zimmerli L, Kalde M, Wanner G, Peck SC, Edwards H, Ramonell K, Somerville CR, Thordal-Christensen H (2004) The PEN1 syntaxin defines a novel cellular compartment upon fungal attack and is required for the timely assembly of papillae. Mol Biol Cell **15**: 5118-5129

Baluska F, Liners F, Hlavacka A, Schlicht M, Van Cutsem P, McCurdy DW, Menzel D (2005) Cell wall pectins and xyloglucans are internalized into dividing root cells and accumulate within cell plates during cytokinesis. Protoplasma **225**: 141-155

Banno H, Hirano K, Nakamura T, Irie K, Nomoto S, Matsumoto K, Machida Y (1993) *NPK1*, a tobacco gene that encodes a protein with a domain homologous to yeast BCK1, STE11, and Byr2 protein-kinases. Mol Cell Biol **13**: 4745-4752

Barlowe C (2010) ER sheets get roughed up. Cell **143**: 665-666

Barlowe C, Orci L, Yeung T, Hosobuchi M, Hamamoto S, Salama N, Rexach MF, Ravazzola M, Amherdt M, Schekman R (1994) COPII: a membrane coat formed by Sec proteins that drive vesicle budding from the endoplasmic reticulum. Cell **77**: 895-907

Barr FA, Short B (2003) Golgins in the structure and dynamics of the Golgi apparatus. Curr Opin Cell Biol **15**: 405-413

Bassham DC, Brandizzi F, Otegui MS, Sanderfoot AA (2008) The secretory system of Arabidopsis. Arabidopsis Book **6**: e0116

Baudisch B, Klosgen RB (2012) Dual targeting of a processing peptidase into both endosymbiotic organelles mediated by a transport signal of unusual architecture. Mol Plant **5**: 494-503

Beck M, Heard W, Mbengue M, Robatzek S (2012) The INs and OUTs of pattern recognition receptors at the cell surface. Curr Opin Plant Biol **15**: 367-374

Bell CJ, Ecker JR (1994) Assignment of 30 microsatellite loci to the linkage map of Arabidopsis. Genomics **19**: 137-144

Bellincampi D, Dipierro N, Salvi G, Cervone F, De Lorenzo G (2000) Extracellular H_2O_2 induced by oligogalacturonides is not involved in the inhibition of the auxin-regulated *rolB* gene expression in tobacco leaf explants. Plant Physiol **122**: 1379-1385

Benschop JJ, Mohammed S, O'Flaherty M, Heck AJ, Slijper M, Menke FL (2007) Quantitative phosphoproteomics of early elicitor signaling in Arabidopsis. Mol Cell Proteomics **6**: 1198-1214

Berglund AK, Pujol C, Duchene AM, Glaser E (2009) Defining the determinants for dual targeting of amino acyl-tRNA synthetases to mitochondria and chloroplasts. J Mol Biol **393**: 803-814

Bhat RA, Miklis M, Schmelzer E, Schulze-Lefert P, Panstruga R (2005) Recruitment and interaction dynamics of plant penetration resistance components in a plasma membrane microdomain. Proc Natl Acad Sci U S A **102**: 3135-3140

Blume B, Nurnberger T, Nass N, Scheel D (2000) Receptor-mediated increase in cytoplasmic free calcium required for activation of pathogen defense in parsley [In Process Citation]. Plant Cell **12**: 1425-1440

Boehm M, Bonifacino JS (2001) Adaptins: the final recount. Mol Biol Cell **12**: 2907-2920

Boevink P, Oparka K, Cruz SS, Martin B, Betteridge A, Hawes C (1998) Stacks on tracks: the plant Golgi apparatus traffics on an actin/ER network. Plant J **15**: 441-447

Boller T (1995) Chemoperception of microbial signals in plant cells. Annu Rev Plant Physiol Plant Mol Biol **46**: 189-214

Boller T, Felix G (2009) A renaissance of elicitors: perception of microbe-associated molecular patterns and danger signals by pattern-recognition receptors. Annu Rev Plant Biol **60**: 379-406

Bolwell GP, Buti VS, Davies DR, Zimmerlin A (1995) The origin of the oxidative burst in plants. Free Radic Res **23**: 517-532

Bonifacino JS, Glick BS (2004) The mechanisms of vesicle budding and fusion. Cell **116**: 153-166

Boudsocq M, Willmann MR, McCormack M, Lee H, Shan L, He P, Bush J, Cheng SH, Sheen J (2010) Differential innate immune

signalling via Ca(2+) sensor protein kinases. Nature **464**: 418-422

Boulaflous A, Faso C, Brandizzi F (2008) Deciphering the Golgi apparatus: from imaging to genes. Traffic **9**: 1613-1617

Brandizzi F, Fricker M, Hawes C (2002a) A greener world: the revolution in plant bioimaging. Nat Rev Mol Cell Biol **3**: 520-530

Brandizzi F, Hanton S, daSilva LL, Boevink P, Evans D, Oparka K, Denecke J, Hawes C (2003) ER quality control can lead to retrograde transport from the ER lumen to the cytosol and the nucleoplasm in plants. Plant J **34**: 269-281

Brandizzi F, Snapp EL, Roberts AG, Lippincott-Schwartz J, Hawes C (2002b) Membrane protein transport between the endoplasmic reticulum and the Golgi in tobacco leaves is energy dependent but cytoskeleton independent: evidence from selective photobleaching. Plant Cell **14**: 1293-1309

Brick DJ, Brumlik MJ, Buckley JT, Cao JX, Davies PC, Misra S, Tranbarger TJ, Upton C (1995) A new family of lipolytic plant enzymes with members in rice, arabidopsis and maize. FEBS Lett **377**: 475-480

Brutus A, Sicilia F, Macone A, Cervone F, De Lorenzo G (2010) A domain swap approach reveals a role of the plant wall-associated kinase 1 (WAK1) as a receptor of oligogalacturonides. Proc Natl Acad Sci USA **107**: 9452-9457

Bryson K, McGuffin LJ, Marsden RL, Ward JJ, Sodhi JS, Jones DT (2005) Protein structure prediction servers at University College London. Nucleic Acids Res **33**: W36-W38

Campbell RE, Tour O, Palmer AE, Steinbach PA, Baird GS, Zacharias DA, Tsien RY (2002) A monomeric red fluorescent protein. Proc Natl Acad Sci USA **99**: 7877-7882

Carter C, Pan S, Zouhar J, Avila EL, Girke T, Raikhel NV (2004) The vegetative vacuole proteome of Arabidopsis thaliana reveals predicted and unexpected proteins. Plant Cell **16**: 3285-3303

Cervone F, Hahn MG, De Lorenzo G, Darvill A, Albersheim P (1989) Host-pathogen interactions. XXXIII. A plant protein converts a fungal pathogenesis factor into an elicitor of plant defense responses. Plant Physiol **90**: 542-548

Chen L, Hamada S, Fujiwara M, Zhu T, Thao NP, Wong HL, Krishna P, Ueda T, Kaku H, Shibuya N, Kawasaki T, Shimamoto K (2010) The Hop/Sti1-Hsp90 chaperone complex facilitates the maturation and transport of a PAMP receptor in rice innate immunity. Cell Host Microbe **7**: 185-196

Chen X, Irani NG, Friml J (2011) Clathrin-mediated endocytosis: the gateway into plant cells. Curr Opin Plant Biol **14**: 674-682

Chinchilla D, Zipfel C, Robatzek S, Kemmerling B, Nurnberger T, Jones JD, Felix G, Boller T (2007) A flagellin-induced complex of the receptor FLS2 and BAK1 initiates plant defence. Nature **448**: 497-500

Chisholm ST, Coaker G, Day B, Staskawicz BJ (2006) Host-microbe interactions: shaping the evolution of the plant immune response. Cell **124**: 803-814

Clough SJ, Bent AF (1998) Floral dip: a simplified method for Agrobacterium-mediated transformation of Arabidopsis thaliana. Plant J **16**: 735-43

Collins NC, Thordal-Christensen H, Lipka V, Bau S, Kombrink E, Qiu JL, Huckelhoven R, Stein M, Freialdenhoven A, Somerville SC, Schulze-Lefert P (2003) SNARE-protein-mediated disease resistance at the plant cell wall. Nature **425**: 973-977

Conner SD, Schmid SL (2003) Regulated portals of entry into the cell. Nature **422**: 37-44

Cote F, Hahn MG (1994) Oligosaccharins: structures and signal transduction. Plant Mol Biol **26**: 1379-1411

D'Enfert C, Wuestehube LJ, Lila T, Schekman R (1991) Sec12p-dependent membrane binding of the small GTP-binding protein Sar1p promotes formation of transport vesicles from the ER. J Cell Biol **114**: 663-670

Dacks JB, Poon PP, Field MC (2008) Phylogeny of endocytic components yields insight into the process of nonendosymbiotic organelle evolution. Proc Natl Acad Sci U S A **105**: 588-593

Dardick C, Ronald P (2006) Plant and animal pathogen recognition receptors signal through non-RD kinases. Plos Pathogens **2**: 14-28

Darvill AG, Albersheim P (1984) Phytoalexins and their elicitors - A defense against microbial infection in plants. Annu Rev Plant Physiol **35**: 243-275

daSilva LL, Snapp EL, Denecke J, Lippincott-Schwartz J, Hawes C, Brandizzi F (2004) Endoplasmic reticulum export sites and Golgi bodies behave as single mobile secretory units in plant cells. Plant Cell **16**: 1753-1771

daSilva LL, Taylor JP, Hadlington JL, Hanton SL, Snowden CJ, Fox SJ, Foresti O, Brandizzi F, Denecke J (2005) Receptor salvage

from the prevacuolar compartment is essential for efficient vacuolar protein targeting. Plant Cell **17**: 132-148

Davidson HW (1995) Wortmannin causes mistargeting of procathepsin D. evidence for the involvement of a phosphatidylinositol 3-kinase in vesicular transport to lysosomes. J Cell Biol **130**: 797-805

De Lorenzo G, D'Ovidio R, Cervone F (2001) The role of polygacturonase-inhibiting proteins (PGIPs) in defense against pathogenic fungi. Annu Rev Phytopathol **39**: 313-335

De Lorenzo G, Ferrari S (2002) Polygalacturonase-inhibiting proteins in defense against phytopathogenic fungi. Curr Opin Plant Biol **5**: 295-299

Decreux A, Thomas A, Spies B, Brasseur R, Van Cutsem P, Messiaen J (2006) In vitro characterization of the homogalacturonan-binding domain of the wall-associated kinase WAK1 using site-directed mutagenesis. Phytochemistry **67**: 1068-1079

Denoux C, Galletti R, Mammarella N, Gopalan S, Werck D, De Lorenzo G, Ferrari S, Ausubel FM, Dewdney J (2008) Activation of defense response pathways by OGs and Flg22 elicitors in Arabidopsis seedlings. Mol Plant **1**: 423-445

Donohoe BS, Kang BH, Staehelin LA (2007) Identification and characterization of COPIa- and COPIb-type vesicle classes associated with plant and algal Golgi. Proc Natl Acad Sci U S A **104**: 163-168

Driouich A, Jauneau A, Staehelin LA (1997) 7-Dehydrobrefeldin A, a naturally occurring brefeldin A derivative, inhibits secretion and causes a cis-to-trans breakdown of Golgi stacks in plant cells. Plant Physiol **113**: 487-492

Dumas B, Sailland A, Cheviet JP, Freyssinet G, Pallett K (1993) Identification of barley oxalate oxidase as a germin-like protein. C R Acad Sci III **316**: 793-798

Eichmann R, Huckelhoven R (2008) Accommodation of powdery mildew fungi in intact plant cells. J Plant Physiol **165**: 5-18

Emanuelsson O, Brunak S, von Heijne G, Nielsen H (2007) Locating proteins in the cell using TargetP, SignalP and related tools. Nat Protoc **2**: 953-971

Emanuelsson O, Nielsen H, Brunak S, von Heijne G (2000) Predicting subcellular localization of proteins based on their N-terminal amino acid sequence. J Mol Biol **300**: 1005-1016

Estevez JM, Kieliszewski MJ, Khitrov N, Somerville C (2006) Characterization of synthetic hydroxyproline-rich proteoglycans with arabinogalactan protein and extensin motifs in Arabidopsis. Plant Physiol **142**: 458-470

Faso C, Chen YN, Tamura K, Held M, Zemelis S, Marti L, Saravanan R, Hummel E, Kung L, Miller E, Hawes C, Brandizzi F (2009) A missense mutation in the Arabidopsis COPII coat protein Sec24A induces the formation of clusters of the endoplasmic reticulum and Golgi apparatus. Plant Cell **21**: 3655-3671

Felix G, Duran JD, Volko S, Boller T (1999) Plants have a sensitive perception system for the most conserved domain of bacterial flagellin. Plant J **18**: 265-276

Foresti O, Denecke J (2008) Intermediate organelles of the plant secretory pathway: identity and function. Traffic **9**: 1599-1612

Fotin A, Cheng Y, Sliz P, Grigorieff N, Harrison SC, Kirchhausen T, Walz T (2004) Molecular model for a complete clathrin lattice from electron cryomicroscopy. Nature **432**: 573-579

Frahry G, Schopfer P (1998) Hydrogen peroxide production by roots and its stimulation by exogenous NADH. Physiol Plant **103**: 395-404

Frei dit FN, Robatzek S (2009) Trafficking vesicles: pro or contra pathogens? Curr Opin Plant Biol **12**: 437-443

Gadella TWJ, Jr., Van der Krogt GNM, Bisseling T (1999) GFP-based FRET microscopy in living plant cells. Trends Plant Sci **4**: 287-291

Galletti R, Ferrari S, De Lorenzo G (2011) Arabidopsis MPK3 and MPK6 play different roles in basal and oligogalacturonide- or flagellin-induced resistance against *Botrytis cinerea*. Plant Physiol **157**: 804-814

Gerber IB, Dubery IA (2003) Fluorescence microplate assay for the detection of oxidative burst products in tobacco cell suspensions using 2',7'-dichlorofluorescein. Methods Cell Sci **25**: 115-122

Godiard L, Grant MR, Dietrich RA, Kiedrowski S, Dangl JL (1994) Perception and response in plant disease resistance. Curr Opin Genet Dev **4**: 662-671

Gomez-Gomez L, Boller T (2000) FLS2: an LRR receptor-like kinase involved in the perception of the bacterial elicitor flagellin in Arabidopsis. Mol Cell **5**: 1003-1011

Griesbeck O, Baird GS, Campbell RE, Zacharias DA, Tsien RY (2001) Reducing the environmental sensitivity of yellow fluorescent protein. Mechanism and applications. J Biol Chem **276**: 29188-29194

Gross P, Julius C, Schmelzer E, Hahlbrock K (1993) Translocation of cytoplasm and nucleus to fungal penetration sites is associated with depolymerization of microtubules and

defence gene activation in infected, cultured parsley cells. EMBO J **12**: 1735-1744

Gruenberg J, van der Goot FG (2006) Mechanisms of pathogen entry through the endosomal compartments. Nat Rev Mol Cell Biol **7**: 495-504

Hanton SL, Brandizzi F (2006) Fluorescent proteins as markers in the plant secretory pathway. Microsc Res Tech **69**: 152-159

Hanton SL, Chatre L, Renna L, Matheson LA, Brandizzi F (2007) De novo formation of plant endoplasmic reticulum export sites is membrane cargo induced and signal mediated. Plant Physiol **143**: 1640-1650

Haseloff J, Siemering KR, Prasher DC, Hodge S (1997) Removal of a cryptic intron and subcellular localization of green fluorescent protein are required to mark transgenic *Arabidopsis* plants brightly. Proc Natl Acad Sci USA **94**: 2122-2127

Haweker H, Rips S, Koiwa H, Salomon S, Saijo Y, Chinchilla D, Robatzek S, Von Schaewen A (2010) Pattern recognition receptors require N-glycosylation to mediate plant immunity. J Biol Chem **285**: 4629-4636

Hawes C, Saint-Jore C, Martin B, Zheng HQ (2001) ER confirmed as the location of mystery organelles in Arabidopsis plants expressing GFP! Trends Plant Sci **6**: 245-246

Hayashi Y, Yamada K, Shimada T, Matsushima R, Nishizawa NK, Nishimura M, Hara-Nishimura I (2001) A proteinase-storing body that prepares for cell death or stresses in the epidermal cells of Arabidopsis. Plant Cell Physiol **42**: 894-899

Heese A, Ludwig AA, Jones JD (2005) Rapid phosphorylation of a syntaxin during the Avr9/Cf-9-race-specific signaling pathway. Plant Physiol **138**: 2406-2416

Hoffmann A, Nebenfuhr A (2004) Dynamic rearrangements of transvacuolar strands in BY-2 cells imply a role of myosin in remodeling the plant actin cytoskeleton. Protoplasma **224**: 201-210

Hoglund A, Donnes P, Blum T, Adolph HW, Kohlbacher O (2006) MultiLoc: prediction of protein subcellular localization using N-terminal targeting sequences, sequence motifs and amino acid composition. Bioinformatics **22**: 1158-1165

Hong Z, Bednarek SY, Blumwald E, Hwang I, Jurgens G, Menzel D, Osteryoung KW, Raikhel NV, Shinozaki K, Tsutsumi N, Verma DP (2003) A unified nomenclature for Arabidopsis dynamin-related large GTPases based on homology and possible functions. Plant Mol Biol **53**: 261-265

Hu J, Shibata Y, Zhu PP, Voss C, Rismanchi N, Prinz WA, Rapoport TA, Blackstone C (2009) A class of dynamin-like GTPases involved in the generation of the tubular ER network. Cell **138**: 549-561

Huckelhoven R (2007) Transport and secretion in plant-microbe interactions. Curr Opin Plant Biol

Huffaker A, Pearce G, Ryan CA (2006) An endogenous peptide signal in Arabidopsis activates components of the innate immune response. Proc Natl Acad Sci USA **103**:

Huffaker A, Ryan CA (2007) Endogenous peptide defense signals in Arabidopsis differentially amplify signaling for the innate immune response. Proc Natl Acad Sci USA **104**: 10732-10736

Hwang I, Robinson DG (2009) Transport vesicle formation in plant cells. Curr Opin Plant Biol **12**: 660-669

Ishikawa M, Soyano T, Nishihama R, Machida Y (2002) The NPK1 mitogen-activated protein kinase kinase kinase contains a

functional nuclear localization signal at the binding site for the NACK1 kinesin-like protein. Plant Journal **32**: 789-798

Jahn R, Scheller RH (2006) SNAREs--engines for membrane fusion. Nat Rev Mol Cell Biol **7**: 631-643

Jares-Erijman EA, Jovin TM (2003) FRET imaging. Nat Biotechnol **21**: 1387-1395

Jelitto-Van Dooren EP, Vidal S, Denecke J (1999) Anticipating endoplasmic reticulum stress. A novel early response before pathogenesis-related gene induction. Plant Cell **11**: 1935-1944

Johnson LN, Noble ME, Owen DJ (1996a) Active and inactive protein kinases: structural basis for regulation. Cell **85**: 149-158

Johnson LN, Noble MEM, Owen DJ (1996b) Active and inactive protein kinases: Structural basis for regulation. Cell **85**: 149-158

Jonak C, Okresz L, Bogre L, Hirt H (2002) Complexity, cross talk and integration of plant MAP kinase signalling. Curr Opin Plant Biol **5**: 415-424

Jones JD, Dangl JL (2006) The plant immune system. Nature **444**: 323-329

Jouannic S, Hamal A, Leprince AS, Tregear JW, Kreis M, Henry Y (1999) Plant MAP kinase kinase kinases structure, classification and evolution. Gene **233**: 1-11

Karimi M, Inze D, Depicker A (2002) GATEWAY vectors for Agrobacterium-mediated plant transformation. Trends Plant Sci **7**: 193-195

Khokhlatchev AV, Canagarajah B, Wilsbacher J, Robinson M, Atkinson M, Goldsmith E, Cobb MH (1998) Phosphorylation

of the MAP kinase ERK2 promotes its homodimerization and nuclear translocation. Cell **93**: 605-615

Kim DH, Eu YJ, Yoo CM, Kim YW, Pih KT, Jin JB, Kim SJ, Stenmark H, Hwang I (2001) Trafficking of phosphatidylinositol 3-phosphate from the trans-Golgi network to the lumen of the central vacuole in plant cells. Plant Cell **13**: 287-301

Kirchhausen T (2000) Three ways to make a vesicle. Nat Rev Mol Cell Biol **1**: 187-198

Knebel W, Quader H, Schnepf E (1990) Mobile and immobile endoplasmic reticulum in onion bulb epidermis cells: short- and long-term observations with a confocal laser scanning microscope. Eur J Cell Biol **52**: 328-340

Koh S, Andre A, Edwards H, Ehrhardt D, Somerville S (2005) Arabidopsis thaliana subcellular responses to compatible Erysiphe cichoracearum infections. Plant J **44**: 516-529

Kohorn BD, Johansen S, Shishido A, Todorova T, Martinez R, Defeo E, Obregon P. Pectin activation of MAP kinase and gene expression is WAK2 dependent. The Plant Journal . 2009.
Ref Type: In Press

Kohorn BD, Kobayashi M, Johansen S, Friedman HP, Fischer A, Byers N (2006) Wall-associated kinase 1 (WAK1) is crosslinked in endomembranes, and transport to the cell surface requires correct cell-wall synthesis. J Cell Sci **119**: 2282-2290

Kombrink E, Somssich IE (1995) Defense responses of plants to pathogens. Adv Bot Res **21**: 1-34

Konieczny A, Ausubel FM (1993) A procedure for mapping Arabidopsis mutations using co-dominant ecotype-specific PCR-based markers. Plant J **4**: 403-410

Konopka CA, Schleede JB, Skop AR, Bednarek SY (2006) Dynamin and cytokinesis. Traffic **7**: 239-247

Kovtun Y, Chiu WL, Tena G, Sheen J (2000) Functional analysis of oxidative stress-activated mitogen-activated protein kinase cascade in plants. Proc Natl Acad Sci USA **97**: 2940-2945

Kovtun Y, Chiu WL, Zeng W, Sheen J (1998) Suppression of auxin signal transduction by a MAPK cascade in higher plants. Nature **395**: 716-720

Krol E, Mentzel T, Chinchilla D, Boller T, Felix G, Kemmerling B, Postel S, Arents M, Jeworutzki E, Al Rasheid KA, Becker D, Hedrich R (2010) Perception of the Arabidopsis danger signal peptide 1 involves the pattern recognition receptor AtPEPR1 and its close homologue AtPEPR2. J Biol Chem **285**: 13471-13479

Krupa A, Preethi G, Srinivasan N (2004) Structural modes of stabilization of permissive phosphorylation sites in protein kinases: distinct strategies in Ser/Thr and Tyr kinases. J Mol Biol **339**: 1025-1039

Krysan PJ, Jester PJ, Gottwald JR, Sussman MR (2002) An Arabidopsis mitogen-activated protein kinase kinase kinase gene family encodes essential positive regulators of cytokinesis. Plant Cell **14**: 1109-1120

Kunze G, Zipfel C, Robatzek S, Niehaus K, Boller T, Felix G (2004) The N Terminus of bacterial elongation factor Tu elicits innate immunity in Arabidopsis plants. Plant Cell **16**: 3496-3507

Kwon C, Bednarek P, Schulze-Lefert P (2008a) Secretory pathways in plant immune responses. Plant Physiol **147**: 1575-1583

Kwon C, Neu C, Pajonk S, Yun HS, Lipka U, Humphry M, Bau S, Straus M, Kwaaitaal M, Rampelt H, El Kasmi F, Jurgens G, Parker J, Panstruga R, Lipka V, Schulze-Lefert P (2008b) Co-option of a default secretory pathway for plant immune responses. Nature **451**: 835-U10

Kyriakis JM, Avruch J (1996) Protein kinase cascades activated by stress and inflammatory cytokines. BioEssays **18**: 567-577

Lacombe S, Rougon-Cardoso A, Sherwood E, Peeters N, Dahlbeck D, van Esse HP, Smoker M, Rallapalli G, Thomma BP, Staskawicz B, Jones JD, Zipfel C (2010) Interfamily transfer of a plant pattern-recognition receptor confers broad-spectrum bacterial resistance. Nat Biotechnol **28**: 365-369

Langhans M, Marcote MJ, Pimpl P, Virgili-Lopez G, Robinson DG, Aniento F (2008) In vivo trafficking and localization of p24 proteins in plant cells. Traffic **9**: 770-785

Langmead B, Trapnell C, Pop M, Salzberg SL (2009) Ultrafast and memory-efficient alignment of short DNA sequences to the human genome. Genome Biol **10**: R25

Latijnhouwers M, Gillespie T, Boevink P, Kriechbaumer V, Hawes C, Carvalho CM (2007) Localization and domain characterization of Arabidopsis golgin candidates. J Exp Bot **58**: 4373-4386

Latijnhouwers M, Hawes C, Carvalho C (2005) Holding it all together? Candidate proteins for the plant Golgi matrix. Curr Opin Plant Biol **8**: 632-639

Lecourieux D, Mazars C, Pauly N, Ranjeva R, Pugin A (2002) Analysis and effects of cytosolic free calcium increases in

response to elicitors in Nicotiana plumbaginifolia cells. Plant Cell **14**: 2627-2641

Lee H, Chah OK, Sheen J (2011a) Stem-cell-triggered immunity through CLV3p-FLS2 signalling. Nature **473**: 376-379

Lee HY, Bowen CH, Popescu GV, Kang HG, Kato N, Ma S, Dinesh-Kumar S, Snyder M, Popescu SC (2011b) Arabidopsis RTNLB1 and RTNLB2 Reticulon-like proteins regulate intracellular trafficking and activity of the FLS2 immune receptor. Plant Cell **23**: 3374-3391

Lee SW, Han SW, Sririyanum M, Park CJ, Seo YS, Ronald PC (2009) A type I-secreted, sulfated peptide triggers XA21-mediated innate immunity. Science **326**: 850-853

Lefebvre B, Furt F, Hartmann MA, Michaelson LV, Carde JP, Sargueil-Boiron F, Rossignol M, Napier JA, Cullimore J, Bessoule JJ, Mongrand S (2007) Characterization of lipid rafts from Medicago truncatula root plasma membranes: a proteomic study reveals the presence of a raft-associated redox system. Plant Physiol **144**: 402-418

Lefebvre B, Klaus-Heisen D, Pietraszewska-Bogiel A, Herve C, Camut S, Auriac MC, Gasciolli V, Nurisso A, Gadella TW, Cullimore J (2012) Role of N-glycosylation sites and CXC motifs in trafficking of medicago truncatula Nod factor perception protein to plasma membrane. J Biol Chem **287**: 10812-10823

Li H, Ruan J, Durbin R (2008) Mapping short DNA sequencing reads and calling variants using mapping quality scores. Genome Res **18**: 1851-1858

Li J, Nam KH (2002) Regulation of brassinosteroid signaling by a GSK3/SHAGGY-like kinase. Science **295**: 1299-1301

Li J, Zhao-Hui C, Batoux M, Nekrasov V, Roux M, Chinchilla D, Zipfel C, Jones JD (2009a) Specific ER quality control components required for biogenesis of the plant innate immune receptor EFR. Proc Natl Acad Sci USA **106**: 15973-15978

Li JF, Park E, Von Arnim AG, Nebenfuhr A (2009b) The FAST technique: a simplified Agrobacterium-based transformation method for transient gene expression analysis in seedlings of Arabidopsis and other plant species. Plant Methods **5**: 6

Lipka U, Fuchs R, Lipka V (2008) Arabidopsis non-host resistance to powdery mildews. Curr Opin Plant Biol **11**: 404-411

Lipka V, Dittgen J, Bednarek P, Bhat R, Wiermer M, Stein M, Landtag J, Brandt W, Rosahl S, Scheel D, Llorente F, Molina A, Parker J, Somerville S, Schulze-Lefert P (2005) Pre- and postinvasion defenses both contribute to nonhost resistance in Arabidopsis. Science **310**: 1180-1183

Lipka V, Kwon C, Panstruga R (2007) SNARE-Ware: The role of SNARE-Domain proteins in plant biology. Annu Rev Cell Dev Biol **23**: 147-174

Livanos P, Galatis B, Quader H, Apostolakos P (2012) Disturbance of reactive oxygen species homeostasis induces atypical tubulin polymer formation and affects mitosis in root-tip cells of Triticum turgidum and Arabidopsis thaliana. Cytoskeleton (Hoboken) **69**: 1-21

Lotze MT, Zeh HJ, Rubartelli A, Sparvero LJ, Amoscato AA, Washburn NR, Devera ME, Liang X, Tor M, Billiar T (2007) The grateful dead: damage-associated molecular pattern molecules and reduction/oxidation regulate immunity. Immunol Rev **220**: 60-81

Lu D, Wu S, Gao X, Zhang Y, Shan L, He P (2010) A receptor-like cytoplasmic kinase, BIK1, associates with a flagellin receptor complex to initiate plant innate immunity. Proc Natl Acad Sci U S A **107**: 496-501

Lu X, Tintor N, Mentzel T, Kombrink E, Boller T, Robatzek S, Schulze-Lefert P, Saijo Y (2009) Uncoupling of sustained MAMP receptor signaling from early outputs in an Arabidopsis endoplasmic reticulum glucosidase II allele. Proc Natl Acad Sci U S A **106**: 22522-22527

Maple J, Moller SG (2007) Mutagenesis in Arabidopsis. Methods Mol Biol **362**: 197-206

Matsuoka K, Bassham DC, Raikhel NV, Nakamura K (1995) Different sensitivity to wortmannin of two vacuolar sorting signals indicates the presence of distinct sorting machineries in tobacco cells. J Cell Biol **130**: 1307-1318

Matz MV, Fradkov AF, Labas YA, Savitsky AP, Zaraisky AG, Markelov ML, Lukyanov SA (1999) Fluorescent proteins from nonbioluminescent Anthozoa species. Nat Biotechnol **17**: 969-973

Matzinger P (2002) The danger model: a renewed sense of self. Science **296**: 301-305

Maxfield FR, McGraw TE (2004) Endocytic recycling. Nat Rev Mol Cell Biol **5**: 121-132

Melotto M, Underwood W, Koczan J, Nomura K, He SY (2006) Plant stomata function in innate immunity against bacterial invasion. Cell **126**: 969-980

Miller E, Antonny B, Hamamoto S, Schekman R (2002) Cargo selection into COPII vesicles is driven by the Sec24p subunit. EMBO J **21**: 6105-6113

Miller EA, Barlowe C (2010) Regulation of coat assembly--sorting things out at the ER. Curr Opin Cell Biol **22**: 447-453

Miller EA, Beilharz TH, Malkus PN, Lee MC, Hamamoto S, Orci L, Schekman R (2003) Multiple cargo binding sites on the COPII subunit Sec24p ensure capture of diverse membrane proteins into transport vesicles. Cell **114**: 497-509

Miya A, Albert P, Shinya T, Desaki Y, Ichimura K, Shirasu K, Narusaka Y, Kawakami N, Kaku H, Shibuya N (2007) CERK1, a LysM receptor kinase, is essential for chitin elicitor signaling in Arabidopsis. Proc Natl Acad Sci USA **104**: 19613-19618

Mizoguchi T, Irie K, Hirayama T, Hayashida N, YamaguchiShinozaki K, Matsumoto K, Shinozaki K (1996) A gene encoding a mitogen-activated protein kinase kinase kinase is induced simultaneously with genes for a mitogen-activated protein kinase and an S6 ribosomal protein kinase by touch, cold, and water stress in Arabidopsis thaliana. Proc Natl Acad Sci U S A **93**: 765-769

Mongrand S, Morel J, Laroche J, Claverol S, Carde JP, Hartmann MA, Bonneu M, Simon-Plas F, Lessire R, Bessoule JJ (2004) Lipid rafts in higher plant cells: purification and characterization of Triton X-100-insoluble microdomains from tobacco plasma membrane. J Biol Chem **279**: 36277-36286

Morel J, Claverol S, Mongrand S, Furt F, Fromentin J, Bessoule JJ, Blein JP, Simon-Plas F (2006) Proteomics of plant detergent-resistant membranes. Mol Cell Proteomics **5**: 1396-1411

Morrison DK, Davis RJ (2003) Regulation of MAP kinase signaling modules by scaffold proteins in mammals. Annu Rev Cell Dev Biol **19**: 91-118

Mossessova E, Bickford LC, Goldberg J (2003) SNARE selectivity of the COPII coat. Cell **114**: 483-495

Nagai T, Ibata K, Park ES, Kubota M, Mikoshiba K, Miyawaki A (2002) A variant of yellow fluorescent protein with fast and efficient maturation for cell-biological applications. Nat Biotechnol **20**: 87-90

Nakagami H, Pitzschke A, Hirt H (2005) Emerging MAP kinase pathways in plant stress signalling. Trends Plant Sci **10**: 339-346

Nakagawa T, Kaku H, Shimoda Y, Sugiyama A, Shimamura M, Takanashi K, Yazaki K, Aoki T, Shibuya N, Kouchi H (2011) From defense to symbiosis: limited alterations in the kinase domain of LysM receptor-like kinases are crucial for evolution of legume-Rhizobium symbiosis. Plant J **65**: 169-180

Nakano A (2002) Spinning-disk confocal microscopy -- a cutting-edge tool for imaging of membrane traffic. Cell Struct Funct **27**: 349-355

Nakano RT, Matsushima R, Nagano AJ, Fukao Y, Fujiwara M, Kondo M, Nishimura M, Hara-Nishimura I (2012) ERMO3/MVP1/GOLD36 Is Involved in a Cell Type-Specific Mechanism for Maintaining ER Morphology in Arabidopsis thaliana. PLoS ONE **7**: e49103

Nakashima M, Hirano K, Nakashima S, Banno H, Nishihama R, Machida Y (1998) The expression pattern of the gene for NPK1 protein kinase related to mitogen-activated protein kinase kinase kinase (MAPKKK) in a tobacco plant: Correlation with cell proliferation. Plant Cell Physiol **39**: 690-700

Nanjo Y, Oka H, Ikarashi N, Kaneko K, Kitajima A, Mitsui T, Munoz FJ, Rodriguez-Lopez M, Baroja-Fernandez E,

Pozueta-Romero J (2006) Rice plastidial N-glycosylated nucleotide pyrophosphatase/phosphodiesterase is transported from the ER-golgi to the chloroplast through the secretory pathway. Plant Cell **18**: 2582-2592

Navarro L, Zipfel C, Rowland O, Keller I, Robatzek S, Boller T, Jones JD (2004) The transcriptional innate immune response to flg22. Interplay and overlap with Avr gene-dependent defense responses and bacterial pathogenesis. Plant Physiol **135**: 1113-1128

Nebenfuhr A, Gallagher LA, Dunahay TG, Frohlick JA, Mazurkiewicz AM, Meehl JB, Staehelin LA (1999) Stop-and-go movements of plant Golgi stacks are mediated by the acto-myosin system. Plant Physiol **121**: 1127-1142

Nekrasov V, Li J, Batoux M, Roux M, Chu ZH, Lacombe S, Rougon A, Bittel P, Kiss-Papp M, Chinchilla D, van Esse HP, Jorda L, Schwessinger B, Nicaise V, Thomma BP, Molina A, Jones JD, Zipfel C (2009) Control of the pattern-recognition receptor EFR by an ER protein complex in plant immunity. EMBO J **28**: 3428-3438

Nelson BK, Cai X, Nebenfuhr A (2007) A multicolored set of in vivo organelle markers for co-localization studies in Arabidopsis and other plants. Plant Journal **51**: 1126-1136

Neumann U, Brandizzi F, Hawes C (2003) Protein transport in plant cells: in and out of the Golgi. Ann Bot **92**: 167-180

Niemes S, Labs M, Scheuring D, Krueger F, Langhans M, Jesenofsky B, Robinson DG, Pimpl P (2010) Sorting of plant vacuolar proteins is initiated in the ER. Plant J **62**: 601-614

Nishihama R, Banno H, Kawahara E, Irie K, Machida Y (1997) Possible involvement of differential splicing in regulation of the activity of Arabidopsis ANP1 that is related to mitogen-

activated protein kinase kinase kinases (MAPKKKs). Plant J **12**: 39-48

Nomura K, DebRoy S, Lee YH, Pumplin N, Jones J, He SY (2006) A bacterial virulence protein suppresses host innate immunity to cause plant disease. Science **313**: 220-223

Nuhse TS, Bottrill AR, Jones AM, Peck SC (2007) Quantitative phosphoproteomic analysis of plasma membrane proteins reveals regulatory mechanisms of plant innate immune responses. Plant J **51**: 931-940

Nurnberger T, Brunner F, Kemmerling B, Piater L (2004) Innate immunity in plants and animals: striking similarities and obvious differences. Immunol Rev **198**: 249-266

Orso G, Pendin D, Liu S, Tosetto J, Moss TJ, Faust JE, Micaroni M, Egorova A, Martinuzzi A, McNew JA, Daga A (2009) Homotypic fusion of ER membranes requires the dynamin-like GTPase atlastin. Nature **460**: 978-983

Paredez AR, Somerville CR, Ehrhardt DW (2006) Visualization of cellulose synthase demonstrates functional association with microtubules. Science **312**: 1491-1495

Park CJ, Bart R, Chern M, Canlas PE, Bai W, Ronald PC (2010) Overexpression of the endoplasmic reticulum chaperone BiP3 regulates XA21-mediated innate immunity in rice. PLoS ONE **5**: e9262

Patterson GH, Lippincott-Schwartz J (2002) A photoactivatable GFP for selective photolabeling of proteins and cells. Science **297**: 1873-1877

Paul MJ, Frigerio L (2007) Coated vesicles in plant cells. Semin Cell Dev Biol **18**: 471-478

Pedley KF, Martin GB (2005) Role of mitogen-activated protein kinases in plant immunity. Curr Opin Plant Biol **8**: 541-547

Pelham HR, Roberts LM, Lord JM (1992) Toxin entry: how reversible is the secretory pathway? Trends Cell Biol **2**: 183-185

Perrin R, Wilkerson C, Keegstra K (2001) Golgi enzymes that synthesize plant cell wall polysaccharides: finding and evaluating candidates in the genomic era. Plant Mol Biol **47**: 115-130

Persson S, Paredez A, Carroll A, Palsdottir H, Doblin M, Poindexter P, Khitrov N, Auer M, Somerville CR (2007) Genetic evidence for three unique components in primary cell-wall cellulose synthase complexes in Arabidopsis. Proc Natl Acad Sci U S A **104**: 15566-15571

Pimpl P, Hanton SL, Taylor JP, Pinto-daSilva LL, Denecke J (2003) The GTPase ARF1p controls the sequence-specific vacuolar sorting route to the lytic vacuole. Plant Cell **15**: 1242-1256

Pimpl P, Taylor JP, Snowden C, Hillmer S, Robinson DG, Denecke J (2006) Golgi-mediated vacuolar sorting of the endoplasmic reticulum chaperone BiP may play an active role in quality control within the secretory pathway. Plant Cell **18**: 198-211

Postel S, Kufner I, Beuter C, Mazzotta S, Schwedt A, Borlotti A, Halter T, Kemmerling B, Nurnberger T (2010) The multifunctional leucine-rich repeat receptor kinase BAK1 is implicated in Arabidopsis development and immunity. Eur J Cell Biol **89**: 169-174

Prasher DC, Eckenrode VK, Ward WW, Prendergast FG, Cormier MJ (1992) Primary structure of the Aequorea victoria green-fluorescent protein. Gene **111**: 229-233

Prinz WA, Grzyb L, Veenhuis M, Kahana JA, Silver PA, Rapoport TA (2000) Mutants affecting the structure of the cortical endoplasmic reticulum in Saccharomyces cerevisiae. J Cell Biol **150**: 461-474

Radhamony RN, Theg SM (2006) Evidence for an ER to Golgi to chloroplast protein transport pathway. Trends Cell Biol **16**: 385-387

Ritzenthaler C, Nebenfuhr A, Movafeghi A, Stussi-Garaud C, Behnia L, Pimpl P, Staehelin LA, Robinson DG (2002) Reevaluation of the effects of brefeldin A on plant cells using tobacco Bright Yellow 2 cells expressing Golgi-targeted green fluorescent protein and COPI antisera. Plant Cell **14**: 237-261

Rizzo MA, Springer GH, Granada B, Piston DW (2004) An improved cyan fluorescent protein variant useful for FRET. Nat Biotechnol **22**: 445-449

Robatzek S (2007) Vesicle trafficking in plant immune responses. Cell Microbiol **9**: 1-8

Robatzek S, Chinchilla D, Boller T (2006) Ligand-induced endocytosis of the pattern recognition receptor FLS2 in Arabidopsis. Genes Dev **20**: 537-542

Robinson DG, Oliviusson P, Hinz G (2005) Protein sorting to the storage vacuoles of plants: a critical appraisal. Traffic **6**: 615-625

Rojo E, Denecke J (2008) What is moving in the secretory pathway of plants? Plant Physiol **147**: 1493-1503

Roos W, Evers S, Hieke M, Tschope M, Schumann B (1998) Shifts of intracellular pH distribution as a part of the signal mechanism leading to the elicitation of benzophenanthridine alkaloids .

Phytoalexin biosynthesis in cultured cells of eschscholtzia californica. Plant Physiol **118**: 349-364

Roux M, Schwessinger B, Albrecht C, Chinchilla D, Jones A, Holton N, Malinovsky FG, Tor M, De Vries S, Zipfel C (2011) The arabidopsis leucine-rich repeat receptor-like kinases BAK1/SERK3 and BKK1/SERK4 are required for innate immunity to Hemibiotrophic and Biotrophic pathogens. Plant Cell **23**: 2440-2455

Rubartelli A, Lotze MT (2007) Inside, outside, upside down: damage-associated molecular-pattern molecules (DAMPs) and redox. Trends Immunol **28**: 429-436

Runions J, Brach T, Kuhner S, Hawes C (2006) Photoactivation of GFP reveals protein dynamics within the endoplasmic reticulum membrane. J Exp Bot **57**: 43-50

Saijo Y, Tintor N, Lu XL, Rauf P, Pajerowska-Mukhtar K, Haweker H, Dong XN, Robatzek S, Schulze-Lefert P (2009) Receptor quality control in the endoplasmic reticulum for plant innate immunity. EMBO J **28**: 3439-3449

Savatin DV, Ferrari S, Sicilia F, De Lorenzo G (2011) Oligogalacturonide-auxin antagonism does not require posttranscriptional gene silencing or stabilization of auxin response repressors in Arabidopsis. Plant Physiol **157**: 1163-1174

Schu PV, Takegawa K, Fry MJ, Stack JH, Waterfield MD, Emr SD (1993) Phosphatidylinositol 3-kinase encoded by yeast VPS34 gene essential for protein sorting. Science **260**: 88-91

Schulze B, Mentzel T, Jehle AK, Mueller K, Beeler S, Boller T, Felix G, Chinchilla D (2010) Rapid heteromerization and phosphorylation of ligand-activated plant transmembrane

receptors and their associated kinase BAK1. J Biol Chem **285**: 9444-9451

Schwessinger B, Zipfel C (2008) News from the frontline: recent insights into PAMP-triggered immunity in plants. Curr Opin Plant Biol **11**: 389-395

Segui-Simarro JM, Coronado MJ, Staehelin LA (2008) The mitochondrial cycle of Arabidopsis shoot apical meristem and leaf primordium meristematic cells is defined by a perinuclear tentaculate/cage-like mitochondrion. Plant Physiol **148**: 1380-1393

Shaner NC, Campbell RE, Steinbach PA, Giepmans BN, Palmer AE, Tsien RY (2004) Improved monomeric red, orange and yellow fluorescent proteins derived from Discosoma sp. red fluorescent protein. Nat Biotechnol **22**: 1567-1572

Shaner NC, Steinbach PA, Tsien RY (2005) A guide to choosing fluorescent proteins. Nat Methods **2**: 905-909

Shih SC, Sloper-Mould KE, Hicke L (2000) Monoubiquitin carries a novel internalization signal that is appended to activated receptors. EMBO J **19**: 187-198

Siemering KR, Golbik R, Sever R, Haseloff J (1996) Mutations that suppress the thermosensitivity of green fluorescent protein. Curr Biol **6**: 1653-1663

Soyano T, Nishihama R, Morikiyo K, Ishikawa M, Machida Y (2003) Nqk1/Ntmek1 Is A MAPKK that acts in the NPK1 MAPKKK-mediated MAPK cascade and is required for plant cytokinesis. Genes & Development **17**: 1055-1067

Spang A (2008) The life cycle of a transport vesicle. Cell Mol Life Sci **65**: 2781-2789

Sparkes I, Tolley N, Aller I, Svozil J, Osterrieder A, Botchway S, Mueller C, Frigerio L, Hawes C (2010) Five Arabidopsis reticulon isoforms share endoplasmic reticulum location, topology, and membrane-shaping properties. Plant Cell **22**: 1333-1343

Sparkes IA, Ketelaar T, de Ruijter NC, Hawes C (2009) Grab a Golgi: laser trapping of Golgi bodies reveals in vivo interactions with the endoplasmic reticulum. Traffic **10**: 567-571

Spear ED, Ng DT (2003) Stress tolerance of misfolded carboxypeptidase Y requires maintenance of protein trafficking and degradative pathways. Mol Biol Cell **14**: 2756-2767

Stagg SM, LaPointe P, Balch WE (2007) Structural design of cage and coat scaffolds that direct membrane traffic. Curr Opin Struct Biol **17**: 221-228

Stamnes MA, Rothman JE (1993) The binding of AP-1 clathrin adaptor particles to Golgi membranes requires ADP-ribosylation factor, a small GTP-binding protein. Cell **73**: 999-1005

Stefano G, Renna L, Hanton SL, Chatre L, Haas TA, Brandizzi F (2006) ARL1 plays a role in the binding of the GRIP domain of a peripheral matrix protein to the Golgi apparatus in plant cells. Plant Mol Biol **61**: 431-449

Sup YH, Panstruga R, Schulze-Lefert P, Kwon C (2008) Ready to fire: Secretion in plant immunity. Plant Signal Behav **3**: 505-508

Swarbreck D, Wilks C, Lamesch P, Berardini TZ, Garcia-Hernandez M, Foerster H, Li D, Meyer T, Muller R, Ploetz L, Radenbaugh A, Singh S, Swing V, Tissier C, Zhang P, Huala

E (2008) The Arabidopsis Information Resource (TAIR): gene structure and function annotation. Nucleic Acids Res **36**: D1009-D1014

Tabata KV, Sato K, Ide T, Nishizaka T, Nakano A, Noji H (2009) Visualization of cargo concentration by COPII minimal machinery in a planar lipid membrane. EMBO J **28**: 3279-3289

Taj G, Agarwal P, Grant M, Kumar A (2010) MAPK machinery in plants: recognition and response to different stresses through multiple signal transduction pathways. Plant Signal Behav **5**: 1370-1378

Takemoto D, Jones DA, Hardham AR (2003) GFP-tagging of cell components reveals the dynamics of subcellular re-organization in response to infection of Arabidopsis by oomycete pathogens. Plant J **33**: 775-792

Tamura K, Shimada T, Ono E, Tanaka Y, Nagatani A, Higashi SI, Watanabe M, Nishimura M, Hara-Nishimura I (2003) Why green fluorescent fusion proteins have not been observed in the vacuoles of higher plants. Plant J **35**: 545-555

Tao Y, Xie Z, Chen W, Glazebrook J, Chang HS, Han B, Zhu T, Zou G, Katagiri F (2003) Quantitative nature of Arabidopsis responses during compatible and incompatible interactions with the bacterial pathogen Pseudomonas syringae. Plant Cell **15**: 317-330

Tatebayashi K, Takekawa M, Saito H (2003) A docking site determining specificity of Pbs2 MAPKK for Ssk2/Ssk22 MAPKKKs in the yeast HOG pathway. EMBO J **22**: 3624-3634

Thilmony R, Underwood W, He SY (2006) Genome-wide transcriptional analysis of the *Arabidopsis thaliana* interaction with the plant pathogen *Pseudomonas syringae* pv. *tomato*

DC3000 and the human pathogen *Escherichia coli* O157:H7. Plant J **46**: 34-53

Titorenko VI, Mullen RT (2006) Peroxisome biogenesis: the peroxisomal endomembrane system and the role of the ER. J Cell Biol **174**: 11-17

Tolley N, Sparkes IA, Hunter PR, Craddock CP, Nuttall J, Roberts LM, Hawes C, Pedrazzini E, Frigerio L (2008) Overexpression of a plant reticulon remodels the lumen of the cortical endoplasmic reticulum but does not perturb protein transport. Traffic **9**: 94-102

Torres MA, Dangl JL (2005) Functions of the respiratory burst oxidase in biotic interactions, abiotic stress and development. Curr Opin Plant Biol **8**: 397-403

Torres MA, Jones JD, Dangl JL (2006) Reactive oxygen species signaling in response to pathogens. Plant Physiol **141**: 373-378

Uemura T, Ueda T, Ohniwa RL, Nakano A, Takeyasu K, Sato MH (2004) Systematic analysis of SNARE molecules in Arabidopsis: dissection of the post-Golgi network in plant cells. Cell Struct Funct **29**: 49-65

Vedrenne C, Hauri HP (2006) Morphogenesis of the endoplasmic reticulum: beyond active membrane expansion. Traffic **7**: 639-646

Vernoud V, Horton AC, Yang Z, Nielsen E (2003) Analysis of the small GTPase gene superfamily of Arabidopsis. Plant Physiol **131**: 1191-1208

Villarejo A, Buren S, Larsson S, Dejardin A, Monne M, Rudhe C, Karlsson J, Jansson S, Lerouge P, Rolland N, von Heijne G, Grebe M, Bako L, Samuelsson G (2005) Evidence for a

protein transported through the secretory pathway en route to the higher plant chloroplast. Nat Cell Biol **7**: 1224-1231

Vitale A, Denecke J (1999) The endoplasmic reticulum - Gateway of the secretory pathway. Plant Cell **11**: 615-628

Vitale A, Hinz G (2005) Sorting of proteins to storage vacuoles: how many mechanisms? Trends Plant Sci **10**: 316-323

Voeltz GK, Prinz WA, Shibata Y, Rist JM, Rapoport TA (2006) A class of membrane proteins shaping the tubular endoplasmic reticulum. Cell **124**: 573-586

Wan J, Zhang XC, Neece D, Ramonell KM, Clough S, Kim SY, Stacey MG, Stacey G (2008) A LysM receptor-like kinase plays a critical role in chitin signaling and fungal resistance in Arabidopsis. Plant Cell **20**: 471-481

Wang D, Weaver ND, Kesarwani M, Dong X (2005) Induction of protein secretory pathway is required for systemic acquired resistance. Science **308**: 1036-1040

Wang J, Cai Y, Miao Y, Lam SK, Jiang L (2009) Wortmannin induces homotypic fusion of plant prevacuolar compartments. J Exp Bot **60**: 3075-3083

Wang L, Jackson WC, Steinbach PA, Tsien RY (2004) Evolution of new nonantibody proteins via iterative somatic hypermutation. Proc Natl Acad Sci U S A **101**: 16745-16749

Wang L, Tsien RY (2006) Evolving proteins in mammalian cells using somatic hypermutation. Nat Protoc **1**: 1346-1350

Wendehenne D, Lamotte O, Frachisse JM, Barbier-Brygoo H, Pugin A (2002) Nitrate efflux is an essential component of the cryptogein signaling pathway leading to defense responses

and hypersensitive cell death in tobacco. Plant Cell **14**: 1937-1951

Whitmarsh AJ, Cavanagh J, Tournier C, Yasuda J, Davis RJ (1998) A mammalian scaffold complex that selectively mediates MAP kinase activation. Science **281**: 1671-1674

Widmann C, Gibson S, Jarpe MB, Johnson GL (1999) Mitogen-activated protein kinase: conservation of a three-kinase module from yeast to human. Physiol Rev **79**: 143-180

Wise RP, Moscou MJ, Bogdanove AJ, Whitham SA (2007) Transcript profiling in host-pathogen interactions. Annu Rev Phytopathol **45**: 329-369

Wurmser AE, Gary JD, Emr SD (1999) Phosphoinositide 3-kinases and their FYVE domain-containing effectors as regulators of vacuolar/lysosomal membrane trafficking pathways. J Biol Chem **274**: 9129-9132

Yamaguchi Y, Huffaker A, Bryan AC, Tax FE, Ryan CA (2010) PEPR2 is a second receptor for the Pep1 and Pep2 peptides and contributes to defense responses in Arabidopsis. Plant Cell **22**: 508-522

Yamaguchi Y, Pearce G, Ryan CA (2006) The cell surface leucine-rich repeat receptor for *At*PEP1, an endogenous peptide elicitor in *Arabidopsis*, is functional in transgenic tobacco cells. Proc Natl Acad Sci USA **103**: 10104-10109

Yoshioka H, Asai S, Yoshioka M, Kobayashi M (2009) Molecular mechanisms of generation for nitric oxide and reactive oxygen species, and role of the radical burst in plant immunity. Mol Cells **28**: 321-329

Yoshioka K (2004) Scaffold proteins in mammalian MAP kinase cascades. J Biochem **135**: 657-661

Zeidler D, Zahringer U, Gerber I, Dubery I, Hartung T, Bors W, Hutzler P, Durner J (2004) Innate immunity in Arabidopsis thaliana: lipopolysaccharides activate nitric oxide synthase (NOS) and induce defense genes. Proc Natl Acad Sci U S A **101**: 15811-15816

Zhang J, Li W, Xiang T, Liu Z, Laluk K, Ding X, Zou Y, Gao M, Zhang X, Chen S, Mengiste T, Zhang Y, Zhou JM (2010) Receptor-like cytoplasmic kinases integrate signaling from multiple plant immune receptors and are targeted by a Pseudomonas syringae effector. Cell Host Microbe **7**: 290-301

Zhang Z, Feechan A, Pedersen C, Newman MA, Qiu JL, Olesen KL, Thordal-Christensen H (2007) A SNARE-protein has opposing functions in penetration resistance and defence signalling pathways. Plant J **49**: 302-312

Zheng H, Kunst L, Hawes C, Moore I (2004) A GFP-based assay reveals a role for RHD3 in transport between the endoplasmic reticulum and Golgi apparatus. Plant J **37**: 398-414

Zipfel C, Kunze G, Chinchilla D, Caniard A, Jones JDG, Boller T, Felix G (2006) Perception of the bacterial PAMP EF-Tu by the receptor EFR restricts *Agrobacterium*-mediated transformation. Cell **125**: 749-760

Zipfel C, Robatzek S, Navarro L, Oakeley EJ, Jones JD, Felix G, Boller T (2004) Bacterial disease resistance in Arabidopsis through flagellin perception. Nature **428**: 764-767